INVESTIGATION OF MICROEMULSIONS AND THEIR MICROSTRUCTURES FOR TRANSDERMAL AND DERMAL DRUG DELIVERY

by

JI ZHANG

A Dissertation submitted to

Graduate School – New Brunswick

Rutgers, The State University of New Jersey

In partial fulfillment of the requirements

For the degree of

Doctor of Philosophy

Graduate Program in Pharmaceutical Science

Written under the direction of

Bozena Michniak-Kohn

And approved by

_____

_____

_____

_____

New Brunswick, New Jersey

OCTOBER, 2017

ABSTRACT OF THE DISSERTATION

Investigation of Microemulsions and Their Microstructures for Transdermal and Dermal Drug Delivery

By JI ZHANG

Dissertation Director:

Professor Bozena Michniak-Kohn

Drug delivery through the skin, transdermally and topically, offers many advantages including reduced systemic toxicity and side-effects, avoidance of the hepatic first pass metabolism, improved patient compliance, enabling sustained or controlled drug release, and enhanced delivery to local target tissues. However, there are many challenges for this route of administration, the major one is the skin barrier function to drug permeation. Many different approaches have been studied and used for enhancing the drug skin permeation. Among them, chemical permeation enhancers and microemulsion formulations are some of widely studied approaches. The thesis work focused on microemulsion (ME) formulations for enhancing transdermal or dermal drug delivery. Specifically, the ME microstructures were investigated and correlated with enhancement effects of drug skin permeation or skin deposition. The results showed that a critical factor influencing ME formulation behavior was the water content that also correlated to the formulation microstructure, and the drug skin permeation increased

significantly corresponding to the microstructure change from W/O, to Bi-continuous, and to O/W. This was the first time that this phenomenon had been systematically studied and reported, the microstructure of a microemulsion affected both hydrophobic and hydrophilic model drugs' transdermal permeation. The extent of trandermal permeation enhancement effect was more significant for hydrophobic drugs than hydrophilic drugs as water content increased and the corresponding microstructure changed in the ME formulation. Furthermore, at fixed water content, increasing oil content would result in higher transdermal permeation enhancement. The model drugs used in the study were lidocaine, ketoprofen, and caffeine, which represented compounds of varied physical and chemical properties. The findings were of practical significance for microemulsion formulation design and development in transdermal drug delivery.

Secondly, in the present study, a combination of analytical methodologies was utilized to examine microemulsion microstructures. It was found that the cooling thermogram generated by Differential Scanning Calorimetry (DSC) provided a simple approach for microstructure determination, which to the author's knowledge, had not been reported before. Extensive DSC cooling experiments had been conducted to analyze three ME systems that had their microstructure characterized and known in the literature. It was showed that DSC derived microstructure results were in complete concordance with literature reports, and thus demonstrated that the cooling DSC method was an effective analytical technique for ME microstructure assessment. The results also showed that the DSC method provided additional advantages over conventional methods for being sensitive, accurate, and versatile. The developed cooling DSC methodology for ME

microstructure analysis would greatly facilitate ME formulation characterization and development in the future.

Finally, dermal delivery of hydrophobic drugs by microemulsion (ME) formulations and effect from ME microstructures were studied. The antifungal drug, clotrimazole (CLOT), was used as the model compound. ME formulations of different microstructures were prepared along water dilution line at fixed oil/(surfactant and co-surfactant) ratio of 1/9 (w/w) using isopropyl myristate as oil, Labrasol and Cremophor EL as surfactant and co-surfactant, and water. Permeation experiments on human cadaver skin were conducted for ME and the control formulations of different CLOT loads. Dermal delivery of CLOT assessed by the dermal drug concentrations was found to be significantly higher for MEs when compared with the control formulation, and the highest concentration was observed with O/W ME, suggesting ME microstructure was an important formulation variable for enhancing dermal delivery. ME gel formulations prepared by incorporating 1.0% (w/w) of Carbopol 980 showed comparable dermal CLOT concentration to MEs but up to 2.4 fold higher than the commercial CLOT cream product, Lotrimin®. Furthermore, FITC used as a model compound for highly hydrophobic drugs, was also studied for its dermal delivery by MEs in porcine skin penetration experiments. Results showed a consistent ME microstructure effect, suggested by significantly higher FITC concentrations in all skin layers, stratum corneum, viable epidermis, and dermis, from O/W ME over Bi-continuous and W/O MEs. Results from the present study highlighted ME microstructure effect on ME dermal delivery of hydrophobic drugs, and provided insight to drug dermal retention and transdermal permeation enhancements and their interplay.

Acknowledgements

I would like to thank sincerely the members in my thesis committee: Drs. Tamara Minko, Guofeng You, and Mark Chandler, for their valuable time, comments and guidance throughout my thesis defense process.

I would like to express my deepest gratitude to my advisor, Dr. Bozena Michniak-Kohn, for her unconditional support, direction, and patience with me over the years when I worked in her research group and without her constant encouragement, assistance and advice, it would not had been possible for me to complete this work which has changed my life forever.

I would like to thank all my laboratory mates and staff in the Center for Dermal Research and the Laboratory of Drug Delivery, New Jersey Center for Biomaterials at Rutgers-The State University of New Jersey for assistance and support I received during my graduate work there.

I would like to thank all professors, teachers, and staffs who had taught or helped me in Department of Pharmaceutics and Graduate Program in Pharmaceutical Sciences, Ernest Mario School of Pharmacy, Rutgers –The State University of New Jersey. Especially, I would like to express my hearted gratefulness to Dr. Tony Kong, Chairman, and Ms. Hui Pung, Secretary of Graduate Program of Pharmaceutical Sciences for their help and support over the years.

In addition, I would like to thank our collaborator Dr. Amnon Sintov, Department of Biomedical Engineering, Faculty of Engineering Sciences, Ben Gurion University of the Negev, Israel, for his help, research advice and collaboration during my research studies.

Table of Contents

List of Tables

List of Illustrations

Chapter 1 . INTRODUCTION AND SPECIFIC AIMS

1.1. Introduction

Drug delivery through the skin/dermal route has been studied widely for many decades. It offers numerous advantages over conventional oral and intravenous routes. These include reducing dosing frequency, avoiding the hepatic first-pass metabolism and GI tract irritation, better patient compliance due to easy dose administration, reducing toxic side effects due to more uniform drug blood levels, and potentially achieving targeted delivery (Subedi et al., 2010; Prausnitz et al., 2008; Paudel et al., 2010).

The worldwide transdermal drug delivery market reached $32 billion in 2015. It is in-track to grow at an annual rate of around 11.6% over the coming decade, and predicted to reach $96.6 billion by 2025, according to the news release on Jan. 20, 2017 by Research and Markets, a leading market research company. Therefore, there are huge opportunities for transdermal and topical drug delivery product developments.

Transdermal products have been used for treatments of many different diseases. They mainly include pain management, women's health, hormonal replacement, Alzheimer's disease and Parkinson's disease, anti-hypertension, and smoking cessation. It can be expected that more transdermal drug products will be developed for treatment of a wider range of diseases as more progress is made in drug delivery technology and more potent drug molecules become available as suitable candidates.

However, transdermal drug delivery also has limitations. The skin barrier function poses the major challenge to drug permeation through the membrane and limits the delivery efficiency. This is why, after more than 30 years since the first transdermal drug product

was approved, there are only about 40 transdermal or dermal products on the US market for about 20 drug molecules, as summarized in Table 1-1 (Subedi et al., 2010)

Table 1-1. Summary of Marketed Transdermal Products in US

Drug	**Disease/treatment**	**Product**
Scopolamine	Motion sickness	Transderm-Scop®
Nitroglycerin	Angina pectoris	Transderm-Nitro®, Nitrodisc®, Deponit®,
Nicotine	Smoking cessation	Minitran®, Nitro-dur®, Nicotinell®, Nicoderm®, Nicostop®, Habitrol®,Nicotrol®, Prostep®
Estradiol	Postmenstrual syndrome	Estraderm®, Estran®, Climaderm®, Climara®, Alora®, Fematrix®, Fempatch®, Vivelle®
Testosterone	Hypogonadism	TestoDermTTS®, AndroDerm®
Clonidine	Hypertension	Catapress-TTS®
Fentanyl	Analgesia	Duragesic®, Matrifen®
Buprenorphine	Analgesia	BuTrans®
Progestin/estrogen	Contraceptives	OrthoEvra®
Estradiol/Norethindrone	Hormone replacement therapy (HRT)	CombiPatch®
Estrogen/Progesterone	HRT	Nuvelle TS®
Selegiline	Depression	EmSam®
Rotigotine	Parkinson’s disease	Neupro®
Methylphenidate	ADHD (Attention deficit hyperactivity disorder)	Daytrana®
Lidocaine	Post-herpetic neuralgia	Lidoderm®, Synera® (lidocaine+Tetracaine)
Ketoprofen, Piroxicam, Diclofenac	Inflammation/pain	Ketotop®, Trast®, Rheumastop®, Nupatch®
Rivastigmine	Alzheimer's disease	Exelon®
Oxybutynin	Hyperactive bladder	Oxytrol® (USA), Kentera® (Europe)
Granisetron	Nausea, vomiting	Sansuco®
Capsaicin	Postherpetic neuralgia	Qutenza®

Many techniques have been developed for enhancing drug transdermal permeation. They can be categorized as physical or chemical approaches. Chemical approaches include prodrug, salt formation, ion pairs, chemical enhancers, and formulation approaches such as microemulsions, liposomes, eutectic mixtures, and co-solvents, etc. (Subedi et al., 2010; Chiranjib et al., 2010).

The use of chemical permeation enhancers is an approach that has been extensively studied. Many different classes of compounds have showed permeation enhancement activity, including alcohols, long chain fatty acids, terpenes, esters, amides, amino acids, and dimethyl sulfoxide (DMSO), etc.

Also among various formulation approaches for enhancing drug skin permeation, the microemulsion approach has been found to be effective and has been extensively studied for the past 20 years. Microemulsion formulations offer advantages of significantly increased drug solubility, ease of preparation, good stability, and effective permeation enhancement for both hydrophobic and hydrophilic drugs. However, there is lack of understanding of the mechanism and controlling factors involving microemulsion permeation enhancement, formulation design and development work have often been conducted arbitrarily rather than in a systematic fashion, which has led to many non-optimized formulations. Specifically, to date there is no systematic study of the impact of ME microstructure on drug permeation enhancement. Therefore, in the present research, the main objective is to study how microemulsion microstructure will affect transdermal drug permeation of different model drugs, including both hydrophobic and hydrophilic ones. Additionally, during the study, it was found that the analytical work needed to determine the ME microstructures was complicated and challenging, and involved a combination of different analytical techniques. Based on a large number of experiments, it was discovered that DSC can be used as one single and effective method for determination of ME microstructure. Finally, efforts were made to expand the study scope by which ME microstructure effect on dermal drug delivery was investigated.

1.2. Specific Aims

The specific aims of this study were:

- To develop a ME system that has high water solubilizing capacity so that ME formulation vehicles with different microstructures could be easily prepared based on this system;
- To characterize ME formulation microstructures using a combination of analytical techniques and based on acquired knowledge, ME formulations of different microstructure containing model drugs were prepared, and tested in skin permeation experiments.
- To investigate the relationship of ME microstructure to model drugs' transdermal permeation enhancement effects. The model drugs included lipophilic lidocaine and ketoprofen, and hydrophilic caffeine. Skin permeation experiments were conducted using Franz diffusion cells and porcine skin. Drug loaded ME formulations of different microstructures were used to treat skin samples and compared side-by-side with control formulations. Skin permeation results were correlated to formulation variables including water content, microstructure, constituent oil type and content. Overall, the goal was to gain further understanding on the ME transdermal delivery enhancement mechanism.
- To demonstrate that DSC is an effective and simple tool for ME microstructure characterization. In the study, DSC method critical running parameters were tested and optimized, three ME systems that had their microstructures been determined in literatures were characterized by the DSC method, and the results were compared with literature reports to show complete agreement.

- To investigate ME formulation variables and microstructure relationship to dermal drug delivery efficiency. In the study, the anti-fungal drug clotrimazole was used as the model hydrophobic drug. Clotrimazole ME formulations of different microstructures were prepared and utilized for skin permeation experiments. The results of the drug skin retention were correlated to ME microstructures in order to gain insight on ME formulation variables for dermal delivery enhancement. Furthermore, ME-gel formulations were studied for skin retention and permeation, and compared side-by-side with a clotrimazole commercial cream product, Lotrimin®.
- To further investigate ME formulations for dermal delivery using FITC fluorescent dye as a model hydrophobic compound. FITC loaded ME formulations of different microstructures were used to treat porcine skin in Franz cell diffusion experiments and FITC skin deposition was measured using fluorescent microscopic imaging analyses.

Chapter 2 . BACKGROUND AND SIGNIFICANCE

2.1. Review of Human Skin Structure

Human skin provides important functions for the body including protection from the environment, prevention of dehydration, regulation of body temperature, production of Vitamin D, and providing sensory perception. Human skin is mainly composed of three structural layers, namely the epidermis, dermis and subcutaneous (hypodermis) layer. The epidermis consists of the stratum corneum, stratum granulosum, stratum spinosum and stratum basale. The dermis contains blood vessels, neuronal nerve endings, sebaceous and sweat glands, and hair follicles as well as collagen and elastin. The hypodermis contains adipocytes. Figure 2-1 illustrates the skin structure (Marieb, 1997).

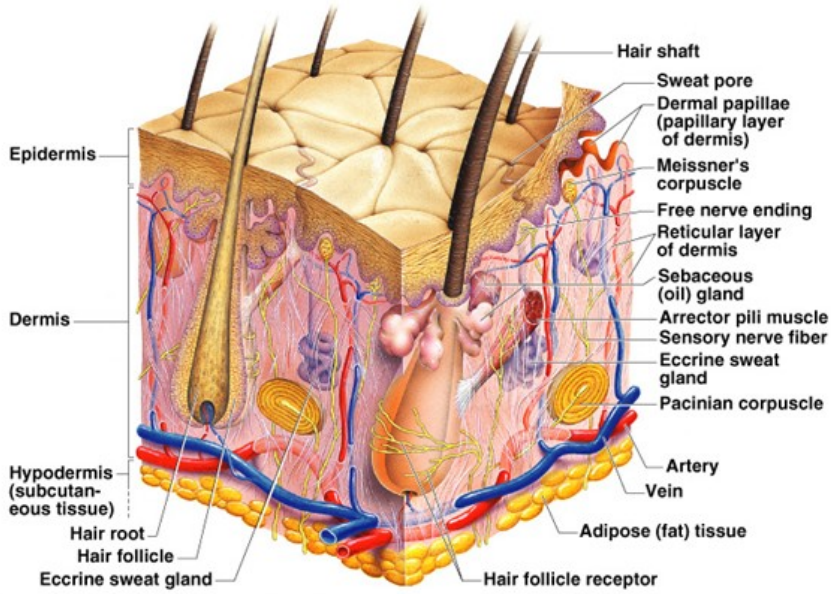

Figure 2-1. Human Skin Structure

Stratum corneum (SC), the outmost thin layer of the epidermis, provides the major barrier of the skin structure. It is composed of layers of dead cornified cells and lipids, proteins

and water. The lipid region has highly crystalline lamellar structure, and is composed of ceramides, cholesterol and fatty acids. The “Brick and Mortar” model is often used to illustrate the structure of SC. Figure 2-2 shows microscopic image of skin cross-section and illustration diagram of SC, epidermis, and dermis (Menon et al., 2012).

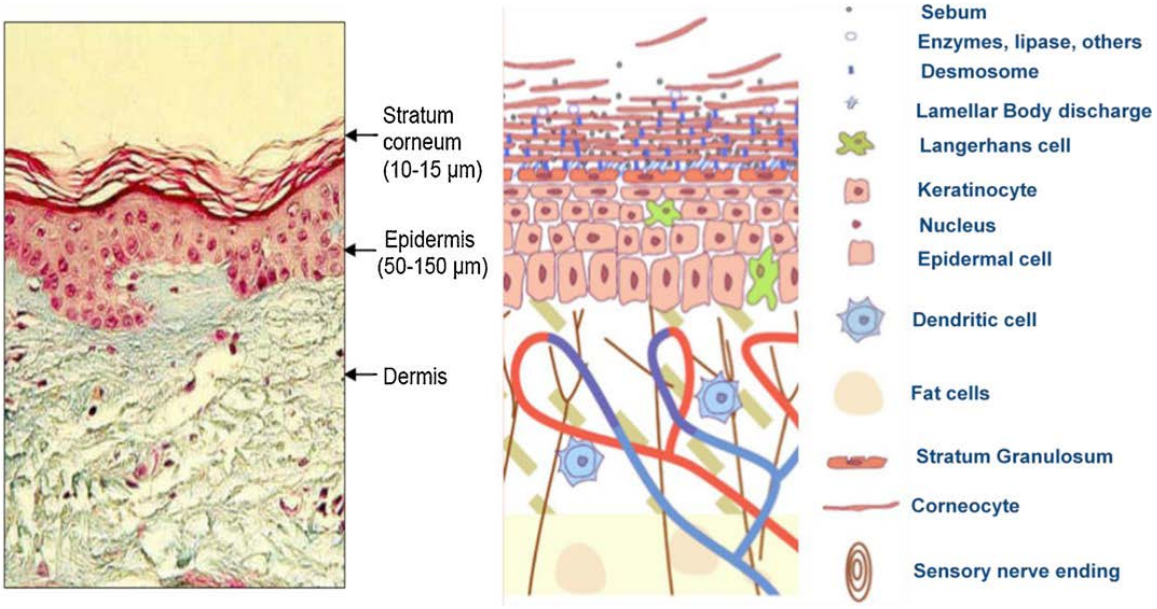

Figure 2-2. Skin Cross-section Microscopic Image and Illustration Diagram of SC, Epidermis, and Dermis

For drug delivery through the skin into the systemic circulation, termed transdermal delivery, or into the skin (epidermis and dermis), termed topical/dermal delivery, there are three major pathways for drug transport through the skin: (1) intercellular, (2) transcellular, and (3) shunt pathways. The intercellular pathway that goes through the lipid regions of SC is considered the main transport route for drug molecules in transdermal or dermal drug delivery. Figure 2-3 illustrates the pathways through the skin SC (Barry, 2001).

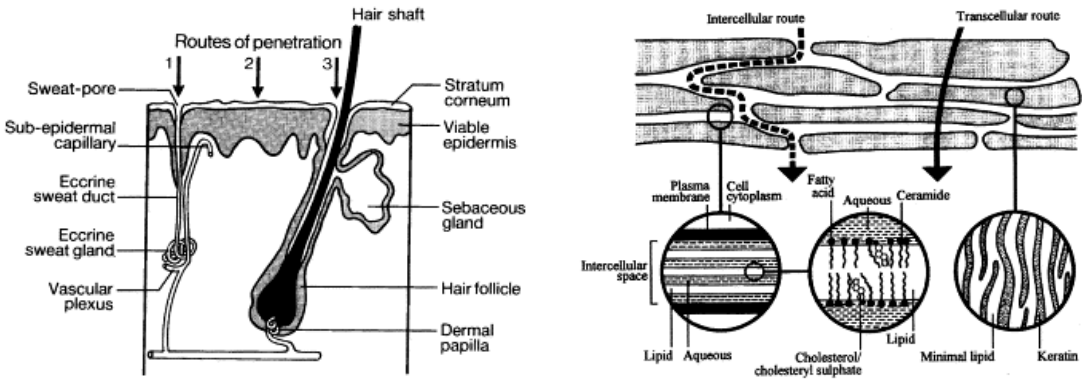

Figure 2-3. Transdermal Drug Delivery Pathways

2.2. Transdermal and Topical Drug Delivery Advantages and Limitations

Drug transdermal and topical deliveries offer some major advantages that can be summarized as follows (Subedi et al., 2010; Prausnitz et al., 2008; Paudel et al., 2010):

- Bypassing the hepatic first-pass metabolism and leading to improvement of bioavailability;
- Reducing gastro-intestinal irritation following oral administration of drugs;
- Reducing toxic side effects due to a more steady state plasma drug level with less peak to trough variations;
- Improved patient compliance due to non-invasive and easy drug administration;
- Feasibility of controlled and sustained drug release;
- Targeting delivery of the drugs to skin or local tissues for certain diseases.

There are also limitations related to transdermal and topical drug delivery, and they include the following (Subedi et al., 2010; Brown et al., 2006) :

- Low drug skin permeation due to the presence of SC barrier ;

- Drug molecules are generally limited to low molecular weight (< 500) and potent compounds (daily dose < 10 mg) for passive permeation dosage forms;
- Drug skin permeation is proportional to the concentration in the formulation and will decrease with the drug release. This route is not suitable for expensive drugs due to drug wasted with patch removal of the patch or formulation being washed off;
- Possible skin irritation and sensitization from the formulation;
- Inter- and intra-subject variability of skin permeability due to patient skin conditions;
- Pre-systemic metabolism, due to enzymes present in skin (e.g. peptidases and esterases), may cause the drug be metabolized to the inactive form.

2.3. Overview of Transdermal and Dermal Drug Permeation Enhancement Approaches

Over the years, various techniques have been developed to overcome the skin barrier function and to make transdermal and topical drug deliveries feasible, they can be classified into physical, chemical or formulation approaches. The physical include iontophoresis (Marro et al., 2001; Guy et al., 2001), electroporation (Hu et al., 2000), sonophoresis and micro-needles (McAllister et al., 2000). These physical techniques are also called active methods (Brown et al, 2006) because an extra driving force is applied to facilitate drug skin permeation. For examples, iontophoretic method applies an electrical field to drive ionized drug molecules across the skin membrane, electroporation

treats the skin with a high electrical voltage for a short period of time, and sonophoresis uses ultrasonic waves to enhance drug penetration.

The chemical and formulation approaches include the use of chemical permeation enhancers (Williams and Barry, 2004), super-saturated formulations (Moser et al., 2001; Pellet et al., 2003), prodrugs (Elias et al., 2003), liposomes, polymeric suspensions and microemulsions (Heuschkel et al., 2008; Kreilgaard, 2002). Drug permeation in these cases is generally considered to be passive because no extra energy is applied. Figure 2-4 shows various approaches that have been used for increasing drug transdermal permeation.

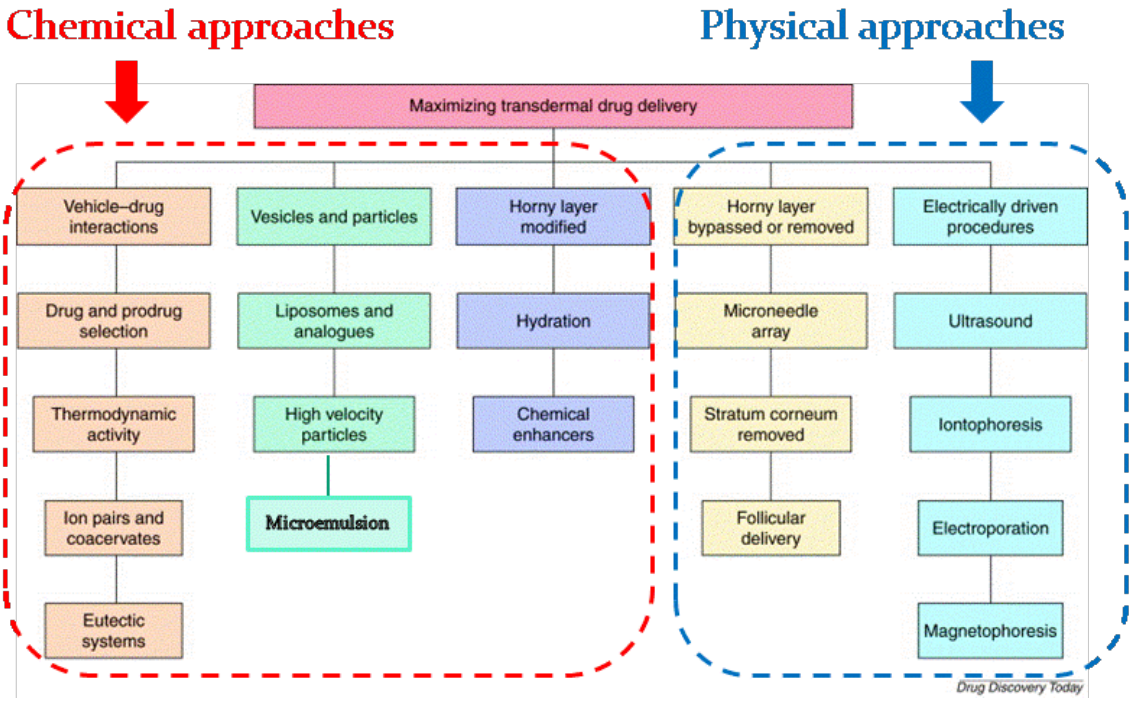

Figure 2-4. Various approaches used for increasing drug transdermal permeation (modified from Chiranjib et al., 2010)

The main focus of the research in this thesis is concentrated on examining the microemulsion formulation approach to drug delivery enhancement.

2.4. Microemulsions for Transdermal / Dermal Drug Delivery

Microemulsions have been extensively studied for application in transdermal and dermal drug delivery. Microemulsion formulations offer several advantages including the ability to increase drug solubility significantly in the vehicle, good formulation stability, ease of preparation, and capability to enhance skin permeation of both hydrophobic and hydrophilic drugs (Heuschkel et al., 2008; Kreilgaard, 2002). However, there is still lack of fundamental understanding of the transdermal permeation enhancement mechanism and the controlling formulation variables for these microemulsion drug delivery systems, despite extensive studies in the area. Specifically, to our knowledge, no study has been reported on systematic investigation of microemulsion microstructure relationship to transdermal permeation enhancement effects. A more detailed review of microemulsions for transdermal and topical delivery is also presented in Chapter 3, 4, and 5. Therefore, the major focus in this study was to characterize microstructures of microemulsion systems and to investigate their relationship to transdermal permeation enhancement effect for several model drugs possessing different physico-chemical properties. The study resulted in a published paper (Zhang and Michniak-Kohn, 2011) and the results are presented in Chapter 3. Additionally, derived from this research work, it was found that DSC could be used as an effective analytical tool for ME microstructure characterization, which in the past, had been very time consuming and complicated, and involved using a combination of several analytical techniques. Therefore, further studies were conducted to develop and optimize the DSC method, and to demonstrate that DSC provides an effective and simple approach for ME microstructure assessment. The study results are presented in Chapter 4. Furthermore, based on data and knowledge acquired in the above

studies, ME microstructure influence on dermal drug delivery efficiency was further investigated, and the study results are presented in Chapter 5. Finally, some initial research was performed on a novel permeation enhancer, bromo-iminosulfurane (DMBIS), which involved its synthesis and study on the enhancing mechanisms. The synthesis work of DMBIS is reported in Appendix B. The skin permeation study on DMBIS which was a collaborated work and led to a published paper (Sintov et al., 2009) is described in Appendix C.

2.5. References for Chapters 1 and 2

Barry, B.W., 2001. Novel mechanism and devices to enable successful transdermal drug delivery. Europ. J. Pharm. Sci. 14, 101-114.

Brown, M.B., Martin, G.P., Jones, S.A., Akomeah, F.K., 2006. Dermal and transdermal drug delivery systems: current and future prospects. Drug Delivery 13, 175-187.

Chiranjib, D.B., Chandira, M., Jayakar B., Sampath, K.P., 2010. Recent advances in transdermal drug delivery system. Int. J. PharmTech. Res. 2 (1), 68-77.

Elias, P.M., Feingold, K.R., Tsai, J., Thornfeldt, C., and Menon, G., 2003. "Metabolic approach to transdermal drug delivery" In: Guy, R.H. and Hadgraft, J., Eds., Transdermal Drug Delivery. Marcel Dekker, New York, pp. 285-304.

Guy, R.H., Delgado-Charro, M.B., Kalia, Y.N., 2001. Iontophoretic transport across the skin. Skin Pharmacol. Appl. Skin Physiol. 14, 35-40.

Heuschkel, S., Goebel, A., Neubert, R.H.H., 2008. Microemulsions – modern colloidal carriers for dermal and transdermal drug delivery. J. Pharm. Sci. 97, 603-631.

Hu, Q., Liang, W., Bao, J., Ping, Q., 2000. Enhanced transdermal delivery of tetracaine by electroporation. Int. J. Pharm. 202, 121-124.

Kreilgaard, M., 2002. Influence of microemulsion on cutaneous drug delivery. Adv. Drug Delivery Rev. 54, s77-s98.

Marieb, E.N., 1997. Human anatomy and physiology. 4th ed., Benjamin Cummings, San Francisco.

Marro, D., Guy, R.H., Delgado-Charro, M.B., 2001. Characterization of iontophoretic permselectivity properties of human and pig skin. J. Control. Release 70, 213-217.

McAllister, D.V., Allen, M.G., Prausnitz, M.R., 2000. Microfabricated microneedles for gene and drug delivery. Ann. Rev. Biomed. Eng. 2, 289-313.

Menon, G.K., Cleary, G.W., Lane, M.E., 2012. The structure and function of the stratum corneum. Int. J. Pharm. 435, 3-9.

Moser K., Kriwet, K., Kalia, Y.N., and Guy, R.H., 2001. Stabilization of supersaturated solution of a lipophilic drug for dermal delivery. Int. J. Pharm. 224 (1-2), 169-176.

Pellet M., Raghavan, S.L., Hadgraft, J., and Davis, A.F., 2003. “The application of supersaturated systems to percutaneous drug delivery” In: Guy, R.H. and Hadgraft, J., Eds., Transdermal Drug Delivery. Marcel Dekker, New York, pp. 305-326.

Prausnitz, M.R., and Langer, R., 2008. Transdermal drug delivery. Nature Biotechnol. 26 (11), 1261-1268.

Sintov, A.C., Zhang, J., Michniak-Kohn, B.B., 2009. Cutaneous biotransformation of N-(4-bromobenzoyl)-S,S-dimethyliminosulfurane and its product, 4-bromobenzamide, leading to percutaneous penetration enhancement of drugs: initial evidence using hydrocortisone. J. Control. Rel. 133, 44-51.

Subedi, R.K., Oh, S.Y., Choi, H-K., 2010. Recent advances in transdermal drug delivery. Arch. Pharm. Res. 33 (3), 339-351.

William, A.C., Barry, B.W., 2004. Permeation enhancers. Adv. Drug Delivery Rev. 56, 603-618.

Zhang, J., Michniak-Kohn, B., 2011. Investigation of microemulsion microstructures and their relationship to transdermal permeation of model drugs: ketoprofen, lidocaine, and caffeine. Int. J. Pharm. 421, 34-44.

Chapter 3 . INVESTIGATION OF MICROEMULSION MICROSTRUCTURES AND THEIR RELATIONSHIP TO TRANSDERMAL PERMEATION OF MODEL DRUGS KETOPROFEN, LIDOCAINE, AND CAFFEINE

3.1. Introduction

One of the major challenges for transdermal drug delivery is to increase the drug permeation through skin tissue by overcoming the skin barrier provided by the stratum corneum. Many different approaches have been developed for this purpose including physical ones such as iontophoresis, sonophoresis, and microneedles, and chemical or formulation ones such as permeation enhancers, co-solvents, liposomes, nano-particle suspensions, and microemulsions. Microemulsion formulation approaches for enhanced drug permeation have been reported in the past two decades. Microemulsions are considered to be modern colloidal drug carrier systems and offer the following advantages: high drug solubilizing capacity, long term stability due to its thermo-dynamic stable system, ease of preparation, and capability to enhance skin permeation for both hydrophobic and hydrophilic drugs (Neubert et al., 2007). Some additional interesting characteristics of a microemulsion are its low viscosity, complex microstructures with their domain sizes in the sub-micro scale (typically 10-100 nm) (Sintov et al., 2004), and many variables in formulation development in term of complex compositions, and a large number of excipients that are available for use.

Microemulsion (ME) formulations can increase drug transdermal permeation, and this has been demonstrated for numerous drugs in past studies (Neubert et al., 2007; Neubert, 2011; Azeem et al., 2009; Kreilgaard, 2000 and 2002; Sintov et al., 2004, 2006;

Hua, 2004). So far, several hypotheses have been proposed on the mechanism for drug permeation enhancement, including increased drug solubility enabling a high concentration gradient toward skin, small droplet sizes and low viscosity of ME facilitating permeation, increased drug thermodynamic activity in the ME vehicle, and the disruption of SC lipid order by ME components, etc. However, there is a lack of systematic approaches in microemulsion formulation design and development mainly because the mechanism and factors controlling transdermal drug permeation enhancement are still not well understood.

Microemulsions exist in various microstructures including droplet-like and bi-continuous types. Since their drug delivery properties are related to the inner structure, there is a need to assign the correct state to the formulation. An appropriate characterization of ME microstructures is highly challenging due to their small particle sizes and fluctuation interfaces (Neubert et al., 2007). The combination of different characterization techniques is required. Typically, the techniques used for microstructure assessment in drug dermal delivery studies include viscosity test, surface tension test, electrical conductivity measurement, DSC, freeze-fracture transmission electron microscope (FF-TEM), small angle neutron scattering (SANS), and pulsed field gradient nuclear magnetic resonance (PFG-NMR). Many research groups have conducted studies focused on ME microstructure characterizations using the above techniques (Djordjevic et al., 2004, 2005; Gasperlin et al., 2004, 2005; Alany et al., 2001; Sintov et al., 2004, 2006). Despite many studies in this area, there is still no clear understanding of microstructure relationship to ME formulation transdermal permeation potential. The reasons, in our view, are as follows: (1) the characterization of ME microstructures is not

a straight forward task, and there is still lack of effective and simple methods to get unambiguous and accurate microstructure information, (2) there is a disconnect between studies on microstructures and those on drug transdermal permeation using ME formulations. The studies focused on microstructure examination were often confined in the structure probing aspect, and not extended to investigate further drug skin permeation. On the other hand, studies on transdermal permeation using ME formulations often only generated inadequate microstructure results or the ME systems in studies only had low water solubilizing capacity so that microstructure relationship to transdermal drug permeation could not be examined fully.

Therefore, the current study was conducted with multiple aims: (1) to explore the most effective techniques and their combination to characterize microemulsion microstructures; (2) to investigate microemulsion microstructure relationship to drug transdermal permeation enhancement for both lipophilic and hydrophilic drugs; (3) to investigate and identify key factors in ME that affect drug permeation potential; and (4) to explore permeation enhancement of microemulsions containing permeation enhancers, Azone and bromo-iminosulfurane (Song et al., 2005). In the study, a microemulsion system was developed, which had high water solubilizing capacity, thus allowing complete microstructure changes to be assessed at different water contents. Microstructures in the ME system were successfully characterized by a combination of techniques of EC, CV, DSC, and DLS. Based on the characterization results, microemulsions with different microstructures were prepared. Drug skin permeation was studied using Franz cell, dermatomed porcine skin and microemulsion formulations containing model drugs ketoprofen, lidocaine, and caffeine.

3.2. Materials and Methods

3.2.1. Materials

Isopropyl myristate (IPM) was purchased from Fisher Scientific (Fair Lawn, NJ). Cremophor EL was obtained from BASF (Ludwigshafen, Germany). Labrasol was obtained as a free sample from Gattefosse (St. Priest Cedex, France). Ketoprofen, lidocaine, caffeine, and ferrocene were purchased from Sigma (St. Louis, MO). Acetonitrile, methanol, and propylene glycol were purchased from Fisher Scientific (Fair Lawn, NJ). Water was distilled water that had been further purified by MilliQ A10 and Elix 10 system.

3.2.2. Pseudo-ternary Phase Diagram Construction

IPM was used as the oil phase (O), Labrasol was used as the surfactant (S), and Cremophor EL was used as co-surfactant (Co-S). First, the mixture of S and Co-S at the w/w ratio of 4:1 was prepared. Next, the mixture of O with S/Co-S was prepared at varying w/w ratios, e.g. 1:9, 2:8, 3:7, etc. Then, 1 gram of the O/(S/Co-S) mixture of the certain ratio was titrated with water step by step, at each step, the H_2O/O/(S/Co-S) mixture was agitated by a vortex mixer to mix thoroughly, and the sample was checked under light versus a dark background. If the sample was an isotropic and clear solution, it was defined as a microemulsion; if the sample was cloudy or showed the phase separation, it was not a microemulsion. The observation, the corresponding O/(S/Co-S) ratio and the water content were recorded at each step of the titration. The boundary point between the microemulsion and the non-microemulsion was defined as the mid-point between points of clear and cloudy samples. The microemulsion system pseudo-ternary phase diagram was constructed by labeling the recorded boundary points in a ternary plot.

3.2.3. Microemulsion Formulation Preparation

The calculated amount of the model drug was weighed into a small glass vial, the exact amount of the O/(S/Co-S) mixture was added in, the compound was dissolved completely by the aid of sonication and vortex mixing. Then, the exact amount of water according to the design of the H_2O/(O/(S/Co-S)) w/w ratio was added in, and mixed well by vortex mixing.

Model drugs, ketoprofen, lidocaine, and caffeine were formulated in microemulsions with different water contents of 20%, 40% and 70% (w/w), representing the specific microstructures, w/o, bi-continuous, and o/w, respectively. The drug loads (w/w %) in the formulations were set constant at 2.5%, 2.5%, and 1.0% for ketoprofen, lidocaine, and caffeine, respectively. Additional microemulsions with permeation enhancers, Azone and bromo-iminosulfurane (Br-IMSF), incorporated at 2% (w/w) were prepared. Propylene glycol (PG) formulations at the same drug loads were prepared and used as the controls. All above described formulations prepared were clear solutions at ambient temperature.

.2.4. Microemulsion Characterization

3.2.4.1. Dynamic light scattering (DLS)

The microemulsion internal phase droplet diameter was determined using a Zetasizer nano series instrument (Zetasizer Nano Series Model: Zen3600, Malvern, Westborough, MA) at room temperature (at 25 °C ± 1 °C).

3.2.4.2. Refraction index

The microemulsion sample refraction index values were measured using a pocket model refractometer (Model PAL-RI, ATAGO, Tokyo, Japan). The measurement was conducted at room temperature by adding 0.3 mL of the sample into the testing well.

3.2.4.3. Electrical conductivity (EC)

The microemulsion microstructure was assessed by EC tests. EC values of the sample were measured using an electric conduct-meter, Oakton ECTestr 11+ (Ockton Instruments, Vernon Hills, IL). The conduct-meter was calibrated using the standard solution of 1413 µS/cm (Ockton Instruments) before testing. Three gram of the oil-surfactant mixture of O/(S/Co-S) ratio 1/9 was titrated by the aqueous phase step by step, at each step, 1 mL of the sample was used for EC measurement at room temperature. The aqueous phase used was 0.9% (w/v) sodium chloride solution.

3.2.4.4. Electro analytical cyclic voltammetry (CV)

The microemulsion microstructure was evaluated by CV tests using a WaveNow Module cyclic voltammetry (CV) instrument with AfterMath software (Pine Research Instruments, Raleigh, NC). The method was based on and modified from that of Mo et al., 2000, 2007. Ferrocene was used as the electro-chemical active probe compound in the experiment. Ferrocene is a very lipophilic compound and will dissolve mainly in oil phase when incorporated in microemulsion. Its diffusion coefficient would be mostly affected by the state of oil phase in microstructure, was measured by CV tests and used to deduce information of microemulsion microstructures. Ferrocene was initially dissolved

in 10 g of oil-surfactant mixture of O/(S/Co-S) ratio 1/9 at the concentration of 0.5 mg/g, and diluted continuously by the aqueous phase (0.2 M KCl solution) while CV was conducted after each step of dilution at room temperature. CV conditions used were as follows: 2 segment run, start at -0.1 V, and end at 0.8 V with sweeping rates: 5, 10, 20, 40, 60, 80, and 100 mV/s. A glossy carbon electrode (surface area, 0.1963 cm^2) was used as the working electrode. A platinum wire and a AgCl/KCl electrode were used as the auxiliary electrode and the reference electrode, respectively. The anodic peak current, i_{pa} (A) at 25 °C will follow Randles-Sevcik equation (Equation 1),

$$i_{pa} = (2.687 \times 10^5) n^{3/2} v^{1/2} D^{1/2} A C \quad (1)$$

Where n is the number of electron transferred in the electro-chemical reaction, v is the sweeping rate (V/s), D is diffusion coefficient of ferrocene (cm^2/s), A is the surface area (cm^2) of the working electrode, and C is the concentration of electroactive probe, ferrocene ($mole/cm^3$). Therefore, based on the slope of the linear regression of i_{pa} vs. $v^{1/2}$ curve, diffusion coefficient of ferrocene, D, can be calculated.

3.2.4.5. Differential scanning calorimetry (DSC)

Microemulsions were tested using a TA Q100 DSC instrument (TA Instruments, New Castle, DE) for exploring the microstructures. Microemulsion sample (7-10 mg) was weighed accurately in an aluminum hermetic sample pan and sealed with the lid quickly to prevent the sample evaporation. DSC tests for blank ME samples were run at the following conditions: equilibrating at 25 °C for 1 minute, cooling the sample at the ramp rate of 5 °C/minute to -70 °C, isothermal for 0.5 minute, heating the sample at the ramp rate of 5 °C/minute to 30 °C. For model drug loaded ME formulation samples, DSC

testing conditions are the same as those for blank ME samples except that the starting equilibration temperature is at 37 °C (for 10 minutes) to mimic the formulation sample temperature in the skin permeation experiment.

3.2.5. In Vitro Skin Permeation Experiment

Fresh porcine skin tissue from the abdomen was harvested from pigs (UMDNJ Dept. of Surgery, Newark, NJ). The tissue was carefully cleaned from fat and muscle, and then dermatomed to a thickness of around 500 μm. The dermatomed skin was then cut into pieces of about 14x14 mm^2 that were stored at -80°C until use. Franz diffusion cells were used for the in vitro permeation study with a receptor (5.1 mL) containing PBS buffer at 37 °C. The skin sample was mounted on the cell and was hydrated for 1 hour prior to the experiment. Then, 150 μL of the microemulsion formulation or the control formulation was added to the donor. Propylene glycol with the same drug load was used as the control. At the time points of 0, 2, 16, 18, 20, 22, and 24 hours, 300 μL of the receptor sample was taken and then replaced with the same amount of the fresh PBS buffer. The permeation samples were assayed immediately by HPLC. The drug steady state permeation flux, J_s, is calculated based on data of time points from 16 to 24 hours.

3.2.6. Model Drug Analyses

The permeation samples were analyzed using an Agilent 1100 HPLC equipped with a Luna C18(2) 5μ 4.6x150 mm column (Phenomenex, Inc., Torrance, CA); Mobile phases were (A) 0.1% H_3PO_4, and (B) acetonitrile. The run was conducted using an isocratic elution at A/B of 45/55, 80/20, and 85/15 for ketoprofen, lidocaine, and caffeine,

respectively. The flow rate was 1 mL/min, the injection volume was 20 µL, and the UV detection wavelength was 258, 215, and 272 nm for ketoprofen, lidocaine, and caffeine, respectively. All assay methods were validated for linearity, inter- and intra-day variability as well as limit of detection.

3.2.7. Statistical Analyses

The skin permeation results are reported as means ± S.D. Data was statistically analyzed using one-way ANOVA test followed by Fisher's post hoc test. Differences between formulations were considered significant when $P < 0.05$.

3.3. Results

3.3.1. Microemulsion Characterization

3.3.1.1. Ternary phase diagram

The constructed pseudo ternary phase diagram is provided in Figure 1. The ME region is identified, in which at the high surfactant content area, a large amount of water can be solubilized without causing phase separation. For example, the oil-surfactant mixture at the O/(S/Co-S) ratio 1/9 can be diluted by water to higher than 95% (w/w) water content and the resulting sample still remained as a microemulsion. Therefore, along this water dilution line it is possible to study the complete course of microemulsion microstructure changes.

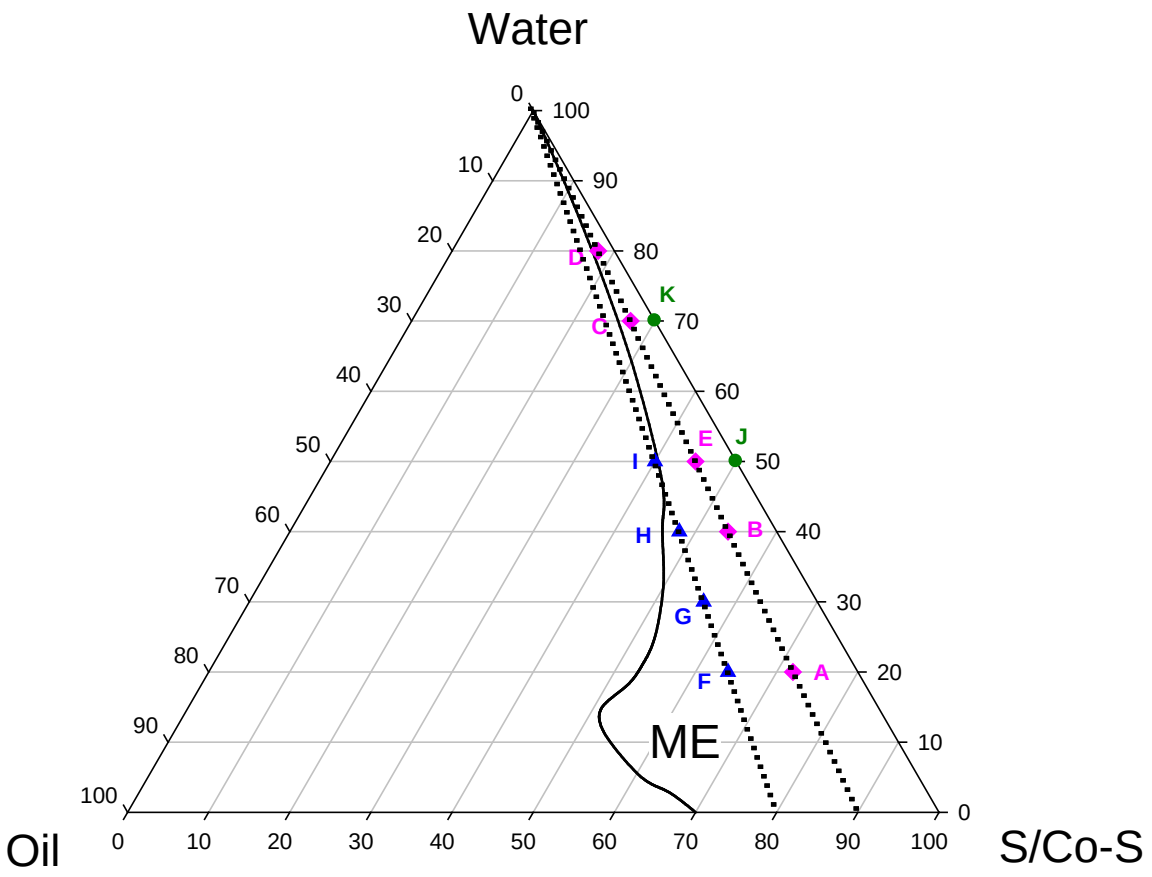

Figure 3-1. A pseudo ternary phase diagram showing the system ME region and positions of ME and micelle formulations used in the permeation study. IPM, Labrasol, and Cremophor EL were used as oil, surfactant, and co-surfactant, respectively.

3.3.1.2. Refraction index

Along the water dilution line of O/(S/Co-S) ratio 1/9, microemulsions with different water content (Φ_w) were prepared and their refraction indexes (RI) were measured. The plot of RI vs Φ_w shows a good linear correlation (R^2 = 0.9996), demonstrating microemulsion optically isotropic nature and high water solubilizing capacity of this ME system (Figure 3-2).

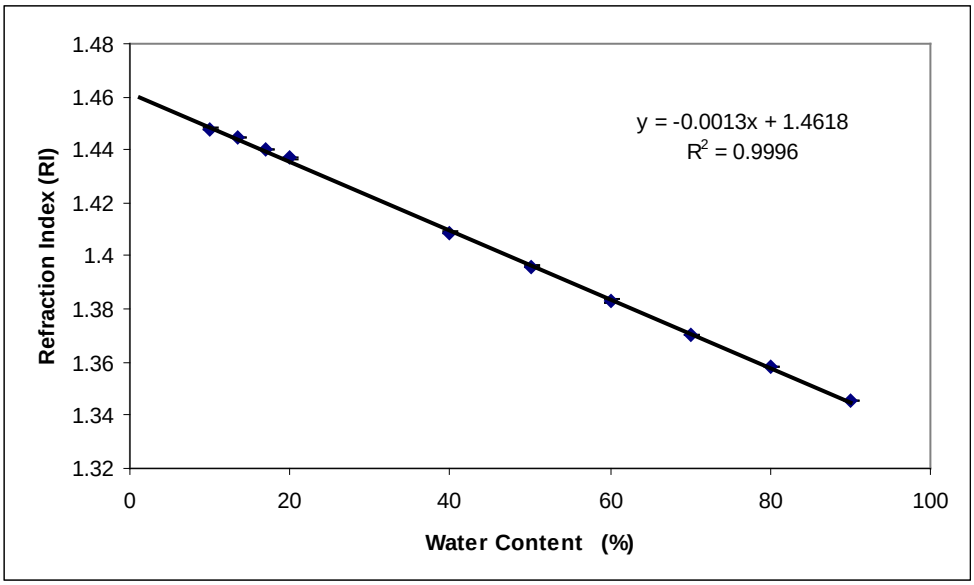

Figure 3-2. Microemulsions along the water dilution line of O/(S/Co-S) ratio 1/9 refraction index (RI) vs. water content (Φ_w) plot with the linear regression.

3.3.1.3. Particle size by Dynamic Light Scattering

Microemulsions were prepared along the water dilution line of O/(S/Co-S) ratio of 1:9. Their apparent droplet sizes assessed by DLS instrument are listed in Table 3-1. As can be seen the microemulsion apparent droplet size decreased significantly as water content increased. For ketoprofen loaded MEs, at high water content (e.g. at Φ_w 70%), O/W droplet size increased significantly as ketoprofen concentration increased, suggesting that ketoprofen molecules were mainly present in the surfactant rich interfacial layers. These results were also consistent with the drug solubility data in different ME excipients reported later.

Table 3-1. Apparent droplet size of microemulsions measured by DLS.

Microemulsion No.	Water Content (w/w %)	Oil Content (w/w %)	S/CoS Content (w/w %)	Drug Load (w/w %)	Enhancer (w/w %)	Droplet Size (nm)
1	20	8	72	None	None	177
2	30	7	63	None	None	86.8
3	40	6	54	None	None	50.0
4	50	5	45	None	None	34.2
5	60	4	36	None	None	22.8
6	70	3	27	None	None	17.3
7	80	2	18	None	None	14.3
8	70	3	27	None	Azone 2%	17.7
9	70	3	27	None	Br-IMSF 2%	22.2
10	70	3	27	Keto 1.0%	None	23.3
11	70	3	27	Keto 2.5%	None	42.3
12	80	2	18	Keto 2.5%	None	64.9
13	70	3	27	Caff 1.0%	None	18.4
14	70	3	27	Caff 1.0%	Azone 2%	21.1

Note: Keto = Ketoprofen; Caff = Caffeine; Br-IMSF = Bromo-iminosulfurane; Define DLS, S and coS.

3.3.1.4. Electrical conductivity

The oil/surfactant mixture of O/(S/Co-S) ratio 1/9 was diluted gradually using the aqueous phase, 0.9% (w/v) NaCl. The EC values of ME, κ, were measured in the dilution process and plotted vs. aqueous content Φ_w, as shown in Figure 3. The κ vs. Φ_w curve could be divided into three parts: parts at low and high aqueous contents, and the part at median aqueous content. Based on previous studies (Mo et al., 2000; Alany et al., 2001;), at low aqueous content, the microstructure is perceived as being w/o. The electrical conductive entities will be the aqueous droplets that are in an isolated state, resulting in the low conductivity at this region. As the aqueous content Φ_w increases, the w/o droplets increase in number and start to aggregate, when the percolation point, Φ_p is reached, w/o droplets begin to contact each other and form inter-connected channels, resulting in a drastic increase of κ. Therefore, the inflection point on the curve of κ vs. Φ_w is indicative

of Φ_p and corresponds to the transformation from a w/o droplet to a bi-continuous ME; At high aqueous content, the microstructure is o/w and the conductive entity is the continuous aqueous phase. As aqueous content Φ_w further increases, κ of the ME is expected to behave like an aqueous solution, increasing linearly. Again, the inflection on the plot of κ vs. Φ_w between the median and the high aqueous regions is indicative of the microstructure transformation from a bi-continuous to an O/W ME; As showed in Figure 3, κ vs. Φ_w curves at low and high Φ_w regions indeed can be approximated by linear fitting and yielded good correlation coefficients, respectively. The curve at the median Φ_w region is non-line and therefore, should correspond to the bi-continuous ME microstructure. Based on the EC results, it can be deduced the the microstructure transition points from W/O to bi-continuous and from bi-continuous to O/W are at water content of about 33% and 60%, respectively.

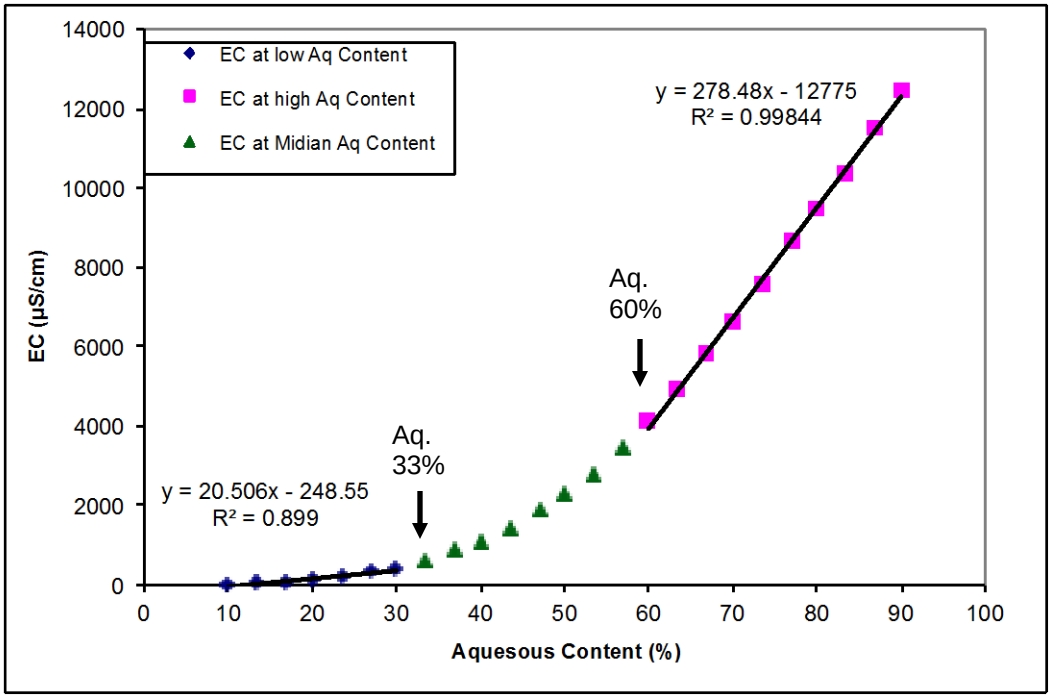

Figure 3-3. Plot of microemulsion electrical conductivity κ vs. aqueous content Φ_w.

3.3.1.5. Electro-chemical method, cyclic voltammetry

The apparent diffusion coefficient, D, of the electro chemical active compound ferrocene was measured in ME samples resulting from the dilution of the oil/surfactant mixture of O/(S/Co-S) ratio 1/9 by the aqueous phase, 0.2 M KCl. The plot of D vs. aqueous content Φ_w is illustrated in Figure 3-4. Similar to the dilution process in the EC measurement experiment, it was expected that the ME microstructure goes through transformation from w/o to bi-continuous to o/w. Based on the previous reports (Mo et al., 2000 and 2007), ferrocene as a lipophilic compound will mainly dissolve in the oil phase, and is expected to have relatively high diffusion coefficient D values in w/o ME, relative low D values in o/w ME, and median D values in bicontinuous ME. Therefore, based on the plot of ferrocene D vs. Φ_w, it can be deduced that microstructure transition points are at Φ_w of around 33% and 60% for changes from W/O to bi-continuous and from bi-continuous to O/W, respectively. These results are consistent with the observations in the EC experiment.

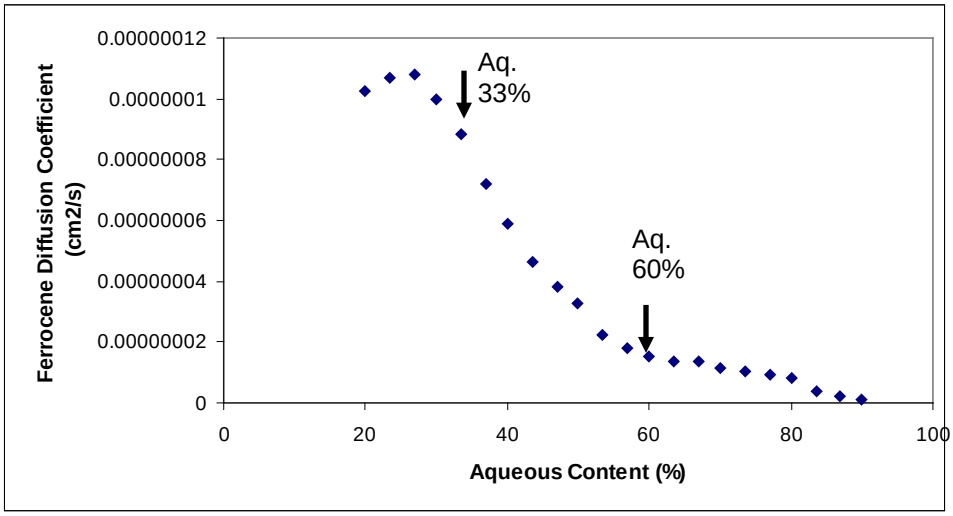

Figure 3-4. Apparent diffusion coefficient, D for ferrocene vs. aqueous content of microemulsions along the water dilution line of oil to surfactant ratio of 1/9.

3.3.1.6. DSC thermal analyses

ME samples were tested using DSC for a cooling and heating cycle. After extensive sample studies, it was found that the cooling DSC thermo-gram provided direct information on ME sample microstructures. Specifically, it was discovered that there are some important characteristics of the cooling thermo-gram related to the oil freezing peak and the water freezing peak. They can be described as follows: (1) ME samples of w/o microstructure did not show the water freezing peak, (2) ME samples of bi-continuous microstructure had the oil freezing peak and the water freezing peak as two distinct and separate peaks, and (3) ME samples of o/w microstructure showed only the water freezing peak as one big single peak in the thermo-gram. Based on these unique traits, the microstructure of a ME sample can be determined by a single DSC run. The DSC cooling thermo-grams of ME samples in microstructure transition regions are illustrated in Figure 3-5. The microstructure transition points along the water dilution line of O/(S/Co-S) ratio 1/9 were easily determined to be at water content of 33% and 59% for microstructure changes from W/O to bi-continuous and from bi-continuous to O/W, respectively. These microstructure transition point results are consistent with results obtained earlier by EC and CV measurements. This above described DSC approach to determine ME microstructures by following the cooling thermo-gram characteristics has not been clearly identified and demonstrated in previous studies to our knowledge. It offers several advantages including a simple test, a small required sample size, and an effective and accurate microstructure determination for both blank and drug loaded MEs. ME formulations loaded with model drugs (ketoprofen 2.5%, lidocaine 2.5%, and caffeine 1.0%) were tested using DSC. The results confirmed that at 37 °C, these model drug loaded ME formulations were indeed in the microstructure of W/O, bicontinuous, and

O/W corresponding to water content of 20%, 40%, and 70%, respectively. Figure 3-6 shows representative DSC cooling thermo-grams of 2.5% lidocaine loaded ME formulations.

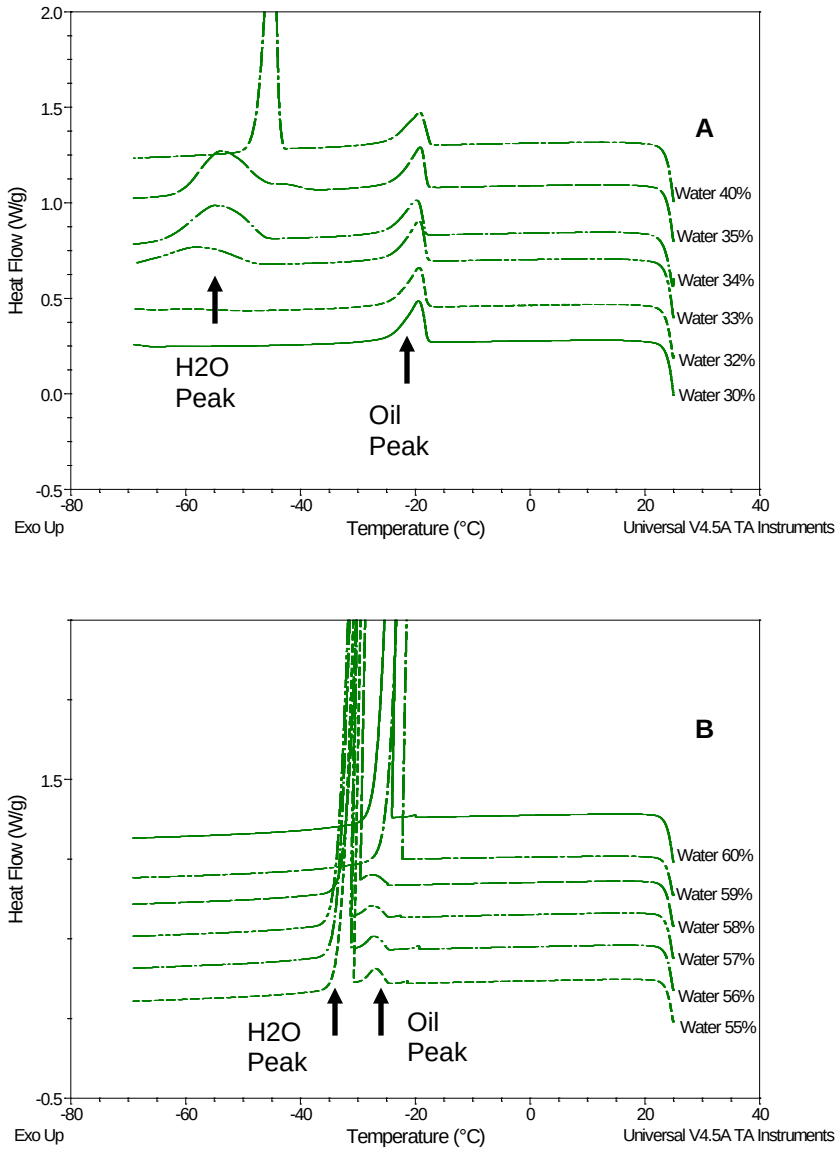

Figure 3-5. DSC cooling thermo-grams of microemulsions at microstructure transition regions: (A) the transition from W/O to bicontinuous ME, and (B) the transition from bicontinuous to O/W ME.

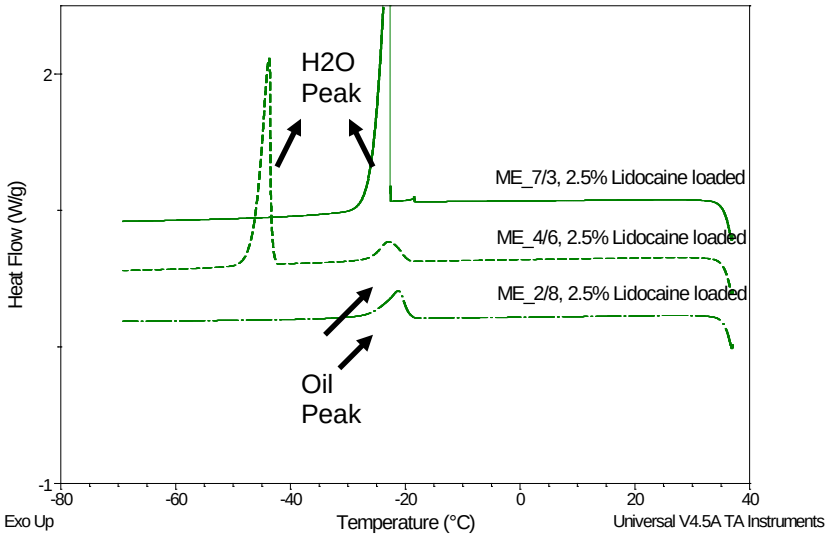

Figure 3-6. DSC cooling thermo-grams of 2.5% lidocaine loaded MEs at 37 °C.

3.3.2. Model Drug Solubility in Microemulsion Excipients

Model drugs, ketoprofen, lidocaine, and caffeine solubility samples in various component excipients used in microemulsion and the control formulations were tested at the ambient temperature (25 °C) and the results are presented in Table 3-2.

Table 3-2. Ketoprofen, lidocaine, and caffeine solubility in selected formulation excipients measured at the ambient temperature

Excipient	Solubility (mg/mL)		
	Ketoprofen	Lidocaine	Caffeine
IPM	12.2	131.3	0.8
IPP	9.2	109.6	NT
Oleic Acid	1.3	184.1	NT
Miglyol 812	10.0	NT	NT
Miglyol 840	16.8	NT	NT
Labrafac	16.1	NT	1.8
Labrasol	154.6	216.9	11.9
Cremophor EL	108.6	110.3	7.6
Ploural Oleique	28	99.0	1.7
PG	151.2	365.7	8.9
Water	0.2	3.7	19.9

Note: NT = “Not Tested”.

3.3.3. Skin Permeation Results

The compositions and microstructures of the microemulsion vehicles used in skin permeation experiments are listed in Table 3-3, and their positions in the pseudo-ternary phase diagram are presented in Figure 3-1.

Table 3-3. Microemulsion vehicle compositions and microstructures.

ME or Micelle Label	Position in Phase Diagram	Water to Oil/Surfactant Ratio	Water (%)	Oil (%)	S/CoS (%)	O/(S/CoS) Ratio	Microstructure
ME_2/8	A	20/80	20	8	72	1/9	W/O
ME_4/6	B	40/60	40	6	54	1/9	bi-continuous
ME_7/3	C	70/30	70	3	27	1/9	O/W
ME_8/2	D	80/20	80	2	18	1/9	O/W
ME_5/5	E	50/50	50	5	45	1/9	bi-continuous
ME_2/8_O	F	20/80	20	16	64	2/8	W/O
ME_3/7_O	G	30/70	30	14	56	2/8	bi-continuous
ME_4/6_O	H	40/60	40	12	48	2/8	bi-continuous
ME_5/5_O	I	50/50	50	10	40	2/8	bi-continuous
Micelle_5/5	J	50/50	50	0	50	0/10	NT
Micelle_7/3	K	70/30	70	0	70	0/10	NT

Note: NT = Not Tested; S = Surfactant; CoS = Co-surfactant;

Initially, drug loaded microemulsions prepared at the fixed oil to surfactant ratio of 1/9 were studied for skin permeation. The results are summarized in Table 3-4, and illustrated in Figures 3-7, 3-8, and 3-9. PG is a known formulation vehicle to offer drug permeation enhancement and was used as the control formulation. For both lipophilic and hydrophilic drugs, microemulsions showed significantly higher or comparable permeation compared with the PG control formulation, therefore, ME formulations provided significant enhancement effects. Drug steady-state permeation flux, J_s, and cumulative permeation amount, Q_{24h}, increased significantly with water content in microemulsions. Since water content is related directly with microstructures, it can be derived that drug permeation is related to microemulsion microstructures, and at the fixed oil to surfactant ratio, the permeation increases in an order of microstructures as follows: W/O < bi-continuous < O/W.

Table 3-4. Skin steady-state permeation fluxes, J_s (mean ± S.D.) and cumulative permeated amounts, Q_{24h} (mean ± S.D.) of model drugs from microemulsions and the control formulations.

Formulation (Vehicle_Drug_Enhancer)	Water (w/w %)	J_s (μg/cm^2 per h)	ER	Q_{24h} (μg/cm^2)
ME_2/8_Keto [a]	20	1.49 ± 0.12	1.86	27.96 ± 1.79
ME_4/6_Keto [a]	40	2.64 ± 0.69	3.30	50.04 ± 15.81
ME_7/3_Keto [a]	70	7.41 ± 1.46	9.27	139.57 ± 34.39
ME_2/8_Keto_Azone [a]	20	1.06 ± 0.45	1.33	18.78 ± 6.74
ME_4/6_Keto_Azone [a]	40	2.19 ± 0.35	2.74	39.95 ± 8.57
ME_7/3_Keto_Azone [a]	70	7.05 ± 1.97	8.82	121.43 ± 29.32
ME_7/3_Keto_Br-IMSF [a]	70	9.23 ± 2.62	11.55	177.15 ± 53.04
PG_Keto [a]	0	0.80 ± 0.29	1.00	9.82 ± 3.28
ME_2/8_Lido [a]	20	7.50 ± 2.17	2.37	142.83 ± 35.94
ME_4/6_Lido [a]	40	9.66 ± 2.36	3.06	194.30 ± 53.94
ME_7/3_Lido [a]	70	26.28 ± 5.66	8.32	505.91 ± 111.87
ME_2/8_Lido_Azone [a]	20	5.98 ± 1.75	1.89	125.22 ± 41.26
ME_4/6_Lido_Azone [a]	40	12.95 ± 1.57	4.10	255.16 ± 26.14
ME_4/6_Lido_Br-IMSF [a]	40	11.23 ± 2.95	3.55	238.18 ± 46.69
ME_7/3_Lido_Azone [a]	70	29.78 ± 4.28	9.42	579.30 ± 88.87
PG_Lido [a]	0	3.16 ± 0.18	1.00	47.78 ± 3.25
ME_2/8_Caff [a]	20	5.44 ± 0.33	1.97	102.07 ± 5.75
ME_4/6_Caff [a]	40	8.86 ± 1.95	3.21	166.63 ± 35.70
ME_7/3_Caff [a]	70	11.63 ± 0.72	4.21	237.79 ± 25.49
ME_2/8_Caff_Azone [a]	20	5.11 ± 1.11	1.85	91.79 ± 16.86
ME_7/3_Caff_Azone [a]	70	10.82 ± 0.76	3.92	204.50 ± 6.86
ME_7/3_Caff_Br-IMSF [a]	70	10.16 ± 0.64	3.68	199.72 ± 7.36
PG_Caff [a]	0	2.76 ± 1.46	1.00	56.32 ± 31.54

Note: Ketoprofen (Keto), Lidocaine (Lido) and Caffeine (Caff) LogP: 3.2, 2.1, & –0.5
For each tested formulation, n = 3 – 5
ER: Enhancement Ratio for drug permeation = J_s in Microemulsion / J_s in PG
[a] Significant difference observed among ME formulations with different water content and the control formulation, $P<0.05$

Figure 3-7 and Table 3-4 showed that ketoprofen permeation fluxes from ME formulations increased significantly ($P<0.05$) with increased water content. Compared with the control, enhancement ratio, ER values were 1.86, 3.30, and 9.27 for ME water content of 20%, 40%, and 70%, corresponding to ME microstructure of W/O,

bicontinuous, and O/W, respectively. The permeation enhancer, Azone incorporated ME formulations (2% w/w load) did not increase the permeation further; While the permeation enhancer, Br-IMSF incorporated ME formulation, ME_7/3_keto_Br-IMSF (2% w/w load) showed to increase J_s further by about 25% compared with the ME formulation without the enhancer ($P < 0.05$), however, the difference was not statistically significant.

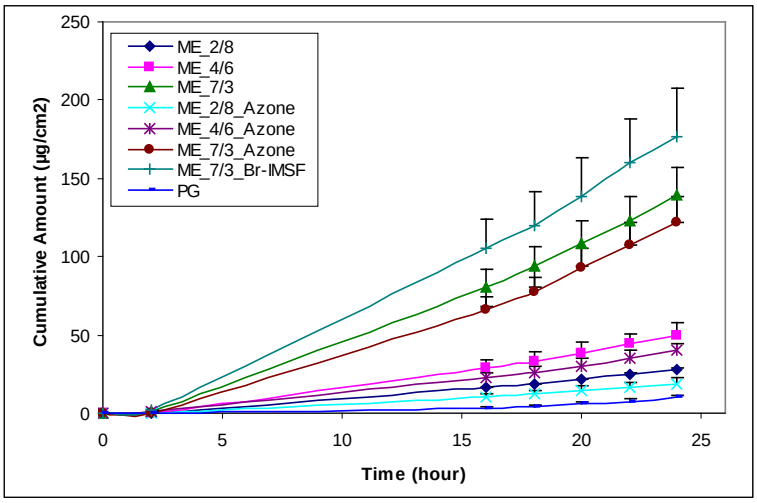

Figure 3-7. Ketoprofen cumulative permeation amount vs. time curves of microemulsions and the control formulation.

Figure 3-8 and Table 3-4 showed lidocaine skin permeation from ME and the control formulations. The results are similar to ketoprofen. For permeation enhancers incorporated ME formulations, at water content of 70%, Azone containing ME provided 13% higher J_s compared to the ME without Azone. At water content of 40%, Azone or Br-IMSF containing MEs resulted in J_s further increases of 16% and 34%, respectively.

However, the differences observed between MEs with and without enhancers were not statistically significant ($P > 0.05$).

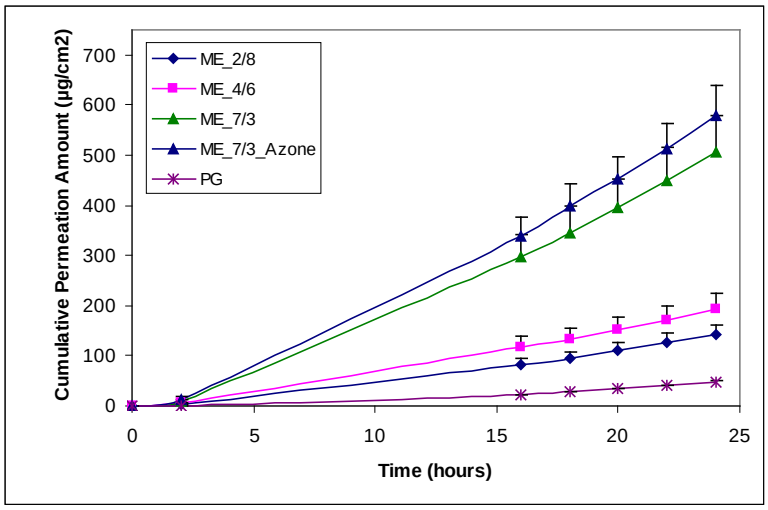

Figure 3-8. Lidocaine cumulative permeation amount vs. time curves of microemulsions and the control formulation.

Figure 3-9 and Table 3-4 showed the permeation of hydrophilic caffeine also increased with water content significantly ($P<0.05$); At water content of 70%, ME formulations with enhancers, Azone or Br-IMSF incorporated resulted in slightly lower but not statistically significant different permeation than MEs without enhancers.

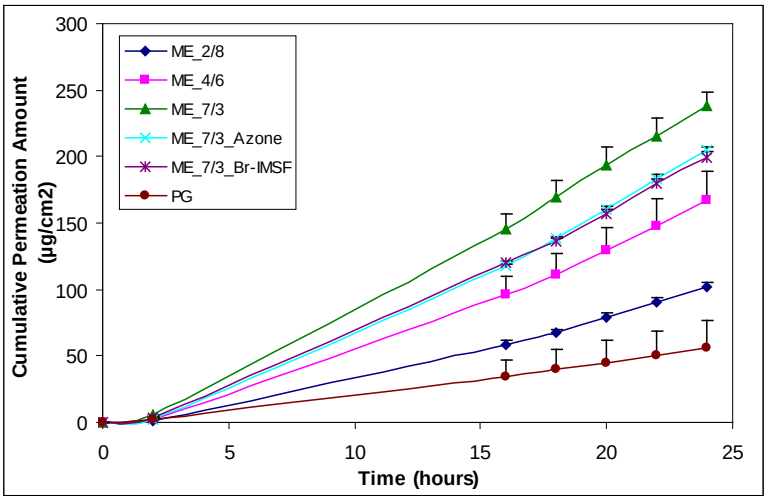

Figure 3-9. Caffeine cumulative permeation amount vs. time curves of microemulsions and the control formulation

Figure 3-10 show ER vs. water content plot for all three model drugs. As water content increased, for lipophilic drug ketoprofen and lidocaine, ER increased in a more pronounced manner, and followed an exponential growth trend, while for hydrophilic caffeine, ER appeared to increase linearly.

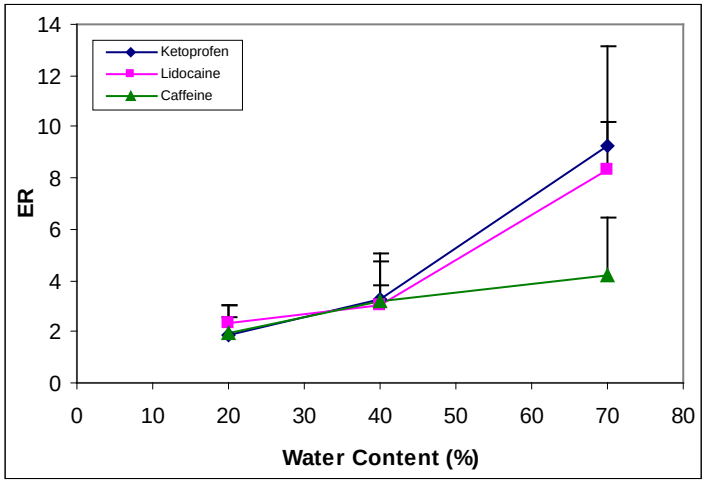

Figure 3-10. Enhancement Ratio, ER from microemulsion formulations vs water content plots for three model drugs, ketoprofen, lidocaine and caffeine (data showing ER + S.D.)

Further ketoprofen permeation experiments were conducted using ME formulations at oil to surfactant ratios of 1/9 and 2/8, and micelle formulations without oil, to investigate the influence of oil content on skin permeation. The results are illustrated in Table 3-5 and Figure 3-11. At the same water content of 50%, ketoprofen permeation J_s increased significantly ($P<0.05$) as oil content increased from 0% to 10%. The results suggest that at the same water content, ketoprofen permeation increases with oil content in the formulation, and micellar formulation (contains no oil) provides the lowest permeation flux. Figure 3-11(A) shows ER values from ME formulations with oil to surfactant ratio of 2/8 are higher than those from ME formulations with oil to surfactant ratio of 1/9 when compared at the same water content, again indicating that increasing oil content will lead to an increase in ketoprofen permeation. Skin permeation results generally bear high variability partly due to skin sample variation among individual animal donors, the ER comparisons based on data from skin of different animals provide a normalized evaluation of the drug permeation and decreased variability from permeation flux data of different animal donors to certain extend.

Figure 3-11(B) shows non-linear exponential fitting of ER vs. water content curves of ME formulations with oil to surfactant ratio of 1/9 and 2/8. Good correlation coefficients (R^2) were obtained, 0.9886 and 0.9968 for MEs of O/S 1/9 and 2/8, respectively. The results demonstrate that the ER of ketoprofen correlates with and appears to increase with water content in an exponential fashion.

Table 3-5. Ketoprofen permeation steady-state flux, J_s (mean ± S.D.) and cumulative permeation amount, Q_{24h} (mean ± S.D.) from microemulsion and micelle formulations.

Formulation (Vehicle_Drug)	Water (w/w %)	O/S	J_s (μg/cm^2 per h)	ER	Q_{24h} (μg/cm^2)
ME_5/5_Keto [a, b, c]	50	1/9	5.29 ± 0.30	7.25	109.84 ± 8.43
ME_5/5_O_Keto [a, b, c]	50	2/8	7.67 ± 1.55	10.51	152.22 ± 37.28
ME_7/3_Keto [a, b, c]	70	1/9	9.92 ± 2.25	13.59	190.37 ± 45.80
ME_8/2_Keto [a, c]	80	1/9	12.92 ± 2.03	17.70	261.60 ± 47.07
Micelle_5/5_Keto [a, b, c]	50	0/10	1.21 ± 0.36	1.66	27.08 ± 6.31
Micelle_7/3_Keto [a, b, c]	70	0/10	3.95 ± 0.96	5.41	69.18 ± 44.82
PG_Keto [a, c]	0	NA	0.73 ± 0.16	1.00	9.07 ± 2.43
ME_2/8_O_Keto [a, d]	20	2/8	0.34 ± 0.05	2.13	5.35 ± 0.30
ME_3/7_O_Keto [a, d]	30	2/8	0.59 ± 0.24	3.69	10.37 ± 4.44
ME_4/6_O_Keto [a, d]	40	2/8	0.88 ± 0.12	5.50	14.67 ± 2.24
ME_5/5_O_Keto [a, d]	50	2/8	1.59 ± 0.41	9.94	25.08 ± 6.78
PG_Keto [a, d]	0	NA	0.16 ± 0.17	1.00	1.95 ± 2.20

Note: NA = "Not Applicable"

For each tested formulation, n = 3-5

O/S : oil to surfactant (and co-surfactant) ratio

[a] Significant difference observed among ME formulations with different water content and the control formulation, $P<0.05$

[b] Significant difference observed among ME and micelle formulations with different oil content, $P<0.05$

[c d] Permeation experiments were conducted using porcine skins from different animals.

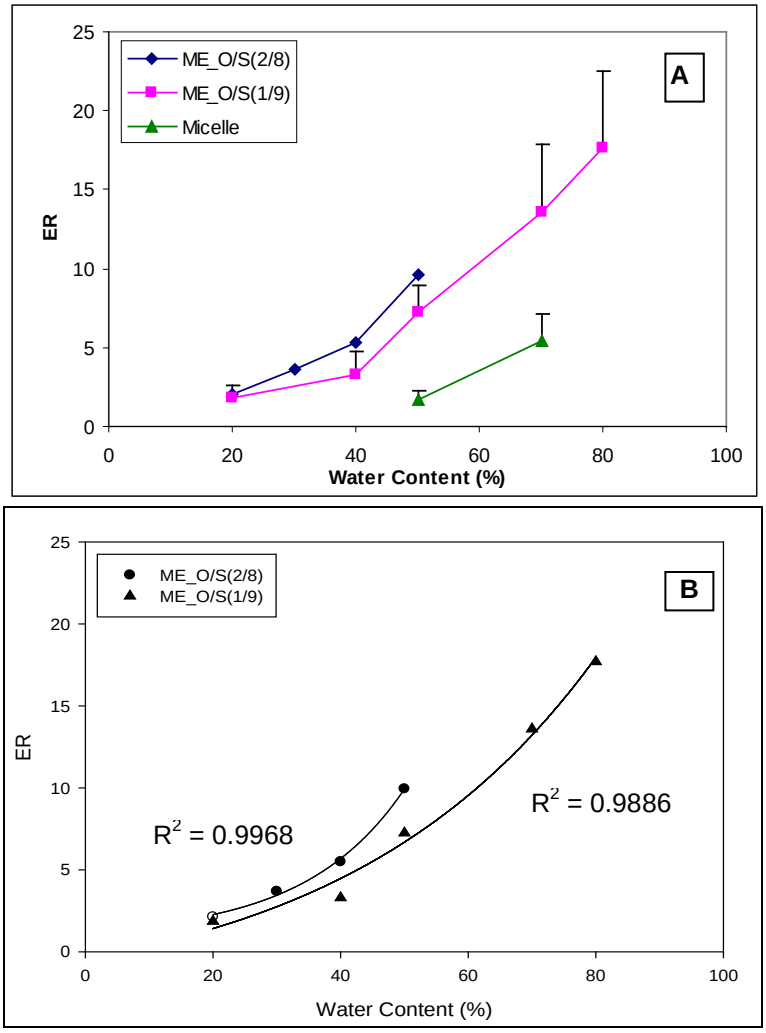

Figure 3-11. (A) ER vs. water content plots for ketoprofen ME and micelle formulations, and (B) Non-linear exponential fitting to ER vs. water content curves.

Additional ketoprofen permeation experiments were conducted using microemulsions with different oils in formulations in order to investigate oil component effects on drug permeation. The results are tabulated in Table 3-6 and illustrated in Figure 3-12. At the same water content of 50%, ketoprofen permeation flux was significantly higher ($P<0.05$) when oil (IPM) content increased from 5% to 10%, this was a reproducible result compared with the same experiment in Table 3-5, although permeation flux data varied due to differences in porcine skin from different animals.

Permeation fluxes also affected for different oils but at the same concentration in formulations. In an increasing order of ketoprofen permeation flux, oils can be ranked as follow: Miglyol 812 < Miglyol 840 < oleic acid < IPM. These results suggest that different oils used in ME formulations will have some effect on the drug permeation. However, the permeation J_s did not show a correlation with the drug solubility in these oils (Table 3-2).

Table 3-6. Ketoprofen permeation steady-state flux, J_s (mean ± S.D.) and cumulative permeation amount, Q_{24h} (mean ± S.D.) from microemulsion formulations containing different oil components.

Formulation (Vehicle_Oil-%Content)	Water (w/w %)	Oil Name	Oil (w/w %)	J_s (μg/cm^2 per h)	Q_{24h} (μg/cm^2)
ME_5/5_IPM_5% [a]	50	IPM	5	2.89 ± 0.56	53.17 ± 10.76
ME_5/5_IPM_10% [a]	50	IPM	10	3.97 ± 0.14	76.01 ± 7.32
ME_5/5_OA_5% [a]	50	OA	5	2.34 ± 0.96	43.82 ± 15.91
ME_5/5_ML812_5% [a]	50	ML840	5	1.57 ± 0.45	30.05 ± 8.64
ME_5/5_ML840_5% [a]	50	ML812	5	1.96 ± 0.63	35.37 ± 10.36

Note: OA=Oleic Acid; ML840=Miglyol 840; ML812=Miglyol812;
For various formulations, n = 3 – 4;
[a] Significant difference observed among ME formulations with different oils or oil contents, $P<0.05$

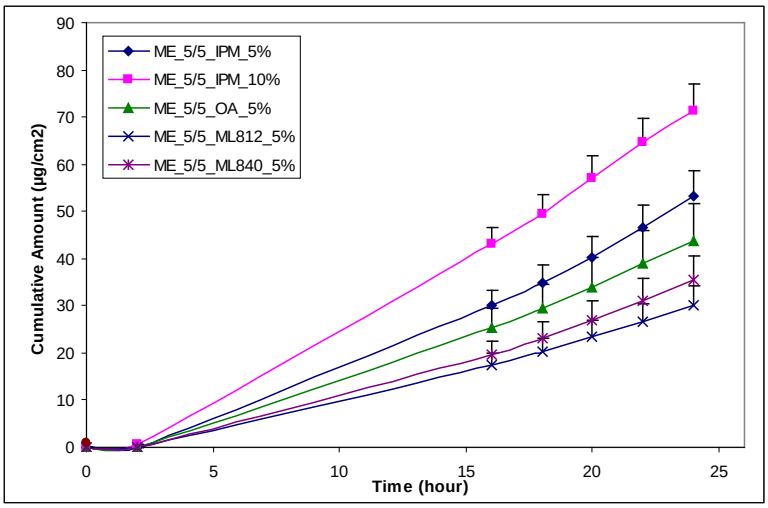

Figure 3-12. Ketoprofen cumulative permeation amount vs. time curves of microemulsion formulations with different oils.

3.4. Discussion

Refraction index (RI) of MEs vs. water content plot showed a good linear correlation (R^2 = 0.9996). The linear relationship between RI and water content reflects the optically isotropic characteristic of ME, which had not been reported before to our knowledge. The linear range of RI vs. water content of MEs can be used to verify the range of ME along the certain water dilution line, and also possibly for ME sample stability monitoring.

Electrical conductivity measurement is the most commonly used method for ME microstructure characterizations. In most previous studies (Djordjevic et al., 2004; Podlogar et al. 2004 and 2005; Lopes et al., 2010;), EC tests were conducted for assessing the phase change of ME samples by gradual dilution using pure water as the aqueous phase. However, this method was often not obvious and effective to determine

microstructure changes in many cases of ME systems with non-ionic surfactants, because of low EC value and no clear inflection points to follow. In this study, a low concentration NaCl salt (0.9% w/v) solution was used as the aqueous phase for the dilution. The resulting EC vs. water content curve showed the three distinct parts, which could be fitted by linear regressions at low and high aqueous phase regions, corresponding to w/o and o/w microstructures. Using this approach, microstructure transition points can be estimated easily and directly. For ME systems using non-ionic surfactants, a low concentration salt solution employed for the dilution was found not to change the ME phase behavior significantly. This observation was consistent with the previous reports (Chaiyana et al., 2010)

The CV method to test ME microstructure has only few reports (Mo et al. 2000, 2007) in the area of electro-chemical study, and has not been applied to ME formulations related to drug delivery. In this study, the results showed that the CV method was an effective approach for deriving microstructure information for ME formulations of drug delivery, and provides complemented results to those from other methods.

A progress has been made in this study when using the DSC technique for ME microstructure characterization. In the previously published studies (Podlogar et al., 2004 and 2005; Boonme et al., 2006; Liu et al., 2009), DSC had been used for the same purpose, but the unique phenomena that led to the ME phase information was not clearly identified. In this study, the following characteristics of the cooling thermo-gram of ME samples were discovered when DSC was conducted at suitable running parameters: (1) the ME sample of w/o structure showed the freezing peak of oil or/and surfactants, but no water freezing peak; (2) the ME sample of bicontinuous structure showed both freezing

peaks of water and oil; (3) the ME sample of o/w structure showed only one large freezing peak of water, but no oil freezing peak. We probably can explain the phenomena by visualizing interactions at a molecular level between different phases. In w/o MEs, water was dispersed molecularly and bound tightly with surfactants, it could not be frozen, so no water freezing peak was observed. As water content increased in bicontinuous MEs, there free water started to be present causing water droplet significant elongation and furthermore the formation of water cylinder or channel structures, therefore, the freezing peak of free bulk water was observed. In o/w MEs, it was either because oil molecules disperse and interact strongly with surfactants and could not be frozen or because water and oil freezing peaks overlaid due to the water peak moving to higher temperature, only one large water freezing peak was observed. Therefore, DSC cooling thermograms reveals direct information of molecular interactions of ME phase components and of microstructures.

Based on these characteristics in cooling thermograms, the microstructure of a ME sample can be determined by a single DSC run. The microstructure transition point can be accurately measured by running a few samples with gradually incremented water content in the transition region. The microstructure results obtained by this DSC approach were consistent with results from EC and CV methods, and thus verified this DSC technique works, at least for the current non-ionic surfactant ME system. Further studies are being conducted using the method for more complex ME sample testing and for other ME systems.

Drug permeation increase with water content of ME systems has been reported by Sintov et al, 2004. However, in the previous study, the ME system could only solubilize

up to 30% water, which prevented the author to draw conclusions regarding drug permeation relationship to different microstructures, which only exist and evolve in a wide range of water content. In this study, because the ME system could solubilize very high percentage of water and along the water dilution line of O/S 1/9 microstructure transitions were fully characterized, we were able to demonstrate that drug permeation correlated with water content and thus with microstructures. Additionally, it was found that lipophilic drug permeation increases with water content in a more pronounced manner that appeared to follow an exponential pattern, while hydrophilic drug permeation increased linearly.

Podlogar's group (2005) studied ketoprofen release from MEs of different water contents, and showed the release rate J_s increased with water content and attributed the phenomena to increased ketoprofen diffusion inside formulations with higher water content. However, over the same range of water content change, the extent of increase of ketoprofen release rate was much less than that of increase of ketoprofen transdermal permeation flux observed in the current study. Therefore, ketoprofen diffusion maybe part of, but not all the cause for the observed transdermal permeation enhancement. For lipophilic drug ketoprofen and lidocaine, the relationship of permeation enhancement with water content can still be explained by the mechanism of increasing drug thermodynamic activity in MEs that have high water content.

Water content and oil content were identified to be two principal factors that affect drug transdermal permeation potential in this study. That is to say increasing water content, or oil content at the fixed water content, or both will lead to the increase of drug permeation. By reviewing literature on microemulsions for transdermal drug delivery, it

was found that most previously reported results are consistent with the two principal factors. Some of the drugs in these reports include both lipophilic and hydrophilic ones: lidocaine, prilocaine hydrochloride, vinpocetine, cyclosporin A, tolterodine, testosterone, ketoprofen, ibuprofen, indomethacin, buspirone hydrochloride, theophylline, lacidipine, capsaicin derivative, and triptolide (Kreilgaard et al., 2000; Sintov et al., 2004; Hua et al., 2004; Liu et al., 2009; Elshafeey et al., 2009; Hathout et al., 2010; Rhee et al., 2001; Chen et al., 2006; Maghraby, 2010; Tsai et al., 2010; Zhao et al., 2006; Gannu et al., 2010; Huang et al., 2008; Chen et al. 2004). Based on observations in the current study and literature reports, we can propose an optimal ME formulation region concept in pseudo-ternary phase diagram. Figure 3-13 illustrated the concept which showing different ME regions in the pseudo-ternary phase diagram. The ME formulation composition of high transdermal drug permeation potential should fall into the regions of high water content (Region W), or the region of balanced water and oil content but low surfactant content (Region I). It is interesting to note that in the literature reports, most of the optimal ME formulations were indeed from Region W, and some of the optimal ME formulations were from Region I (Rhee et al., 2001; Chen et al., 2004; Liu et al., 2009).

There are some reports that are not consistent with our proposed ME optimal concept of high water content, balanced oil content and low surfactant content. These reports (Baroli et al., 2000; Peltola et al., 2003; Yuan et al., 2006; Zhu et al., 2008) had the optimal ME formulations containing relatively high surfactant mixture contents. In all these cases, the ME systems under investigations used short chain alcohol such as ethanol as the co-surfactant. Because ethanol is a well-known permeation enhancer itself (Gao and Singh, 1998), higher surfactant mixture content increased the ME formulation permeation

potential. Therefore, we can view the ME systems using ethanol as co-surfactant are exceptional to the above proposed optimal ME formulation region concept.

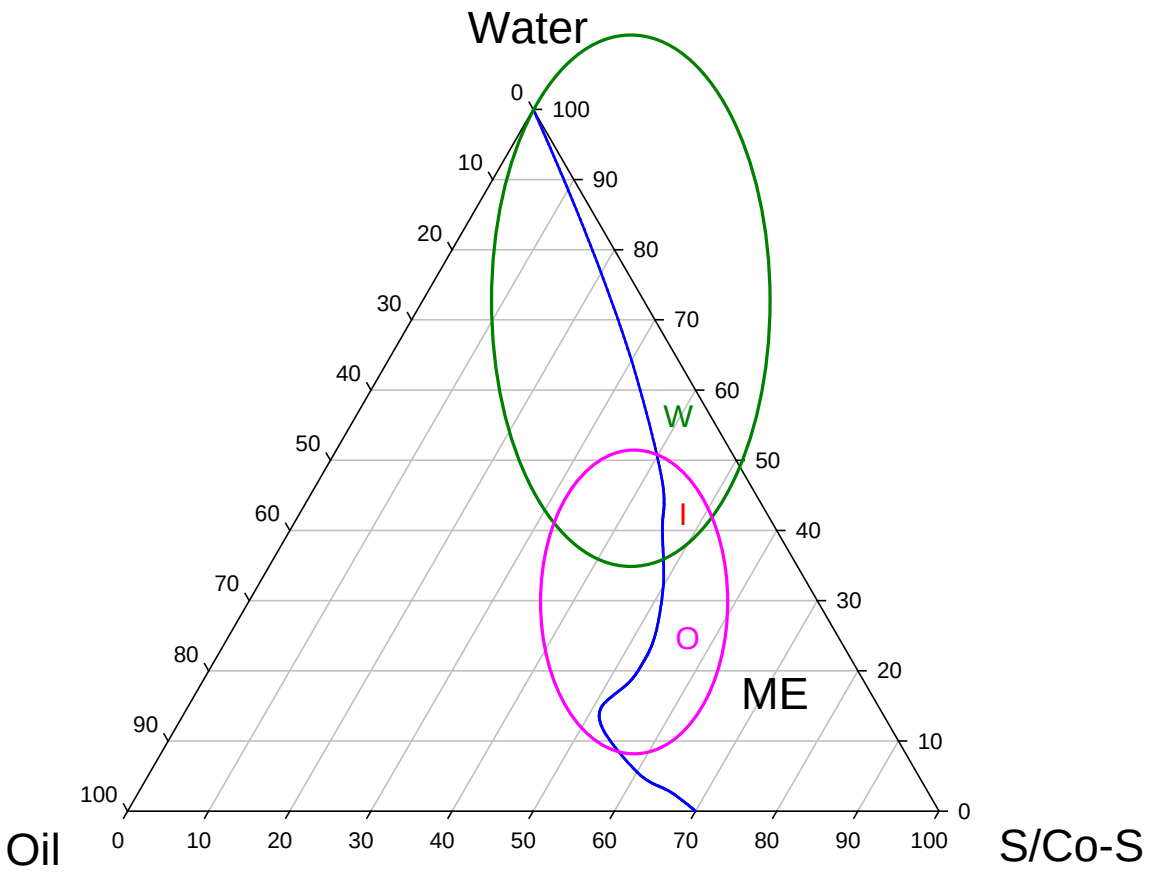

Figure 3-13. Microemulsion pseudo-ternary phase diagram with labeled regions of high water content, W (in green), high oil content, O (in purple), and balanced water and oil content, I (in purple)

Although we report water content and oil content are the two key factors affecting drug transdermal permeation enhancement, which are the focus of this study, there are other factors that also play a role in controlling drug permeation, for example, the surfactant to co-surfactant (S/Co-S) ratio (Kreilgaard et al., 2000; Sintov et al., 2004; Hua et al., 2004; Rhee et al., 2001; Maghraby, 2008; Huang et al., 2008). In ME formulation

development, it is necessary to optimize S/Co-S ratio, which were showed to be unique for the different ME systems. Additionally, it was showed that different oils used in ME will have some effect on drug transdermal permeation in the study which had IPM, oleic acid, Miglyol 812, and Miglyol 840 being tested.

3.5. Conclusions

Microemulsion formulations showed significant transdermal permeation enhancement effect for lipophilic and hydrophilic model drugs, ketoprofen, lidocaine, and caffeine. The two key factors that strongly influenced drug transdermal permeation potential from ME formulations were water content and oil content. Drug permeation increased with water content, for hydrophobic drugs, permeation appeared to increase in an exponential manner while for hydrophilic drugs, permeation appeared to increase linearly. Transdermal drug delivery potential is also related to ME microstructures, along a given water dilution line, in an increasing order of drug permeation it was identified: W/O < bicontinuous < O/W. At the same water content, increasing oil content will lead to higher drug permeation. The above observations provide practical guidance to ME transdermal formulation development. ME formulations with permeation enhancer, Azone or Bromo-imnosulfurane incorporated in general did show significant further permeation enhancement effect. Additionally, different oil components used in microemulsions were shown to have some influence on drug permeation. Characterizations of ME microstructure is important for gaining insight into permeation enhancement mechanisms and for developing ME formulations. This was achieved by successful utilization of a combination of testing techniques, e.g. DSC, CV, EC and DLS.

The DSC technique was further developed in the study, which allowed an easy and accurate determination of ME microstructures.

3.6. References

Alany, R.G., Tucker, I.G., Davies, N.M., Rades, T., 2001. Characterizing colloidal structures of pseudoternary phase diagrams formed by oil/water/amphiphile systems. Drug Dev. Industrial Pharmacy 27(1), 31-38.

Azeem, A., Khan, Z.I., Aqil, M., Ahmad, F.J., Khar, R.K., Talegaonkar, S., 2009. Microemulsion as a surrogate carrier for dermal drug delivery. Drug Dev. Industrial Pharmacy 35, 525-547.

Baroli, B., Lopez-Quintela, M.A., Delgado-Charro, M.B., Fadda, A.M., Blanco-Mendez, J., 2000. Microemulsion for topic delivery of 8-methoxsalen. J. Control. Rel. 69, 209-218.

Boelsma, E., Tanojo, H., Bodde, H.E., Ponec, M., 1996. Assessment of the potential irritancy of oleic acid on human skin: Evaluation in vitro and in vivo. Toxicol. In Vitro 10, 729-742.

Boonme, P., Krauel, K., Graf, A., Rades, T., Junyaprascert, V.B., 2006. Characterization of Microemulsion Structures in the Pseudoternary Phase Diagram of Isopropyl Palmitate/Water/Brij 97:1-Butanol. AAPS PharmSciTech 7(2), E1-E6.

Chaiyana, W., Saeio, K., Hennink, W.E., Okonogi, S., 2010. Characterization of potent anticholinesterase plant oil based microemulsion. Inter. J. Pharm. 401, 32-40.

Chen, H., Chang, X., Weng, T., Zhao, X., Gao, Z., Yang, Y., Xu, H., Yang, X., 2004. A study of microemulsion systems for transdermal delivery of triptolide. J. Control. Rel. 98, 427-436.

Chen, H., Chang, X., Du, D., Li, J., Xu, H., Yang, X. 2006. Microemulsion-based hydrogel formulation of ibuprofen for topical delivery. Inter. J. Pharm. 315, 52-58.

Djordjevic, L., Primorac, M., Stupar, M., Krajisnik, D., 2004. Characterization of caprylocaproyl macrogoglycerides based microemulsion drug delivery vehicles for an amphiphilic drug. Inter. J. Pharm. 271, 11-19.

Djordjevic, L., Primorac, M., Stupar, M., 2005. In vitro release of diclofenac diethylamine from caprylocaproyl macrogoglycerides based microemulsions. Inter. J. Pharm. 296, 73-79.

Elshafeey, A.H., Kamel, A.O., Fathallal, M.M., 2009. Utility of nanosized microemulsion for transdermal delivery of tolterodine tartrate: Ex-Vivo permeation and in-Vivo pharmacokinetic studies. Pharm. Res. 11, 2446-2453.

El Maghraby G.M., 2008. Transdermal delivery of hydrocortisone from eucalyptus oil microemulsion: Effects of cosurfactants. Inter. J. Pharm. 355, 285-292.

El Maghraby, G.M., 2010. Self-microemulsifying and microemulsion systems for transdermal delivery of indomethacin: Effect of phase transition. Colloids and Surfaces B: Biointerfaces. 75, 595-600.

Gannu, R., Palem, C.R., Yamsani, V.V., Yamsani, S.K., Yamsani, M.R., 2010. Enhanced bioavailability of lacidipine via microemulsion based transdermal gels: Formulation optimization, ex vivo and in vivo characterization. Inter. J. Pharm. 388, 231-241.

Gao, S., Singh, J., 1998. Effect of oleic acid/ethanol and oleic acid/propylene glycol on the in vitro percutaneous absorption of 5-fluorouracil and tamoxifen and the macroscopic barrier property of porcine epidermis. Int. J. Pharm. 156, 45-55.

Hathout, R.M., Woodman, T.J., Mansour, S., Mortada, N.D., Geneidi, A.S., Guy, R.H., 2010. Eur. J. Pharm. Sci. 40, 188-196.

Heuschkel, S., Goebel, A., Neubert, R.H.H., 2008. Microemulsions—modern colloidal carrier for dermal and transdermal drug delivery. J. Pharm. Sci. 97(2), 603-631.

Hua, L., Weisan, P., Jiayu, L., Ying, Z., 2004. Preparation evaluation, and NMR characterization of vinpocetine microemulsion for transdermal delivery. Drug Dev. Industrial Pharmacy 30(6), 657-666.

Huang, Y.B., Lin, Y.H., Lu, T.M., Wang, R.J., Tsai, Y.H., Wu, P.C., 2008. Transdermal delivery of capsaicin derivative-sodium nonivamide acetate using microemulsions as vehicles. Inter. J. Pharm. 349, 206-211.

Kreilgaard, M., Pedersen, E.J., Jaroszewski, J.W., 2000. NMR characterization and transdermal drug delivery potential of microemulsion systems. J Controlled Release 69, 421-433.

Kreilgaard, M., 2002. Influence of microemulsions on cutaneous drug delivery. Advanced Drug Delivery Reviews 54(suppl. 1), s77-s98.

Liu, H., Wang, Y., Lang, Y., Yao, H., Dong, Y., Li, S., 2009. Bicontinuous cyclosporine A loaded water-AOT/Tween 85-isopropylmyristate microemulsions: structural characterization and dermal pharmacokinetics in vivo. J. Pharm. Sci. 98(3), 1167-1176.

Lopes, L.B., Vandewall, H., Li, H.T., Venugopal, V., Li, H.K., Naydin, S., Hosmer, J., Levendusky, M., Zheng, H., Bentley, M.V.L.B., Levin, R., Hass, M.A., 2010. Topical delivery of lycopene using microemulsions: enhanced skin penetration and tissue antioxidant activity. J. Pharm. Sci. 99(3), 1346-1357.

Mo, C., Zhong, M., Zhong, Q., 2000. Investigation of structure and structural transition in microemulsion systems of sodium dodecyl sulfonate + n-heptane + n-butanol + water by cyclic voltammetric and electrical conductivity measurements. J. Electroanalytical Chem. 493, 100-107.

Mo, C., Li, X., 2007. Microstructure and structural transition in coconut oil microemulsion using semidifferential electroanalysis. J. Colloid and Interface Sci. 312, 355-362.

Mou, D., Chen, H., Du, D., Mao, C., Wan, J., Xu, H., Yang, X., 2008. Hydrogel-thickened nanoemulsion system for topical delivery of lipophilic drugs. Inter. J. Pharm. 353, 270-276.

Neubert, R.H.H., 2011. Potential of new nacocarriers for dermal and transdermal drug delivery. Eur. J. Pharm. Biopharm. 77, 1-2.

Peltola, S., Saarinen-Savolainen, P., Kiesvaara, J., Suhonen, T.M., Urtti, A., 2003. Microemulsions for topical delivery of estradiol. Inter. J. Pharm. 254, 99-107.

Podlogar, F., Gasperlin, M., Tomsic, M., Jamnik, A., Rogac, M.B., 2004. Structural characterization of water-Tween 40 / Imwiter 308 – isopropyl myristate microemulsions using different experimental methods. Inter. J. Pharm. 276, 115-128.

Podlogar, F., Rogac, M.B., Gasperlin, M., 2005. The effect of internal structure of selected water-Tween 40 – Imwitor 308 – IPM microemulsions on ketoprofen release. Inter. J. Pharm. 302, 68-77.

Rhee, Y.S., Choi, J.G., Park, E.S., Chi, S.C., 2001. Transdermal delivery of ketoprofen using microemulsions. Inter. J. Pharm. 228, 161-170.

Sintov, A.C., Shapiro, L., 2004. New microemulsion vehicle facilitates percutaneous penetration in vitro and cutaneous drug bioavailability in vivo. J. Control. Release 95, 173-183.

Sintov, A.C., Botner, S., 2006. Transdermal drug delivery using microemulsion and aqueous systems: Influence of skin storage conditions on the in vitro permeability of diclofenac from aqueous vehicle systems. Inter. J. Pharm. 311, 55-62.

Sintov, A.C., Brandys-Sitton, R., 2006. Facilitated skin penetration of lidocaine: combination of a short-term iontophoresis and microemulsion formulation. Inter. J. Pharm. 316, 58-67.

Song, Y., Xiao, C., Mendelsohn, R., Zheng, T., Strekowski, L., Michniak, B., 2005. Investigation of iminosulfuranes as novel transdermal penetration enhancers: enhancement activity and cytotoxicity. Pharm. Res. 22(11), 1918-1925.

Tsai, Y.H., Chang, J.T., Chang, J.S., Huang, C.T., Huang, Y.B., Wu, P.C., 2011. The effect of component of microemulsions on transdermal delivery of buspirone hydrochloride. J. Pharm. Sci. 100, 2358-2365.

Yuan, Y., Li, S., Mo, F., Zhong, D., 2006. Investigation of microemulsion system for transdermal delivery of meloxicam. Inter. J. Pharm. 321, 117-123.

Zhao, X., Liu, J.P., Zhang, X., Li, Y., 2006. Enhancement of transdermal delivery of theophylline using microemulsion. Inter. J. Pharm. 327, 58-64.

Zhu, W., Yu, A., Wang, W., Dong, R., Wu, J., Zhai, G., 2008. Formulation design of microemulsion for dermal delivery of penciclovir. Inter. J. Pharm. 360, 184-190.

Chapter 4 . INVESTIGATION OF DSC APPROACH FOR CHARACTERIZATION OF MICROEMULSION FORMULATION MICROSTRUCTURES

4.1. Introduction

Microemulsions are optically transparent and isotropic dispersions composed of oil, surfactants and water. The formulations using ME as vehicles have been widely studied for transdermal and topical drug delivery (Heuschkel et al., 2008; Azeem et al., 2009; Sintov et al., 2004; Kreilgaard et al., 2002; Hua et al., 2004). ME formulations offer several advantages: high drug solubilizing capacity, long term vehicle stability due to their thermodynamic stability, ease of preparation, and capability to enhance skin permeation for both hydrophobic and hydrophilic drugs (Heuschkel et al., 2008).

Microemulsions exist in various microstructures including droplet-like and bicontinuous types. Since their drug delivery properties are related to the inner structure, there is a need to assign the correct microstructure to the formulation. An appropriate characterization of ME microstructures is challenging due to the small particle sizes and interface fluctuations (Heuschkel et al., 2008). A combination of different characterization techniques is required. Typically, the techniques used for microstructure examination in transdermal formulation studies include measurement of viscosity (Sintov et al., 2004; Djordjevic et al., 2004), surface tension (Dong et al., 2011; Podlogar et al., 2005), electrical conductivity (Alany et al., 2001; Djordjevic et al., 2005; Sintov et al., 2004; Mo et al., 2007), DSC (Podlogar et al., 2004, 2005; Liu et al., 2009; Lopes et al., 2010), and freeze-fracture transmission electron microscopy (FF-TEM) (Kuntsche et al.,

2011; Alany et al, 2001; Dong et al., 2011), small angle X-ray scattering (SAXS) (Podlogar et al., 2005), and pulsed field gradient nuclear magnetic resonance (PFG-NMR) (Kreilgaard et al., 2000; Hua et al., 2004).

FF-TEM is currently the most direct and unambiguous method to examine the microstructures of ME formulations, but the method is a complicated one that requires expensive equipment, elaborate sample preparation and careful effort to discriminate true structural features from artifacts (Alany et al. 2001). Most other methods above are indirect methods that monitor one of the corresponding physico-chemical parameters with the change of the ME composition to deduce microstructure information. Large numbers of tests are required, and it is necessary to use several testing techniques in combination, however, the results are often not clear for the determinations of microstructures and the phase transition points. Therefore, there is a need for a simple and effective method to analyze ME formulation microstructures. A DSC method has been developed and used in our lab for this purpose, and some initial results were reported (Zhang and Michniak-Kohn, 2011). The current study tries to validate the DSC method further by analyzing more ME systems with known microstructure information, and also to investigate DSC experimental parameter effects of the sample size, the cooling rate, and the initial isothermal temperature in order to optimize the DSC analytical conditions.

4.2. Materials and Methods

4.2.1. Materials

Isopropyl myristate (IPM) was purchased from Fisher Scientific (Fair Lawn, NJ). Isopropyl palmitate (IPP) and tetraglycol were purchased from Sigma (Rehovot, Israel), Cremophor EL and RH40 were obtained from BASF (Ludwigshafen, Germany). Labrasol was obtained as a free sample from Gattefosse (St. Priest Cedex, France). 1-Butanol was purchased from Alfa Aesar (Ward Hill, MA). Oleic acid, Sorbitan mono-laurate (Span 20), Polyoxyethylene 20 sorbitan mono-oleate (Tween 80), ketoprofen, and caffeine were purchased from Sigma (St. Louis, MO). Glyceryl oleate was obtained from Uniqema (Bromborough Pool, The Wirral, UK). Propylene carbonate was purchased from Aldrich (Sigma-Aldrich Inc., St. Louis, MO). Acetonitrile, methanol, ethanol, and propylene glycol were purchased from Fisher Scientific (Fair Lawn, NJ). Water was distilled water that had been further purified by MilliQ A10 and Elix 10 system.

4.2.2. Summary Literature Results of Three ME Systems

Four ME systems have been selected for the current study based on literature reports, their microstructure information were known and are summarized in Table 4-1. ME System #1 was previously studied in our lab. ME System #2 and #3 were chosen mainly based on available freeze-fracture transmission electron microscopy (FF-TEM) data which provided unambiguous microstructure information. ME System #4 was an opportunity to determine the ruggedness of the DSC method, as the later DSC characterization was conducted by a different laboratory by different analysts, and using a different DCS model .

Table 4-1. Summary of ME systems used in the current study

ME System #	Composition				Characterization Methods	Reference
	Oil	Surfactant	Co-surfactant	Km		
1	IPM	Labrasol	Cremophor EL	4/1	EC, DSC Cyclic voltametry	Zhang & Michniak-Kohn, 2011
2	OA	Cremophor RH40	Ethanol	2/1	FF-TEM, EC, Viscosity, Surface tension, Density	Dong et al., 2011
3a	EO	Tween 80/ Span 20, 3/2	1-butanol	7/3	FF-TEM, EC, Viscosity, Microscopy	Alany et al., 2001
3b	EO	Tween 80/ Span 20, 3/2	None	n/a		

Note: The abbreviations used in the table are listed below: EC=electrical conductivity, FF-TEM=freeze-fracture transmission electron microscopy, DLS=dynamic light scattering, OA=oleic acid, EO=ethyl oleate, Km=surfactant/co-surfactant ratio (w/w).

4.2.3. Further Characterization of ME System #1

4.2.3.1. Pseudo-ternary phase diagram construction

ME System #1 was reported previously (Zhang and Michniak-Kohn, 2011). The phase diagram construction procedure is briefly described as follows: first, the mixture of Surfactant (S) and Co-surfactant (Co-S) at the w/w ratio (K_m) of 4:1 was prepared. Next, the mixture of Oil (O) with S/Co-S was prepared at varying w/w ratios, e.g. 1:9, 2:8, 3:7, etc. Then, one gram of the O/(S/Co-S) mixture of the certain ratio was titrated with water step by step, at each step, the H_2O/O/(S/Co-S) mixture was mixed thoroughly using a vortex mixer, and the sample was checked under light versus a dark background. If the sample was an isotropic and clear solution, it was defined as a microemulsion; if the sample was cloudy or showed the phase separation, it was not a microemulsion. The observation, the corresponding O/(S/Co-S) ratio and the water content were recorded at each step of the titration. The boundary point between the microemulsion and the non-microemulsion was defined as the mid-point between points of clear and cloudy samples.

The microemulsion system pseudo-ternary phase diagram was constructed by labeling the recorded boundary points in a ternary plot.

4.2.3.2. Microemulsion formulation preparation

The calculated amount of the model drug was weighed into a small glass vial, the exact amount of the O/(S/Co-S) mixture was added in, and the compound was dissolved completely by the aid of sonication and vortex mixing. Then, the exact amount of water according to the design of the H_2O/(O/(S/Co-S)) w/w ratio was added in, and mixed well by vortex mixing.

Model drugs, ketoprofen, and caffeine were formulated in ME System #1 vehicles along the water dilution line of oil to surfactant ratio of 1/9 (denoted in the text as DL10) with varied water content in the regions of phase transitions. The drug loads (w/w %) in the formulations were constant at 2.5%, and 1.0% for ketoprofen, and caffeine, respectively. All above described formulations prepared were clear solutions at ambient temperature.

4.2.3.3. Electrical conductivity (EC) tests for ME System #1

The ME microstructures of System #1 were assessed by EC tests. EC values of the sample were measured using an electric conductivity-meter, Oakton ECTestr 11+ (Ockton Instruments, Vernon Hills, IL). The conductivity-meter was calibrated using the standard solution of 1413 µS/cm (Ockton Instruments) before testing. Three grams of the oil-surfactant mixture of O/(S/Co-S) ratio 1/9 was titrated along DL10 at the ambient temperature (25 °C ± 1 °C) by aqueous phase step by step, at each step, 1 mL of the

sample was used for EC measurement at the ambient temperature. The aqueous phase used was 0.9% (w/v) sodium chloride solution. Similarly, the oil-surfactant mixture of O/(S/Co-S) ratio 2/8 was titrated along DL20 by the aqueous phase, and the EC values for the ME samples were recorded.

4.2.4. Differential Scanning Calorimetry (DSC)

Microemulsion microstructures (for systems #1- #3) were evaluated using a TA Q100 DSC instrument (TA Instruments, New Castle, DE). Microemulsion sample (7-10 mg) was weighed accurately in an aluminum hermetic sample pan and sealed with the lid quickly to prevent the sample evaporation. DSC tests for ME samples were run at the following conditions: equilibration at 25 °C, staying isothermal for 2 minute, cooling the sample at the ramp rate of 5 °C/minute to -80 °C (-70 °C in some cases), staying isothermal for 0.5 minute, and heating the sample at the ramp rate of 5 °C/minute to 30 °C. To study the sample size effect, the sample weights were varied from 2 to 12 mg for tests. To study the cooling rate effect, the cooling rates at 1, 3, 5, 8, and 10 °C/minute were tested. To study the initial isothermal temperature effect, the temperature at 37 °C was tested in an attempt to simulate the formulation sample temperature during a transdermal permeation experiment.

4.3. Results

4.3.1. Microemulsion Microstructure Characterizations

4.3.1.1. ME Systems #1 and #3

4.3.1.1.1. Ternary phase diagram

The constructed pseudo ternary phase diagrams are presented in Figure 4-1. The ME region for ME Systems #1 and #4 were identified, in which at the 'high surfactant content' area, a large amount of water can be solubilized without causing phase separation. For example, the oil-surfactant mixture along DL10 in System #1 can be diluted by water to higher than 95% (w/w) water content and the resulting sample still remained as a microemulsion. Therefore, along DL10, it is possible to study the complete course of microemulsion microstructure changes in System #1. Along the dilution line DL20 (System #1), the oil-surfactant mixture can be diluted by water up to 49% (w/w) water content to reach the boundary of the ME region. The microstructure transition points (Figure 4-1 points: A, B, and C) along DL10 and DL20 were determined by DSC and EC methods which are presented in next sections.

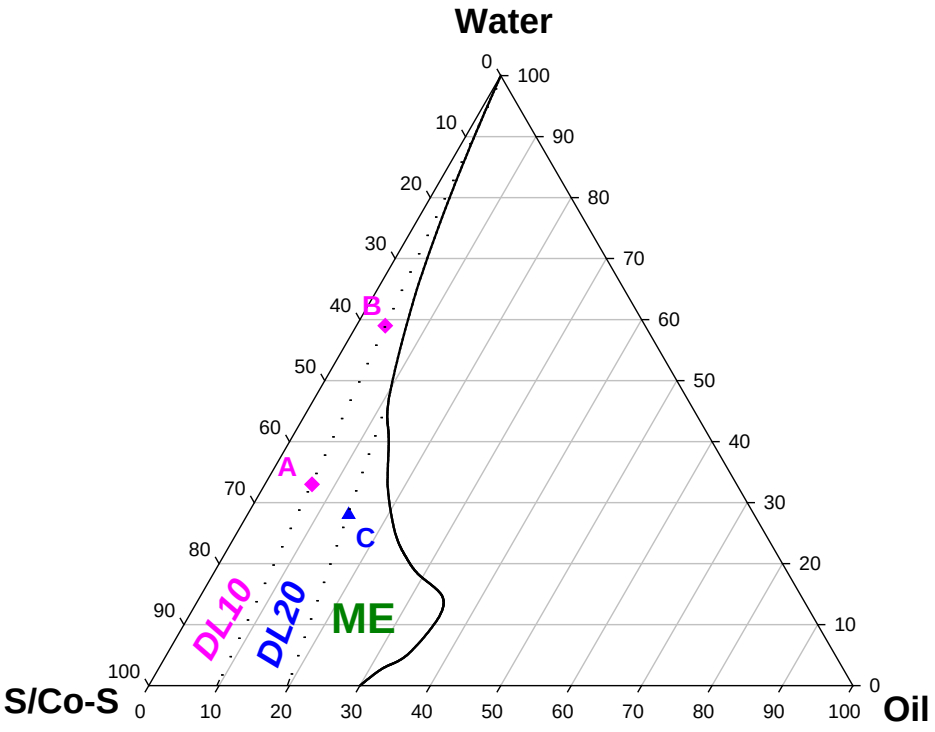

Figure 4-1. Pseudo-ternary phase diagrams of ME System #1

4.3.1.1.2. Electrical conductivity tests

The oil/surfactant mixture of System #1 and #4 was diluted by the aqueous phase, 0.9% (w/v) NaCl, gradually. EC values of ME, κ, were measured in the dilution process and plotted vs. aqueous content Φ_w, as shown in Figure 4-2. The κ vs. Φ_w curve could be divided into three parts: parts at low and high aqueous contents, and the part at median aqueous content. Based on previous studies (Mo et al., 2000; Alany et al., 2001), at low aqueous content, the microstructure was perceivably being as W/O. The electrical conductive entities would be the aqueous droplets that were in isolated state, resulting in the low conductivity at this region, and the κ vs. Φ_w curve in the region could be approximated well by the linear fitting. As the aqueous content Φ_w increases, the W/O droplets increased in number and started to aggregate, when the percolation point, Φ_p was

reached, W/O droplets began to contact each other and formed inter-connected channels, resulting in a drastic increase of κ. Therefore, the turning point from the slow linear increase to a quick non-linear climbing on the curve of κ vs. Φ_w was indicative of Φ_p and corresponded to the transformation from a W/O droplet to a bi-continuous ME; At high aqueous content, the microstructure was O/W and the conductive entity was the continuous aqueous phase. As aqueous content Φ_w further increased, κ of the ME was expected to behave like an aqueous solution, increasing linearly. Again, the turning point from the non-linear increase to the linear climbing on the plot of κ vs. Φ_w between the median and the high aqueous regions was indicative of the microstructure transformation from a bi-continuous to an O/W ME; As shown in Figure 2A for DL10 in System #1, κ vs. Φ_w curves at low and high Φ_w regions indeed could be approximated by linear fittings and yielded good correlation coefficients, respectively. The curve at the median Φ_w region was non-linear and therefore, should correspond to the bi-continuous ME microstructure. Based on the EC results, it could be deduced microstructure transition points from W/O to bi-continuous and from bi-continuous to O/W were at water content of about 33% and 60%, respectively. In contrast, ME samples of System #1 along DL20 were also measured for EC during the dilution process, the obtained κ vs. Φ_w plot (Figure 4-2B) showed to contain two parts, the low aqueous and median aqueous content parts. Similarly, it was deduced that the microstructure transition point from W/O to bi-continuous was at water content of about 27% and no transition from bi-continuous to O/W was visible based on the plot.

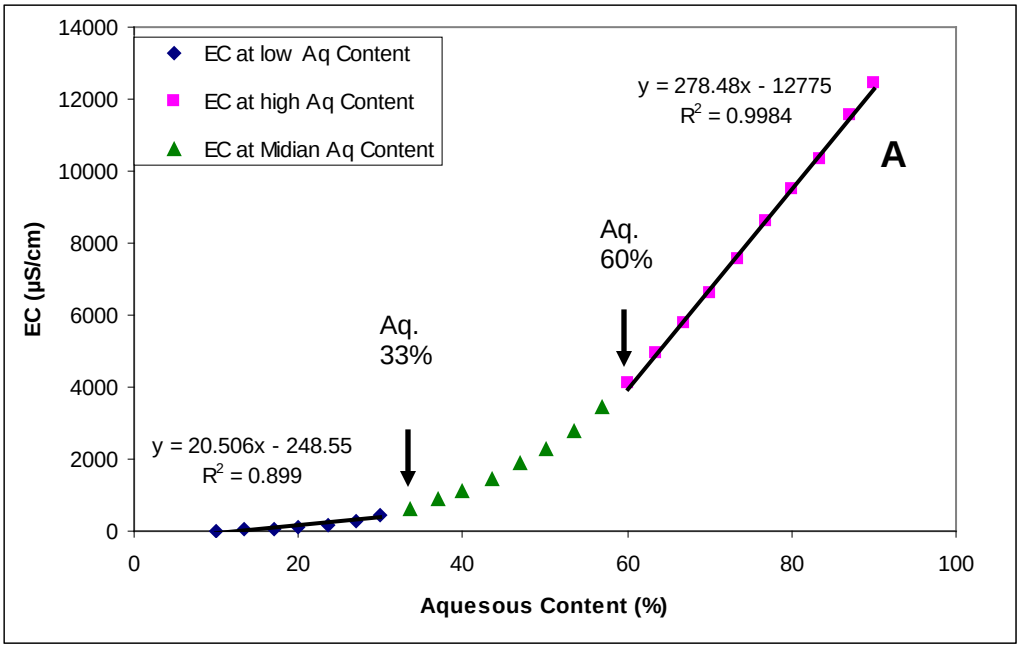

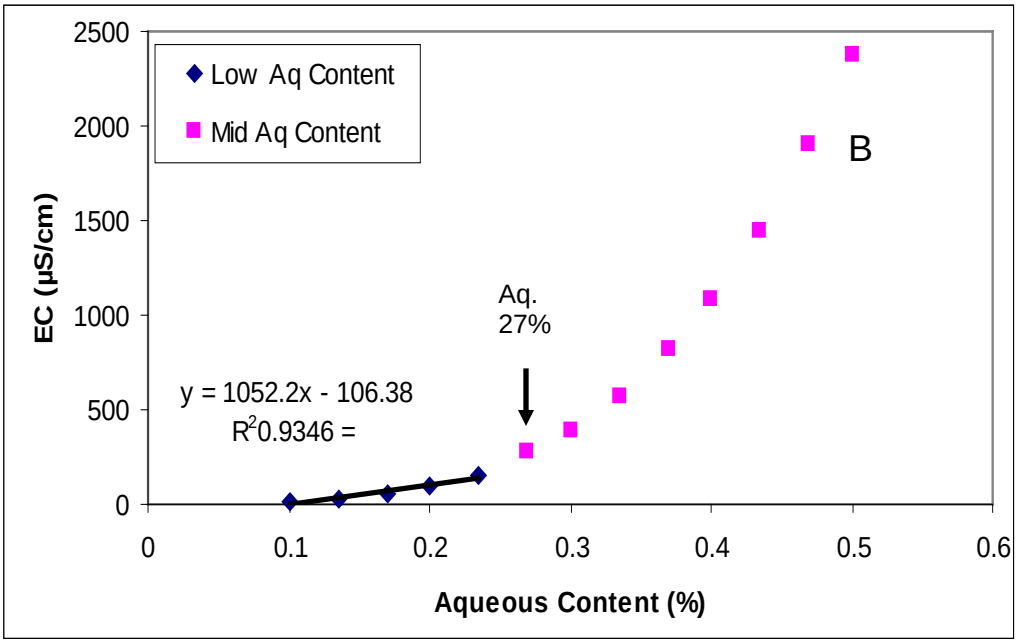

Figure 4-1. Plots of ME electrical conductivity κ vs. aqueous content Φ_w, for ME samples along System #1 DL10 (A), and along DL20 (B)

4.3.1.1.3. DSC characterization of ME System #1

ME samples were tested using DSC with a cooling and heating cycle. After extensive sample studies, it was found that the cooling DSC thermo-gram provided direct information on ME sample microstructures. Specifically, it was discovered that there were some important characteristics of the cooling thermo-gram related to the oil freezing peak and the water freezing peak. They could be described as follows: (1) ME samples of W/O microstructure did not show the water freezing peak, (2) ME samples of bi-continuous microstructure had the oil freezing peak and the water freezing peak as two distinct and separate peaks, and (3) ME samples of O/W microstructure showed only the water freezing peak as one big single peak in the thermo-gram. Based on these unique traits, the microstructure of a ME sample could be determined by a single DSC run. The DSC cooling thermo-grams of ME samples along DL10 and DL20 in microstructure transition regions are illustrated in Figure 4-3A to 4-3D. The microstructure transition points along DL10 were easily determined to be at water content of 33% and 59% for microstructure changes from W/O to bi-continuous and from bi-continuous to O/W, respectively. The microstructure transition point from W/O to bi-continuous along DL20 was determined to be at water content of 28%. These microstructure transition point results were consistent with results obtained earlier by EC measurements.

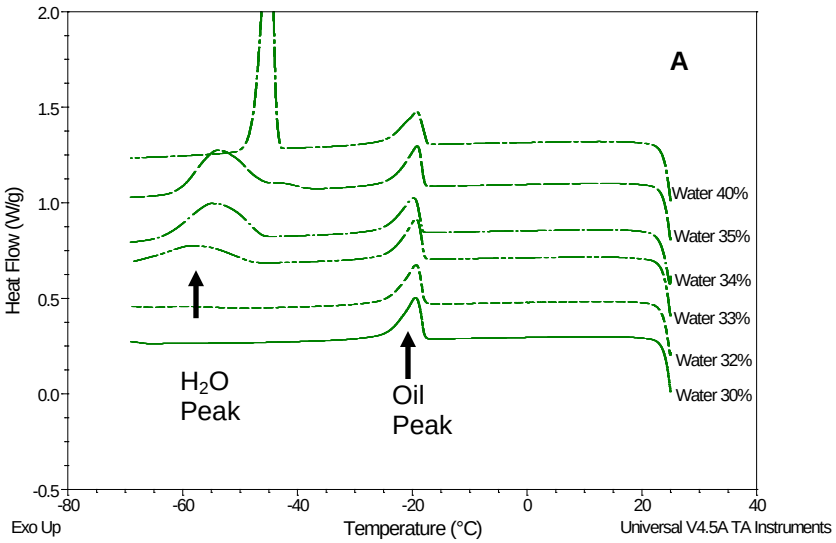
A
Heat Flow (W/g)
2.0
1.5
1.0
0.5
0.0
-0.5
Water 40%
Water 35%
Water 34%
Water 33%
Water 32%
Water 30%
H2O Peak
Oil Peak
-80
-60
-40
-20
0
20
40
Exo Up
Temperature (°C)
Universal V4.5A TA Instruments

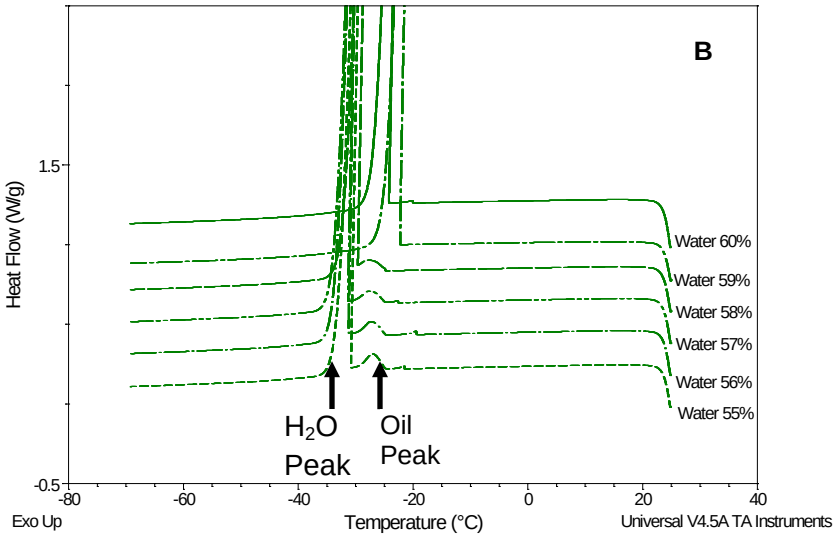
B
Heat Flow (W/g)
1.5
-0.5
Water 60%
Water 59%
Water 58%
Water 57%
Water 56%
Water 55%
H2O Peak
Oil Peak
-80
-60
-40
-20
0
20
40
Exo Up
Temperature (°C)
Universal V4.5A TA Instruments

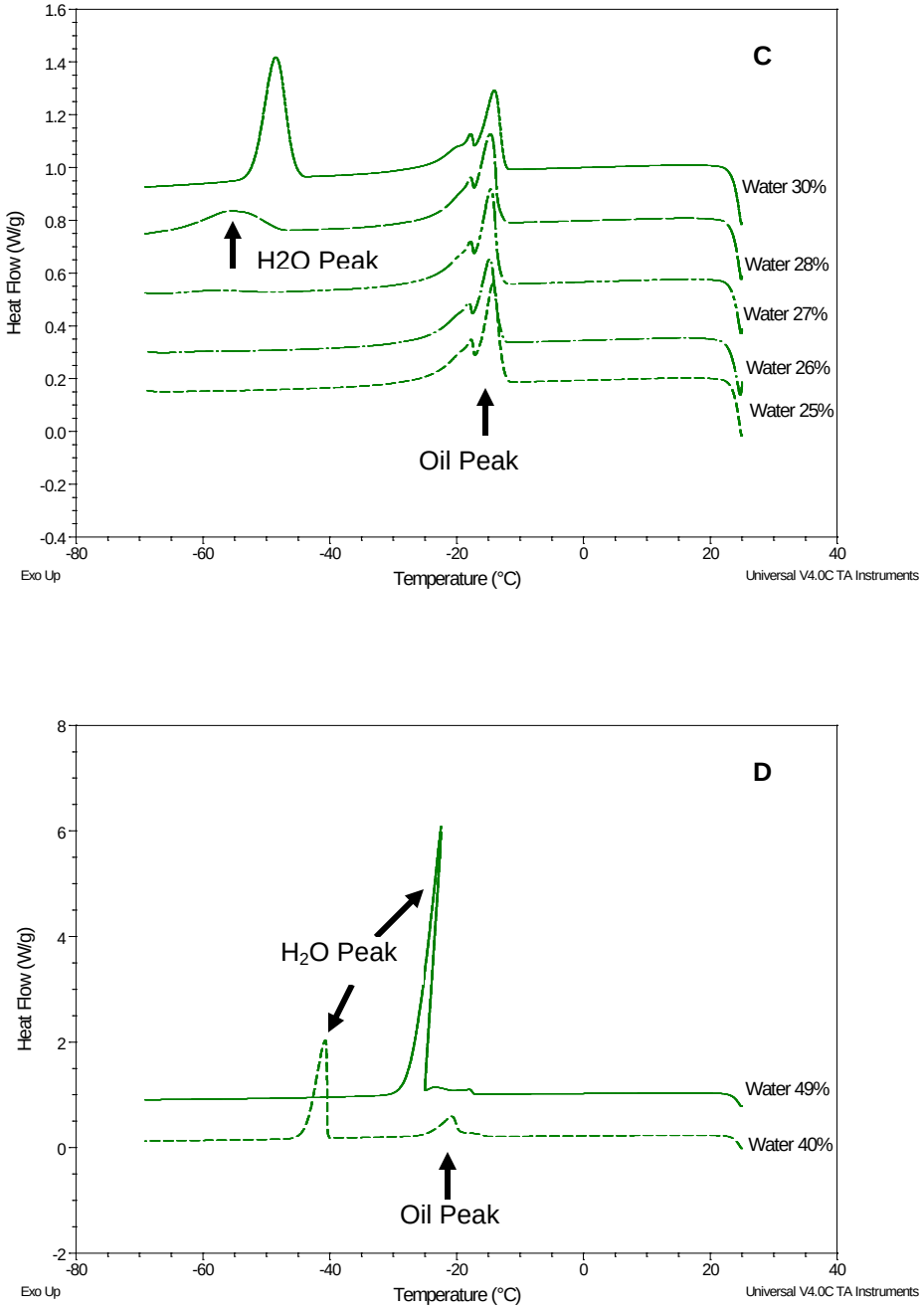

Figure 4-2. ME System #1 sample DSC cooling thermo-grams at microstructure transition or border regions: (A) the transition from W/O to bi-continuous ME along DL10, (B) the transition from bi-continuous to O/W ME along DL10, (C) the transition from W/O to bi-continuous along DL20, and (D) the ME border region along DL20.

4.3.1.2. DSC characterization of ME System #2

ME samples of System #2 along DL10 with water contents of 20%, 40%, and 80% had been characterized to be of microstructures of W/O, bi-continuous, and O/W, respectively (Dong et al, 2011). The above three samples were prepared and analyzed by the DSC method and the results are shown in Figure 4-4. For ME samples of ME System #2, the oleic acid's freezing peak was very small in the cooling thermograms probably due to strong interaction of oleic acid and surfactants. The samples of water content of 20%, 40%, and 80% (denoted as ME(OA)_20/80, ME(OA)_40/60, and ME(OA)_80/20, respectively) were in microstructures of W/O, bi-continuous, and O/W, respectively, based on the cooling thermogram traits. The cooling thermogram of ME(OA)_20/80 did show no water freezing peak; The cooling thermogram of ME(OA)_40/60 did show both freezing peaks of water and oleic acid; The cooling thermogram of ME(OA)_80/20 showed only the water freezing peak. Therefore, the results from the DSC analyses of microstructures of ME #2 were consistent with those observed by the FF-TEM method reported by Dong's group.

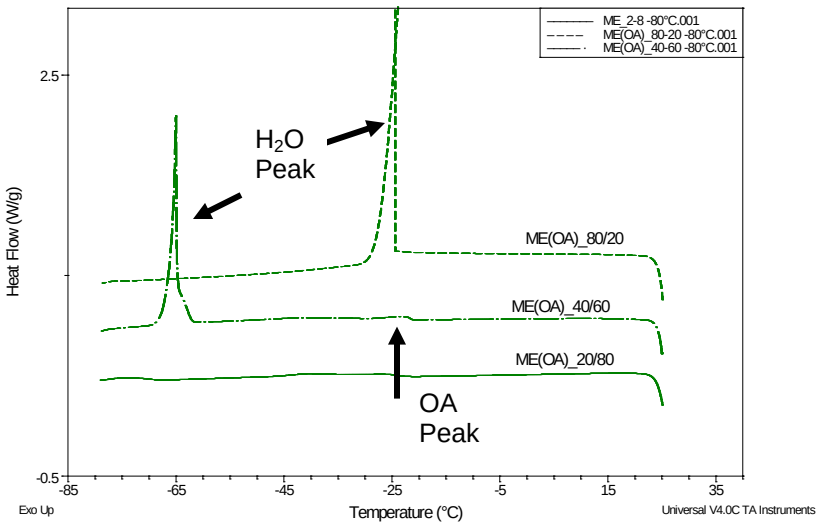

Figure 4-3. DSC freezing thermograms of samples of ME System #2. Samples Labeled as ME(OA)_20/80, ME(OA)_40/60, and ME(OA)_80/20 containing water contents of 20%, 40%, and 80% (w/w), respectively

4.3.1.3. DSC characterization of ME System #3

ME samples of System #3 along DL40 with or without co-surfactant had been thoroughly characterized by Alany et al. (2001) using the FF-TEM method and other methods. For the system with 1-butanol as the co-surfactant (denoted as System #3a), samples with water contents of 7.5%, 15%, and 35% were of microstructures, W/O, bicontinuous, and O/W, respectively. The above three samples were prepared and analyzed by the DSC method and the results are presented in Figure 4-5, 4-6, and 4-7.

Figure 4-5 shows the DSC cooling thermograms of ME samples of water content of 7.5%. One sample was prepared using H_2O (denoted as ME(EO(S-Butano))_75/925), while the other sample was prepared using deuterated water-D_2O (denoted as ME(D2O-(EO(S-Butano)))_75/925). The reason of testing the ME sample containing deuterated

water was to check whether the freezing peak was indeed a water freezing peak, that is because the deuterated water in ME formulations exhibits higher freezing and melting temperatures than hydrogenated water (Senatra et al., 1998; Senatra, 2000). In this case, the freezing peaks at around –67 °C were at the same temperature for both ME samples, indicating the peak was not a water-freezing peak. Further DSC testing of the O/S/Co-S mixture sample suggested that the peak was related to the surfactants. Therefore, there was no water-freezing peak observed for the samples in the DSC cooling thermogram, suggesting the samples were of W/O microstructures.

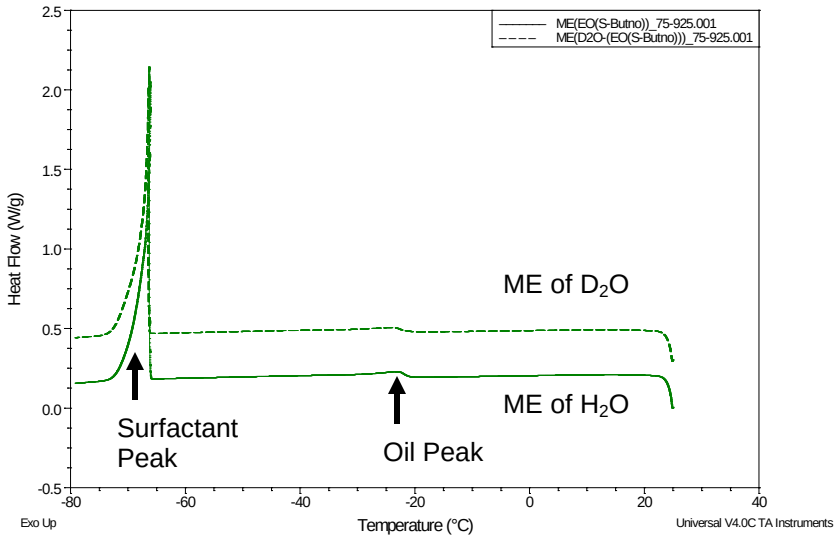

Figure 4-4. DSC cooling thermograms of ME System #3a samples containing 7.5% (w/w) of water and deuterated water, respectively.

Figure 4-6 shows the results of ME samples of System #3a containing 7.5%, 15%, and 35% water content. There were both water and oil freezing peaks observed for ME samples of 15% and 35% water content, suggesting they were of bi-continuous

microstructures. These results were consistent with those of Alany's study in which the microstructures were ascertained from the FF-TEM examinations.

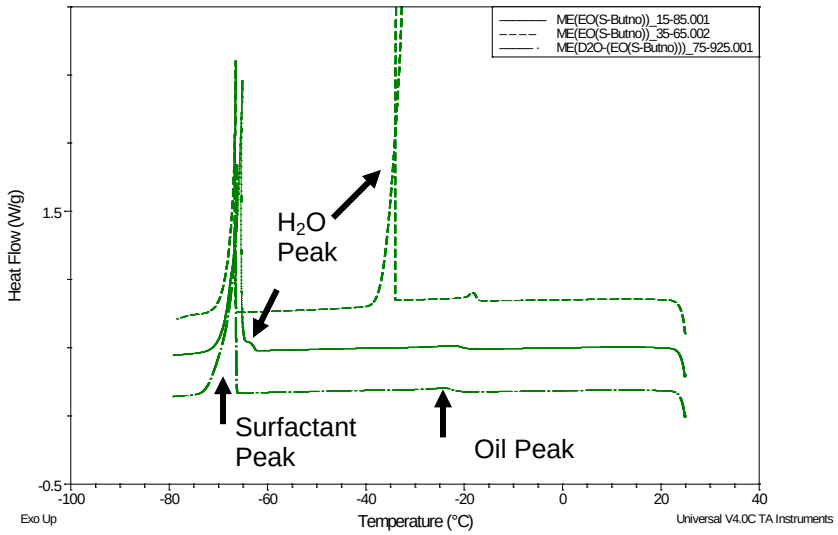

Figure 4-5. DSC cooling thermograms of ME System #3a samples of water contents, 7.5%, 15%, and 35% (w/w), respectively

Figure 4-7 shows the DSC cooling and heating thermograms of ME samples of System #3a containing 13%, 14%, and 15% water content. On the cooling thermogram of the ME sample of 15% water, the water-freezing peak just started to emerge which suggests the phase transition point from W/O to bi-continuous microstructure was at water content of 15%. This transition point result was also in an excellent agreement with that derived from the viscosity analysis in Alany's study.

The heating thermograms in this case also show a clear water-melting peak for ME samples of water content of 14% and 15%, respectively. The observations of water freezing and melting peaks are in general corresponding, suggesting the formation bulk water related to water in the continuous phase, although the heating thermogram showed

the difference of 1% water content from that of the cooling thermogram. Based on large number of DSC analyses in our investigations, the cooling thermogram water freezing peak in general always provided clearer pattern to follow than the heating thermogram in terms of microstructure assessment, therefore, the cooling thermograms in the DSC method were focused on in the study.

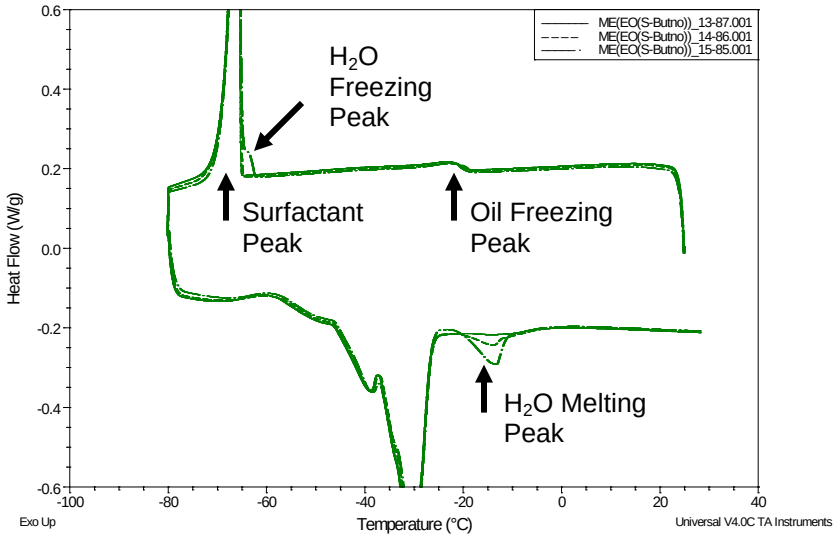

Figure 4-6. DSC cooling and heating thermograms of ME System #3a samples of water contents, 13%, 14%, and 15% (w/w), respectively.

ME System #3b did not contain the co-surfactant, 1-butanol. The samples of this system with water contents of 5% and 12.5% were analyzed by DSC, and results are presented in Figure 4-8. As can be seen, no water freezing peak was observed in the cooling thermograms, the sample microstructures were of W/O, which were consistent with Alany's data. Again in these experiments, ME samples prepared using deuterated water were utilized to rule out a peak in cooling thermograms being water freezing peak.

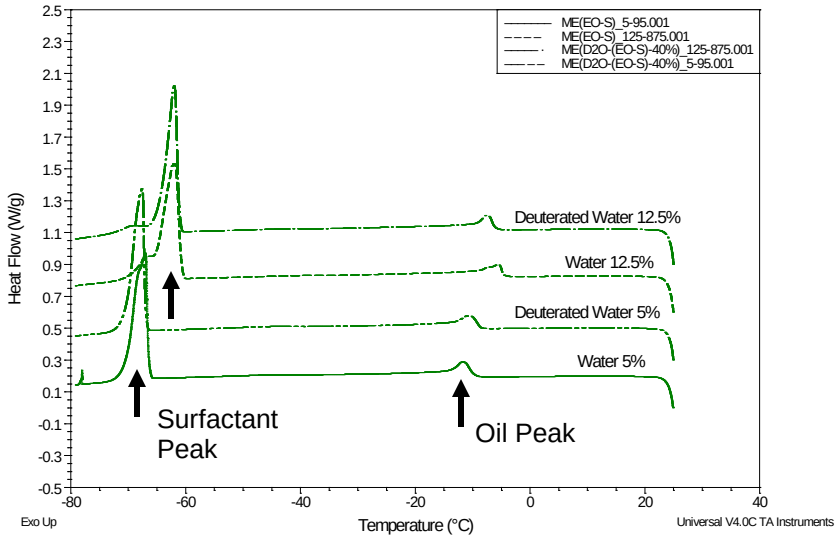

Figure 4-7. DSC cooling thermograms of ME System 3b samples of water (or deuterated water) contents, 5% and 12.5%, respectively.

4.3.1.5. Summary of the microemulsion DSC characterization results

The DSC characterization results of four ME systems are summarized in the Table 4-2. The results showed ME microstructure information derived from DSC analyses were in complete agreement with literature reports, and demonstrated the DSC method's validity and applicability for ME microstructure determination.

Table 4-2. Summary of DSC analysis results of microstructures of ME systems

ME System #	Dilution Line	Microstructure Results by DSC		Observation
1	DL10	Transition point from W/O to Bi-c: Φ_w 33% Transition point from Bi-c to O/W: Φ_w 60%		Consistent with EC result
	DL20	Transition point from W/O to Bi-c: Φ_w 28%		
2	DL10	ME water content	Microstructure	Consistent with FF-TEM results of Dong's group
		20%	W/O	
		40%	Bi-c	
		80%	O/W	
3a	DL40	ME water content	Microstructure	Consistent with FF-TEM results of Alany's group
		7.5%	W/O	
		15%	Bi-c	
		35%	Bi-c	
		37%	Bi-c	
3b	DL40	ME water content	Microstructure	
		5%	W/O	
		12.5%	W/O	
Note: "Bi-c" stands for bi-continuous microstructure.				

4.3.2. DSC Cooling Rate Effect

A cooling run of DSC analysis of the ME sample is a dynamic course, during which several processes occurred at the same time. The obvious ones include: (1) the cooling of the sample, (2) the re-equilibration of phase components at the lower temperature, and (3) the nucleation of phase components upon freezing. Therefore, the cooling rate is a major factor affecting the cooling thermogram. In principle, the cooling rate should be set fast enough to prevent the phase component re-equilibration so that the cooling thermogram is more reflective to the ME sample initial state. However, the cooling rate cannot be too fast to surpass the instrument capacity, causing the poor baseline. The cooling rate effect of DSC run was evaluated by analyzing the ME samples of System #1 along DL10. The results are presented in Figure 4-9 to 4-12.

Figure 4-9 shows that for a ME sample of W/O microstructure (with 20% water), the varied cooling rate did not affect the cooling thermograms significantly, although a slight shifting to a lower temperature of the oil freezing peak was observed. The almost same heating thermograms also indicate that the frozen states of the ME sample at the end of the freezing cycles were the same although different cooling rates were used to conduct the cooling.

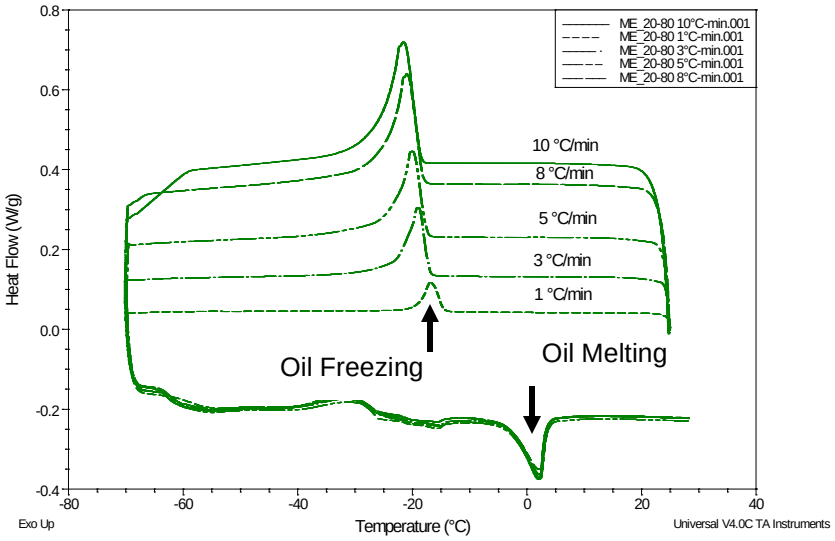

Figure 4-8. DSC cooling and heating thermograms of the ME sample of System #1 with 20% water content tested at varied cooling rates

Figure 4-10 shows that for a ME sample of W/O microstructure (with 30% water) but at the phase transition region, the varied cooling rate affected the cooling thermograms significantly. At 1 °C/min rate, a water-freezing peak was observed in the cooling thermogram, while no water-freezing peak was observed under other higher cooling rates. The heating thermograms resulted from 1 °C/min cooling rate showed to be very different, indicating that the frozen state of the ME sample at the end of the freezing

cycle was different from those at other cooling rates. At high cooling rates of 8 and 10 °C/min, the based lines of the cooling thermograms degraded close to the end of the cooling cycle. Therefore, the cooling rate of 5 °C/min is the most suitable for the analysis of this ME sample.

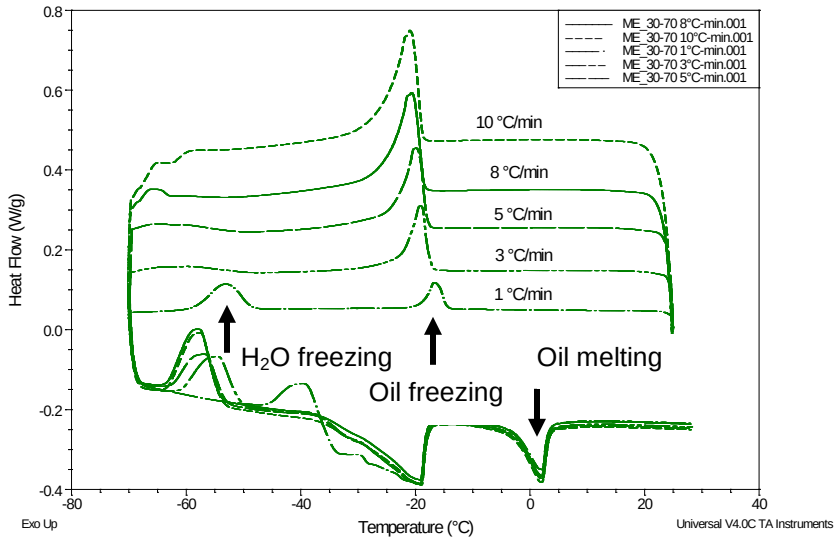

Figure 4-9. DSC cooling and heating thermograms of the ME sample of System #1 with 30% water content tested at varied cooling rates

Similarly, Figure 4-11 and 4-12 show that the cooling rate will affect to some extent either the cooling thermograms or the state of the corresponding ME sample in the end of the cooling cycle. Based on all results from Figure 4-9 to 4-12, the cooling rate of 5 °C/min is considered the optimal rate for the DSC analyses of all ME samples with different microstructures.

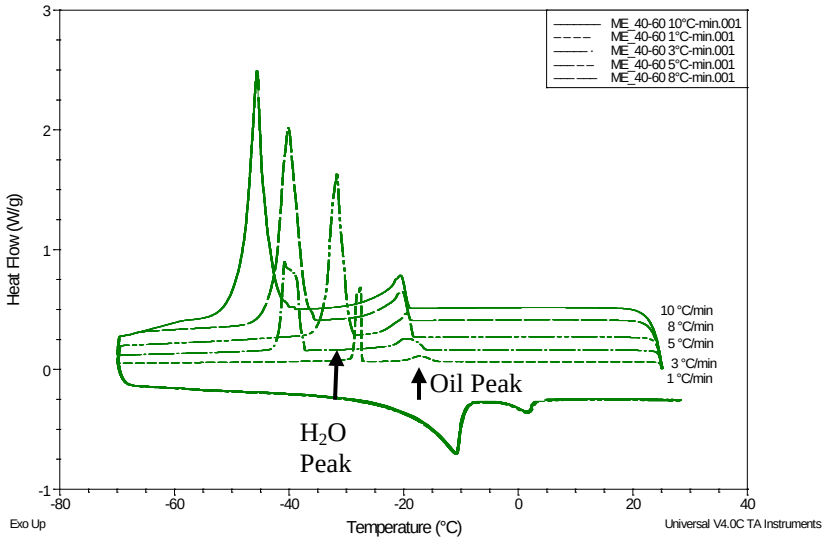

Figure 4-10. DSC cooling and heating thermograms of the ME sample of System #1 with 40% water content tested at varied cooling rates.

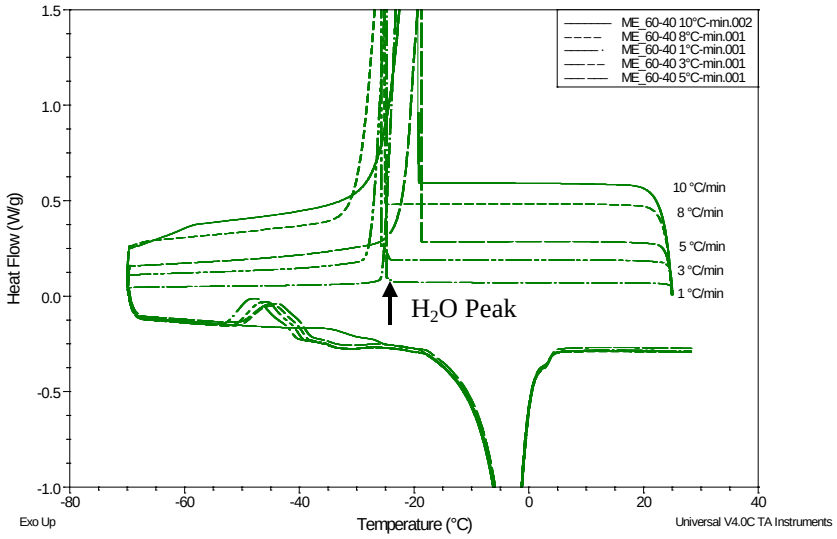

Figure 4-11. DSC cooling and heating thermograms of the ME sample of System #1 with 60% water content tested at varied cooling rates.

4.3.3. DSC Sample Size Effect

A ME sample of ME System #1 was tested with varying sample weights to evaluate the sample size effect on DSC cooling thermograms. The results (Figure 4-13) show that the sample size in the range from 2 mg to 12 mg did not cause a significant difference in cooling thermograms under the current instrument conditions. However, it is recommended to narrow the sample size in the range of 6 to 10 mg to reduce possible variation because in theory, the sample size contributes to the DSC signal time constant and will affect the DSC thermogram to some extent.

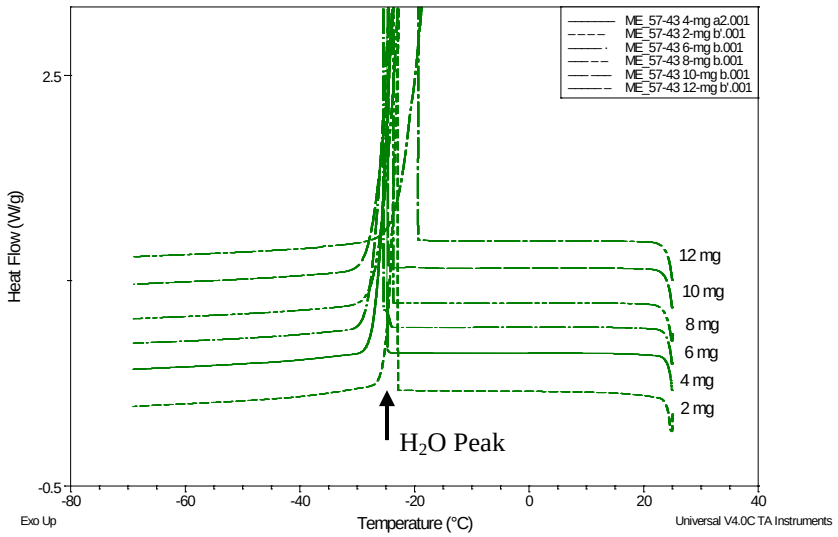

Figure 4-12. DSC cooling thermograms of the ME samples of various sample sizes from 2 mg to 12 mg.

4.3.4. Measurement of ME Samples at the Initial Isothermal Temperature of 37 °C

The current DSC approach offers a unique advantage for ME microstructure characterization, it enables an easy analysis of the ME sample microstructures at a temperature different from the ambient one. Specifically, the human body temperature is

37 °C and therefore, microstructure information of the ME formulation at 37 °C is of particular interest since the formulation will be eventually subjected to this temperature once applied in vivo. In order to assess the microstructure information at a particular temperature, the DSC test can be easily conducted by setting the initial isothermal temperature at that temperature.

Figure 4-14 and 4-15 show DSC cooling thermograms at 37 °C of ME samples of System #1 at two different phase transition regions. Based on the results, at 37 °C the phase transition point of the system from W/O to bicontinuous was at water content of 32% and was similar to that at 25 °C, while the phase transition point from bicontinuous to O/W was at water content of 57% and was slightly lower than that at 25 °C. These kinds of determination would be more challenging to do if using other probing methods, e.g. surface tension or electric conductivity measurements.

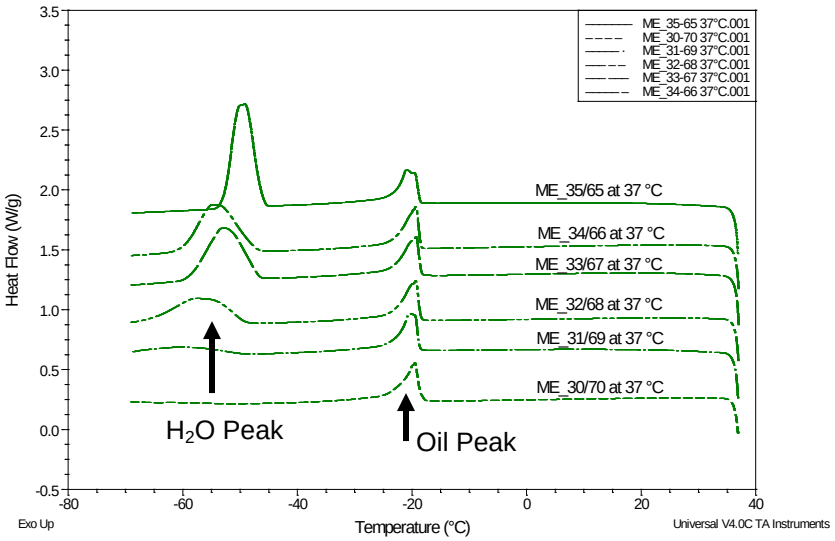

Figure 4-13. DSC cooling thermograms of the ME samples with various water contents at the transition from W/O to bicontinuous microstructures at 37 °C.

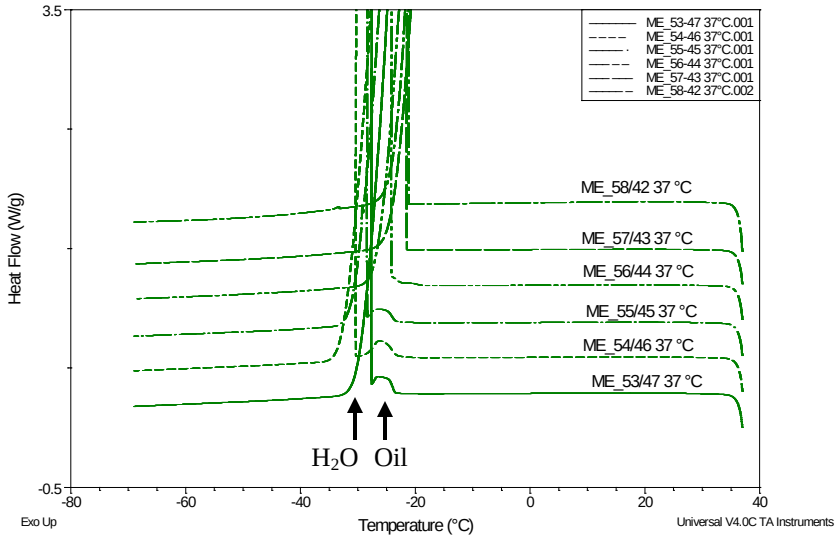

Figure 4-14. DSC cooling thermograms of the ME samples with various water contents at the transition from bicontinuous to O/W microstructures at 37 °C.

4.3.5. DSC Testing of ME formulations Containing Model Drugs: Ketoprofen and Caffeine

ME formulation samples of System #1 with the lipophilic model drug Ketoprofen (2.5% w/w) were prepared along the water dilution line DL10. Microstructures and phase transition points of the formulation samples were determined conveniently by the DSC method as illustrated by the cooling thermograms in Figure 4-16 and 4-17. The ME formulation transition points from W/O to bi-continuous, and from bi-continuous to O/W were tested to be at water content of 31% and 59%, respectively. These transition points are similar to those of blank ME vehicles.

Similarly, ME formulation samples with the hydrophilic model drug caffeine (1.0% w/w) were also prepared along the water dilution line DL10. The ME formulation transition points from W/O to bi-continuous, and from bi-continuous to O/W were tested

to be at water content of 31% and 58% (Figure 4-18 and 4-19), respectively. Both model drugs did not affect much the phase transition points of the ME samples compared with the blank ME vehicles, suggesting they did not interfere significantly interactions of surfactants with oil and water.

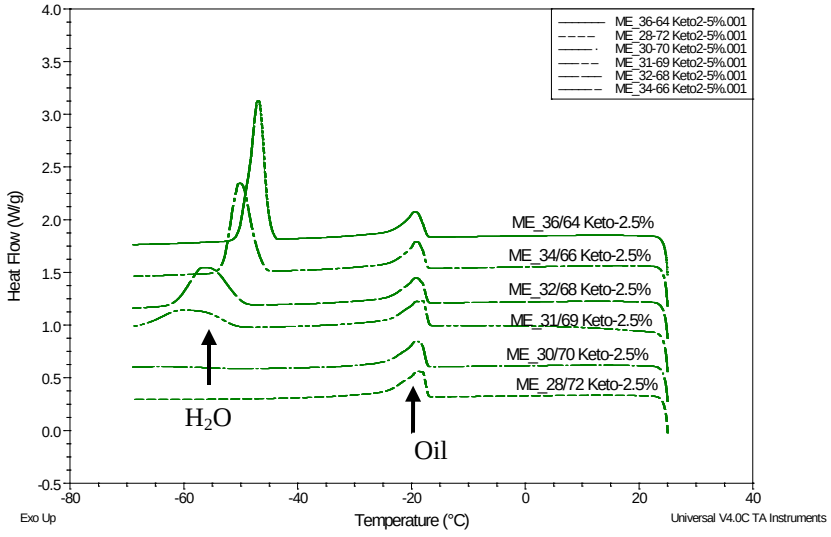

Figure 4-15. DSC cooling thermograms of the ME formulation samples with Loaded Model drug, ketoprofen 2.5% at various water contents in the transition region from W/O to Bi-continuous microstructures

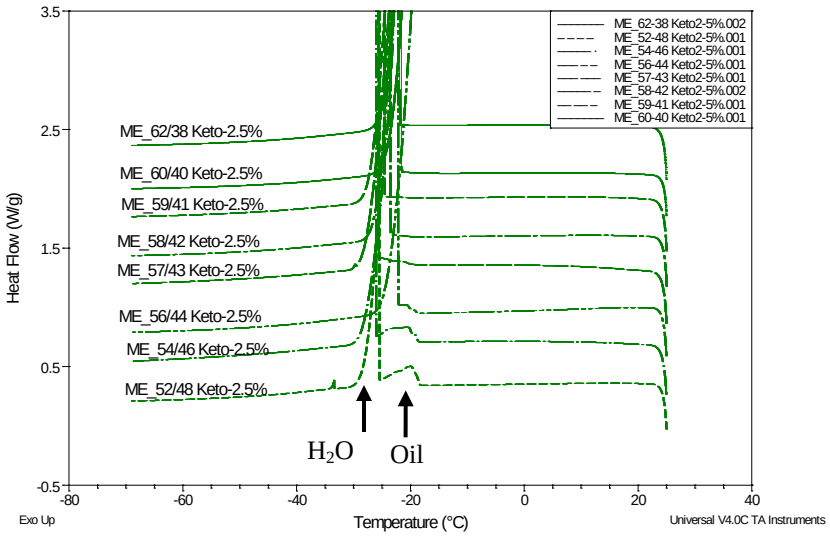

Figure 4-16. DSC cooling thermograms of the ME formulation samples with loaded model drug, ketoprofen 2.5% at various water contents in the transition region from bicontinuous to O/W microstructures

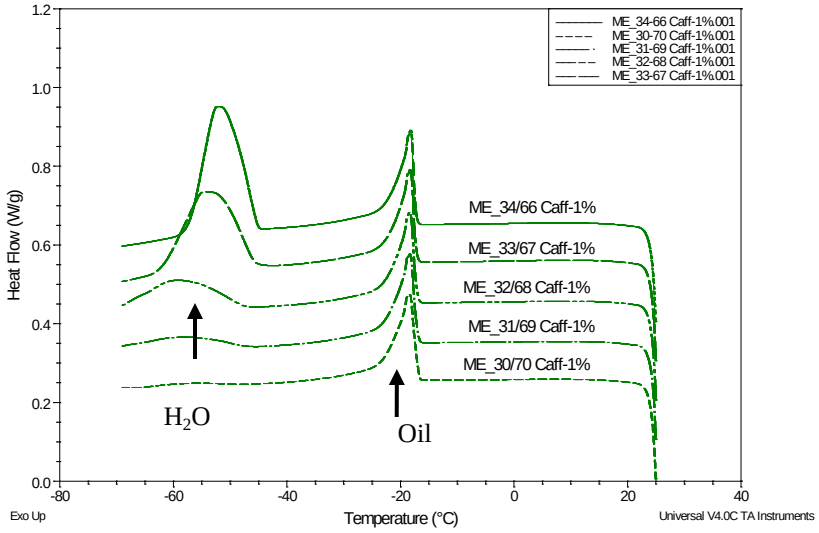

Figure 4-17. DSC cooling thermograms of the ME formulation samples with Loaded Model drug, caffeine 1.0% at various water contents in the transition region from W/O to bicontinuous microstructures.

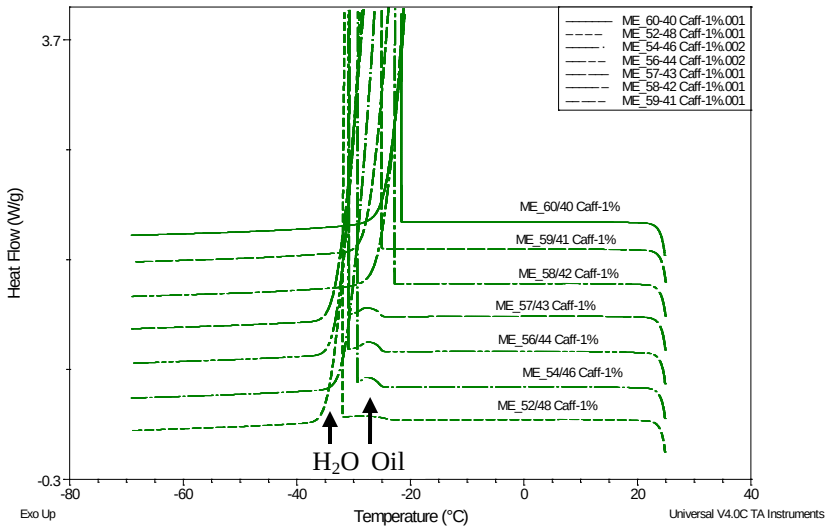

Figure 4-18. DSC cooling thermograms of the ME formulation samples with loaded Model drug, caffeine 1.0% at various water contents in the transition region from bicontinuous to O/W microstructures.

4.4. Discussion

A significant progress has been made in the current study in applying the DSC technique for ME microstructure characterization. In the previously published studies (Podlogar et al., 2004 and 2005; Boonme et al., 2006; Liu et al., 2009), DSC had been used for the same purpose, but the unique characteristics in the cooling thermograms that led to the ME microstructure information was not clearly identified. We probably can explain the observed phenomena in cooling thermograms by visualizing interactions at a molecular level between different phase components. In W/O MEs, water was dispersed molecularly and bound tightly with surfactant molecules, it could not be frozen or frozen at much lower temperature than -80 °C, so no water-freezing peak was observed. As water content increased into the bi-continuous MEs, the “free” or “unbound” bulk water started to form, resulting in significant elongation of the water droplets and furthermore

the formation of water cylinder or channel structures, therefore, the freezing peak of free bulk water was observed. In O/W MEs, water becomes the continuous phase, oil freezing peaks were buried under the water peak due to the complete encompass of oil droplets by water and the increasingly large water freezing peak moving to higher temperature. Therefore, DSC cooling thermo-grams reveal direct information of molecular interactions of ME phase components and of microstructures.

The DSC method can potentially be useful in studying the loaded drug interaction with ME formulation components. As an example, Figure 4-20 presents DSC cooling and heating thermograms of ME vehicle and formulation samples of System #1 and Micelle vehicle. From the cooling thermograms (Figure 4-20A), it was determined that ME vehicle and formulations were of O/W microstructure. From the heating thermograms (Figure 4-20B), it could be derived that ketoprofen disturbed surfactant mutual interaction as suggested by the elimination of the surfactant interaction peak, while caffeine did not show such effect.

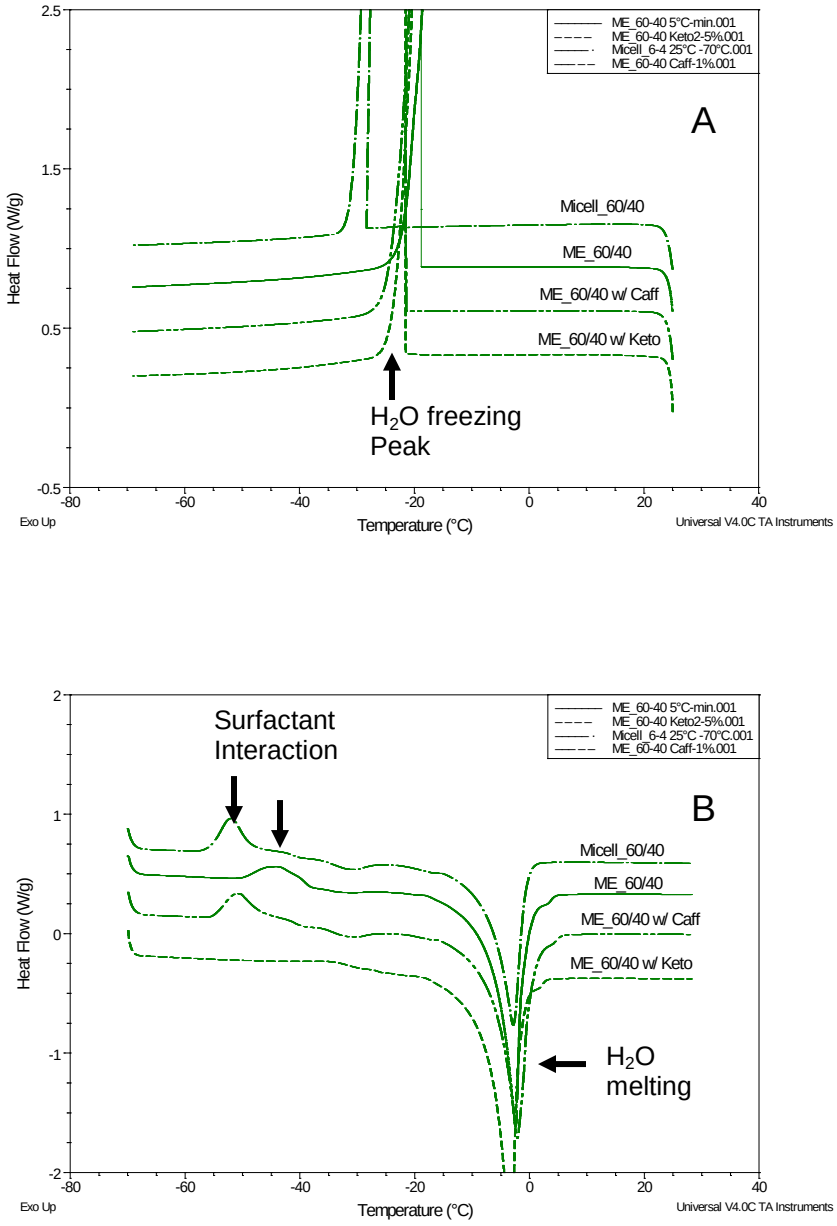

Figure 4-19. The DSC testing results of ME vehicle, formulation, and micellar vehicle: cooling thermograms (A), and heating thermograms (B.)

In this paper, common ME systems most often used as transdermal drug formulation vehicles were studied using the DSC approach. The common ME systems

referred here are typically made of fatty acids or fatty acid esters as oil component, non-ionic surfactants as the surfactant component, and are with or without short chain alcohol as the co-surfactant. However, there are other types of ME systems, e.g. systems made of phospholipid based surfactants, or sugar based surfactants or ionic surfactants. In order to understand if the described DSC method is applicable to these systems, further studies are needed.

Based on extensive DSC analyses results, it was also found for the current DSC method, the determination of ME transition point from W/O to bi-continuous was accurate and consistent, while the determination of ME transition from bi-continuous to O/W carried slightly higher variability. One possible reason was ME sample microstructures were very dynamic during this transition. Therefore, DSC observed data with the viability are very likely the true reflection of ME system microstructure status characteristics in the region.

4.5. Conclusions

The DSC method for characterization of ME microstructures was investigated in a systematic way. By generating DSC data derived microstructure information that were consistent with those reported in literatures, the developed DSC method for ME microstructure assessment was demonstrated to be applicable to common ME systems and very effective and accurate. The method offers several advantages: easy analysis of microstructure by a single DSC run, convenient determination of phase transition points, and feasible for probing of microstructure information of the ME sample at different

temperatures of interest. Further studies should focus on testing more ME systems and combining both cooling and heating thermograms to derive more information on ME microstructure and the interaction between the drug and formulation components at the microscopic level. Knowledge of ME microstructures and drug interaction at these microstructure domains will provide important insights to drug release and delivery from ME formulations.

4.6. References

Alany, R.G., Tucker, I.G., Davies, N.M., Rades, T., 2001. Characterizing colloidal structures of pseudoternary phase diagrams formed by oil/water/amphiphile systems. Drug Dev. Industrial Pharmacy 27(1), 31-38.

Azeem, A., Khan, Z.I., Aqil, M., Ahmad, F.J., Khar, R.K., Talegaonkar, S., 2009. Microemulsion as a surrogate carrier for dermal drug delivery. Drug Dev. Industrial Pharmacy 35, 525-547.

Boonme, P., Krauel, K., Graf, A., Rades, T., Junyaprascert, V.B., 2006. Characterization of microemulsion structures in the pseudoternary phase diagram of isopropyl palmitate/water/brij 97:1-butanol. AAPS PharmSciTech 7(2), E99-E104.

Djordjevic, L., Primorac, M., Stupar, M., Krajisnik, D., 2004. Characterization of caprylocaproyl macrogoglycerides based microemulsion drug delivery vehicles for an amphiphilic drug. Inter. J. Pharm. 271, 11-19.

Djordjevic, L., Primorac, M., Stupar, M., 2005. In vitro release of diclofenac diethylamine from caprylocaproyl macrogoglycerides based microemulsions. Inter. J. Pharm. 296, 73-79.

Dong, X., Ke, X., Liao, Z., 2011. The microstructure characterization of meloxicam microemulsion and its influence on the solubility capacity. Drug Dev. Ind. Pharm. 37, 894-900.

Heuschkel, S., Goebel, A., Neubert, R.H.H., 2008. Microemulsions—modern colloidal carrier for dermal and transdermal drug delivery. J. Pharm. Sci. 97(2), 603-631.

Hua, L., Weisan, P., Jiayu, L., Ying, Z., 2004. Preparation evaluation, and NMRcharacterization of vinpocetine microemulsion for transdermal delivery. Drug Dev. Industrial Pharmacy 30(6), 657-666.

Kreilgaard, M., Pedersen, E.J., Jaroszewski, J.W., 2000. NMR characterization and transdermal drug delivery potential of microemulsion systems. J Controlled Release 69, 421-433.

Kreilgaard, M., 2002. Influence of microemulsions on cutaneous drug delivery. Advanced Drug Delivery Reviews 54(suppl. 1), s77-s98.

Kuntsche, J., Horst, J.C., Bunjes, H., 2011. Cryogenic transmission electron microscopy (cryo-TEM) for studying the morphology of colloidal drug delivery systems. Int. J. Pharm. 417, 120-137.

Lee, P.J., Langer, R., Shastri, V.P., 2003. Novel microemulsion enhancer formulation for simultaneously delivery of hydrophilic and hydrophobic drugs. Pharm. Res. 20, 264-269.

Liu, H., Wang, Y., Lang, Y., Yao, H., Dong, Y., Li, S., 2009. Bicontinuous cyclosporine A loaded water-AOT/Tween 85-isopropylmyristate microemulsions: structural characterization and dermal pharmacokinetics in vivo. J. Pharm. Sci. 98(3), 1167-1176.

Lopes, L.B., Vandewall, H., Li, H.T., Venugopal, V., Li, H.K., Naydin, S., Hosmer, J., Levendusky, M., Zheng, H., Bentley, M.V.L.B., Levin, R., Hass, M.A., 2010. Topical delivery of lycopene using microemulsions: enhanced skin penetration and tissue antioxidant activity. J. Pharm. Sci. 99(3), 1346-1357.

Mo, C., Zhong, M., Zhong, Q., 2000. Investigation of structure and structural transition in microemulsion systems of sodium dodecyl sulfonate + n-heptane + n-butanol + water by cyclic voltammetric and electrical conductivity measurements. J. Electroanalytical Chem. 493, 100-107.

Mo, C., Li, X., 2007. Microstructure and structural transition in coconut oil microemulsion using semidifferential electroanalysis. J. Colloid and Interface Sci. 312, 355-362.

Neubert, R.H.H., 2011. Potential of new nacocarriers for dermal and transdermal drug delivery. Eur. J. Pharm. Biopharm. 77, 1-2.

Podlogar, F., Gasperlin, M., Tomsic, M., Jamnik, A., Rogac, M.B., 2004. Structural characterization of water-Tween 40 / Imwiter 308 – isopropyl myristate microemulsions using different experimental methods. Inter. J. Pharm. 276, 115-128.

Podlogar, F., Rogac, M.B., Gasperlin, M., 2005. The effect of internal structure of selected water-Tween 40 – Imwitor 308 – IPM microemulsions on ketoprofen release. Inter. J. Pharm. 302, 68-77.

Sintov, A.C., Shapiro, L., 2004. New microemulsion vehicle facilitates percutaneous penetration in vitro and cutaneous drug bioavailability in vivo. J. Control. Release 95, 173-183.

Sintov, A.C., Levy, H.V., Botner, S., 2010. Systemic delivery of insulin via the nasal route using a new microemulsion system: In vitro and in vivo studies. J. Control. Release 148, 168-176.

Zhang, J., Michniak-Kohn, B., 2011. Investigation of microemulsion microstructures and their relationship to transdermal permeation of model drugs: ketoprofen, lidocaine, and caffeine. Int. J. Pharm. 421:34-44.

Chapter 5 . INVESTIGATION OF MICROEMULSION AND MICROEMULSION GEL FORMULATIONS FOR DERMAL DELIVERY OF CLOTRIMAZOLE

5.1. Introduction

Microemulsions (MEs) are single optically isotropic and thermodynamically stable dispersions of oil, water, and surfactants with droplet sizes in the submicron range (Lee at al., 2003). As formulation vehicles, they offer high drug solubilizing capacity, long term stability, ease of preparation, and capability to enhance skin permeation for hydrophobic and hydrophilic drugs (Heuschkel et al., 2008; Kreilgaard, 2001). For over two decades, extensive studies have been conducted on MEs for transdermal and dermal drug delivery, although the drug skin permeation enhancement effect from MEs has been well established, the mechanism is still not completely elucidated. One main reason is that a microemulsion is a complex system that has many variables. Recent research provided more insights, from the point of view of understanding mechanisms, they can be categorized into the following: (a) formulation constituent/excipient permeation enhancer effect: oil is a critical excipient that impacts drug solubility and skin permeation (Thomas et al., 2014; Ren et al., 2014; Pepe et al., 2012; Montenegro et al., 2011; Lopes et al., 2009) and so are the surfactant and co-surfactant (Hoppel et al., 2015; Montenegro et al., 2011; Todosijevic et al., 2015). Additional excipients can be formulated in order to improve drug solubility and skin permeation, e.g. β-cyclodextrin (Mora et al., 2014); (b) ME composition and its optimization: Response-Surface Model (RSM) in conjunction with experimental design has been increasingly used by different research groups for ME formulation optimization (Ge et al., 2014; Zhao et al., 2014; Tsai et al., 2015). Results from composition studies generally support the observation that for hydrophobic drugs,

increased water or oil content and decreased surfactant content help to achieve higher drug skin permeation (Zhang and Michniak-Kohn, 2011; Hoppel et al., 2014 and 2015; Ge et al., 2014; Bhatia et al., 2013; Tsai et al., 2015; Kreilgaard, 2001); (c) microstructure influence: ME droplet shape or size may have effects on drug permeation enhancement (Mahrhauser et al., 2015; Sintov, 2015). Model drug skin permeation study results have been correlated with ME microstructures in several publications (Sintov et al., 2014; Zhang and Michniak-Kohn, 2011;Cavalcanti et al., 2016); and (d) ME-gel formulations: many research studies were conducted on ME-gel formulations in order to explore transdermal or dermal product development (Wan et al., 2015; Ge et al., 2014; Fouad et al., 2013; Zhu et al., 2009).

Despite extensive studies, there is a lack of information on ME microstructure influence on drug dermal delivery and on relationships between drug skin retention and transdermal permeation in such cases. Previously, our group reported on investigation of ME microstructure influence on both hydrophobic and hydrophilic model drug transdermal permeation (Zhang and Michniak-Kohn, 2011). In the present work, our main objective is to investigate ME microstructure effect on hydrophobic drug dermal delivery. Clotrimazole is a widely used anti-fungal with its main target tissue at the viable epidermis and dermis. There are few reports on CLOT dermal delivery by ME formulations (Hashem et al., 2011), to our knowledge, no work had been reported on CLOT delivery by MEs using different microstructures. Therefore, we used CLOT as a model hydrophobic drug, and conducted the study in a systematic way in which ex vivo human cadaver skin permeation experiments were run using Franz diffusion cells and ME formulations of different microstructures containing varied CLOT loads. Additionally,

ME-gel formulations were also studied and compared with a commercial CLOT cream, Lortrimin®, with the objective to assess dermal delivery efficiency and potential for topical product development. Furthermore, FITC (cLogP of 6.8, by ACDLabs v.11) was also used as a model compound to study its skin deposition delivered by MEs using porcine skin permeation experiments and fluorescent microscopy.

5.2. Materials and Methods

5.2.1. Materials

Clotrimazole,Fluorescein IsoThiocynate (FITC), dioxane, and propylene carbonate (PC)wereall purchased from Sigma-Aldrich, St. Louis, MO, USA. Labrasol was a sample provided by Gattefosse. Isopropyl myristate (IPM), Cremophor EL, propylene glycol (PG),triethanolamine (TEA), methanol, acetonitrile, water and PBS tablets were purchased from Fisher Scientific, Waltham, MA, USA. Carbopol 980 was purchased from Lubrizol, Wickliffe, OH, USA. Lotrimin® was purchased from local CVS pharmacy store. Human cadaver skin samples were purchased from Skin Bank NY Firefighters, NY, USA, were stored at -80 °C until use.

5.2.2. Preparation of ME Formulations

A microemulsion system used was developed, and its ternary phase diagram construction and microstructure characterization were reported in the previous study (Zhang and Michniak-Kohn, 2011). Briefly, the system used IPM as oil phase, Labrasol and Cremophor EL as surfactant and co-surfactant, and water as aqueous phase. ME formulations were prepared along the water dilution line of Oil/(Surfactant and co-surfactant) 1/9 (w/w). Model drugs, CLOT or FITC, were dissolved in the mixture of IPM/(Labrasol/Cremophor EL, 4/1 (w/w)) with the aid of sonication, then, the right amount of water was added in based on the corresponding water content and mixed by

vortex shaking to obtain the formulation which was an isotropic and transparent solution. Table 5-1 lists formulations used in the study, their labels, compositions and corresponding micro-structures.

5.2.3. Preparation of ME Gel Formulations

ME-gel formulations were prepared based on ME_5/5 and ME_65/35. Carbopol980 was used as the gelling agent at 1.0% (w/w). The preparation followed partially the method reported by Zhu et al. (2009). The drug loaded ME formulation was first prepared, 1.0% (w/w) of Carbopol980 was added and allowed to swell overnight at room temperature, then, the formulation was gelled by adjusting its pH to 6.8 ± 0.2 by the addition of TEA.

Table 5-1. Summary of formulations, their labels, compositions, and micro-structure information.

Formulation Label	Model Drug	Drug Load % (w/w)	Oil/(Surf./Co-surf.) % (w/w)	H_2O% (w/w)	Microstructure
PC	CLOT	1.0	None	None	Solution
ME_2/8_CLOT-0.5%		0.5	80	20	W/O
ME_4/6_CLOT-0.5%		0.5	60	40	Bi-continuous
ME_5/5_CLOT-0.5%		0.5	50	50	Bi-continuous
ME_7/3_CLOT-0.5%		0.5	30	70	W/O
ME_2/8_CLOT-1 %		1.0	80	20	W/O
ME_5/5_CLOT-1%		1.0	50	50	Bi-continuous
ME_65/35_CLOT-1%		1.0	35	65	O/W
Micelle_5/5_CLOT-1%		1.0	50 [a]	50	Micelle
ME_5/5_gel_CLOT-1% [b]		1.0	50	50	Bi-continuous
ME_65/55_gel_CLOT-1% [b]		1.0	35	65	O/W
ME_2/8_FITC-0.1 %	FITC	0.1	80	20	W/O
ME_4/6_FITC-0.1%		0.1	60	40	Bi-continuous
ME_7/3_FITC-0.1%		0.1	30	70	O/W

Note: [a] Micelle_5/5_CLOT-1% contained only surfactant/co-surfactant, no oil.
[b]ME_gel formulations contain 1% (w/w) of Carbopol980 with pH adjusted to 6.8 using TEA.

5.2.4. Measurement of CLOT Solubility in Formulation Excipients and Various Vehicles

CLOT was weighed into a 4-mL glass vial, then, 2 mL of the tested excipient or vehicle was added in order to obtain a suspension. The sample vial was put in a shaker and agitated under constant speed of 600 rpm at 37.0 ± 0.1 °C overnight. One mL of the sample was pipetted into a micro-centrifuge tube and this was centrifuged at 14,000 rpm at 37 °C for 10 min. One hundred µL of the supernatant was taken and diluted using methanol and then placed in a HPLC vial. The prepared sample was analyzed using HPLC to determine solubility of CLOT.

5.2.5. Skin Permeation Study

5.2.5.1. Skin permeation experiment

Dermatomed human cadaver skin was defrosted, cut into 14x14 mm pieces, and soaked in PBS buffer to hydrate for 15 min before permeation experiments. Skin pieces from two donors were used in the study, which were harvest from their body backs. The donors are male Hispanic and White, aged 47 and 50, and death due to atherosclerotic corona and hypertension, respectively. For the study comparing ME formulations of the same CLOT load, skin samples from the same human donor were used in order to reduce data variability. Permeation experiments were conducted using Franz diffusion cells (Permegear, Hellertown, PA, USA), which had a donor diffusion area of 0.64 cm^2 and receptor volume of 5.1 mL. In order to conduct the permeation experiment, the skin samples were sandwiched between the donor and the receptor with the stratum corneum layer facing the donor, 0.15 mL of solution formulation or 0.3 mL of gel/cream formulation was added into the donor, and this was occluded using Parafilm®. The receptor was filled with medium under constant stirring, and was kept at 37.0 ± 0.2 °C by circulating water bath jacket. PBS buffer/Dioxane, 9/1 (v/v)was used as the receptor

medium, which provided sink conditions for permeation of CLOT (Ning et al., 2005). Skin permeation experiments for all formulations were run for 24 hours unless otherwise specified. Replicates3 to 6 were conducted for each formulation.

5.2.5.2. Permeation analytical sample preparation

At the end of the permeation experiment, three different types of analytical samples were prepared for HPLC assay to assess CLOT dermal retention and transdermal permeation: (1) Dermal samples, (2) Stratum Corneum Epidermis (SCE) samples, and (3) transdermal permeation samples.

One mL of receptor medium was filled into a HPLC vial which served as the transdermal permeation sample. The skin sample was wiped clean (twelve times using Kim wipes®), and the skin tat had been treated with the formulation was cut out using a 10 mm biopsy punch. This sample was then subjected to 60 ºC water treatment for 60 seconds, and peeled to separate SCE and dermal layers according to an established method (Puglia et al., 2001).The SCE sample was placed in a 50-mL plastic centrifuge tube and 10 mL of methanol was added to extract the sample by vortex shaking for 2 min and sonicated in a water bath for 1 hour. The sample was then filtered through a 0.22 µm PTFE syringe filter (Whatman) and filled into a HPLC vial, which served as SCE sample. The weight of dermal sample was recorded and it was then cut into 12-14 pieces and placed in a plastic homogenization tube which contained metal milling beads. Then 1-mL of methanol was added and the sample was homogenized at speed of 600 rpm for 15 min. Following this treatment, 0.5 mL of the methanol solution was taken and filtered using a 0.2 µm syringe-less filter device (Mini-UniPrep™, polypropylene filter medium, Whatman), and this then served as the Dermal sample. HPLC analyses of these samples were conducted in order to determine CLOT concentrations.

5.2.6. HPLC Analytical Method

Clotrimazole concentrations were assayed using a HPLC method. An Agilent Zorbax Eclipse XDB phenyl column 4.6x250 mm and a mobile phase of 0.005% H_3PO_4/ acetonitrile, 45/55 (v/v), were used. The method was conducted under the following conditions: column at ambient temperature, flow rate at 1 mL/min, UV detection at 210 nm, injection volume of 10 µL, and run time of 8 min. The method was validated for reproducibility and linearity with a dynamic linear range from 0.1 to 100 µg/mL. Skin permeation sample concentrations were determined by the CLOT peak area calibrated by bracketing external CLOT standards.

5.2.7. FITC Skin Deposition Study by Fluorescent Microscopy

FITC ME formulation skin penetration experiments were conducted using porcine skin, which was harvested by dermatoming the skin to a thickness of 800 µm from the back portion of freshly slaughtered pigs (pig tissues were supplied from the University of Medicine and Dentistry of New Jersey), and skin samples were stored at -80 °C until use. The experiment was similar to the human skin permeation experiment described in Section 2.5.1. Replicates of three Franz cell tests for each formulation were run. Receptor medium was PBS buffer, 0.15 mL of ME formulations containing 0.1% (w/w) FITC was added into the donor, and skin samples were treated for 12 hours, then were cleaned from excess formulation and rinsed under running DI H_2O for 10 seconds, and were then blotted dried using a paper towel. The skin samples were frozen in OCT medium on a sample holder placed on dry ice, and then sectioned to obtain the cross-sectional slices of 8µm thickness at -22 °C using a cryostat microtome (Leica CryoStat, CM3050S, Wetzlar, Germany). The skin slices were collected on glass slides and were examined by fluorescent microscopy under GFP light (Zeiss Fluorescent microscope with

AxioCamMRm camera). Fluorescent intensity of different skin layers on images were quantitatively analyzed by Image-J software, which correlated to FITC deposition concentrationsin the SC, viable Epidermis (vE,), and Dermal (D) layers. Small integration boxes of 400 to 600 squared pixel areas were drawn in the different skin layers for intensity quantification, box locations were at the skin depth (counted from SC surface down into the dermis) of 0-20 μm, 70-100 μm, and 200 to 250 μm for SC, vE, and D layers, respectively. Results were reported as (means ± S.D.) that were calculated based on n=30 readings from 6 skin slices of 3 Franz cell treated skin samples for each formulation.

5.2.8. Statistical Analysis of Data

Skin permeation experiments for each formulation were conducted three to six times. Results were expressed at means ± S.D. Student t-tests were employed to assess difference between mean values, and the statistically significant differences were defined as $P < 0.05$.

5.3. Results and Discussion

5.3.1. CLOT Solubility in Formulation Excipients and Vehicles

CLOT solubility data at 37 °C in formulation excipients and various vehicles are presented in Table 5-2. As expected, CLOT solubility is high in surfactant/co-surfactant mixture, Labrasol/Cremophor EL (73.8 mg/mL), moderate in oil, IPM (9.3 mg/mL), and extremely low in aqueous PBS ($5x10^{-5}$ mg/mL). In ME vehicles, CLOT solubility decreased approximately linearly when the water content increased from 20% to 70% (w/w) as shown in Figure 5-1. It can be assumed that at the same CLOT load, if the water content increases in MEs in the same range, resulting in ME microstructure changes from W/O to bi-continuous, then to O/W, the thermodynamic activity of CLOT in ME

formulations will increase accordingly due to decreasing solubility in the ME vehicle. PBS/Dioxane (9/1, v/v) was used as the receptor fluid in the CLOT permeation study, CLOT solubility in the fluid was found to be 7.1 µg/mL which meets sink conditions due to overall CLOT concentration being much lower in the Franz cell receptor during the skin permeation experiment.

Table 5-2. CLOT solubility at 37 °C in formulation excipients and vehicles issue belowin Table with font size and color. Define IPM, PBS and S.

Formulation Excipients	Solubility (mg/mL)	ME Vehicle	Solubility (mg/mL)
Labrasol/Cremophor EL (4/1, w/w)	73.8	ME_2/8	30.7
IPM/(S+CoS) (1/9, w/w)	69.9	ME_4/6	23.1
IPM (oil)	9.3	ME_5/5	16.8
Propylene Carbonate (PC)	39.7	ME_65/35	13.9
PBS	$5.0x10^{-5}$	ME_7/3	9.1
PBS/Dioxane (9/1, v/v)	$7.1x10^{-3}$		

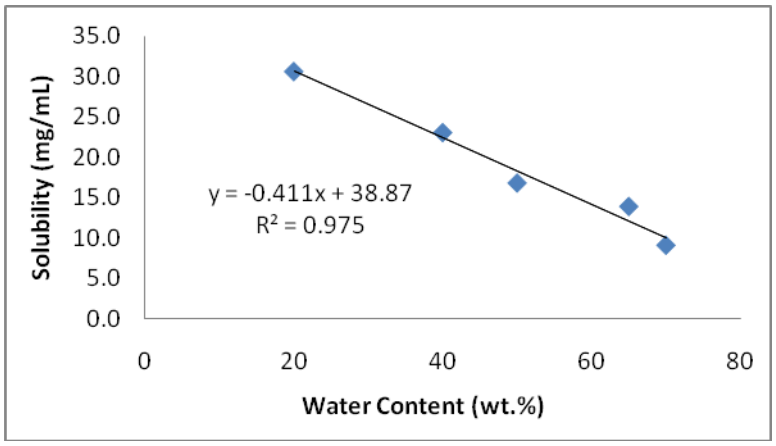

Figure 5-1. CLOT solubility in ME vehicles vs. water content

5.3.2. Skin Permeation Tests for MEs Containing 0.5% (w/w) of CLOT

Human cadaver skin permeation test results for ME formulations containing 0.5% (w/w) of CLOT are presented in Table 5-3 and Figure 5-2. CLOT dermal delivery can be directly observed based on CLOT concentrations in skin SCE and dermal layers. In this study, dermal layer CLOT concentration is used as the index for evaluating CLOT dermal

delivery efficiency. As can be seen, dermal CLOT concentration from ME_7/3 is significantly higher than other MEs ($P<0.05$), being 2.0, 2.2, and 1.8 fold of that of ME_2/8, ME_4/6, and ME_ 5/5, respectively. ME_7/3 of O/W microstructure provided the highest CLOT dermal delivery with a moderate increase when compared to ME_2/8, ME_4/6, and ME_5/5, which were of W/O, and bi-continuous microstructures, respectively. No significant differences in CLOT dermal delivery were observed among these MEs. Therefore, O/W type ME shows superiority for CLOT dermal delivery over W/O and bi-continuous MEs.

CLOT transdermal delivery was assessed by CLOT cumulative permeated amount over 24 hours, Q_{24hr}, in the study. The Q_{24hr} value for ME_7/3 is significantly higher than other MEs ($P<0.05$), being 21.4, 2.7, and 1.7 fold of that of ME_2/8, ME_4/6, and ME_5/5, respectively. These results of significantly increased CLOT transdermal permeation from MEs of increasing water content are expected, and are in concordance with literature reports on many other drugs in ME transdermal studies (Hoppel et al., 2014; Zhang and Michniak-Kohn, 2011;Lee et al., 2003).

Table 5-3. Human Cadaver Skin PermeationStudy Results from ME Formulations containing 0.5% (w/w) of CLOT.

Formulation	Dermis Conc. ($\mu g/cm^2$)	SCE Conc. ($\mu g/cm^2$)	Q_{24hr} ($\mu g/cm^2$)
ME_2/8_CLOT-0.5%	0.54 ± 0.27	1.59 ± 0.60	0.07 ± 0.16
ME_4/6_CLOT-0.5%	0.50 ± 0.20	2.50 ± 1.12	0.55 ± 0.10
ME_5/5_CLOT-0.5%	0.60 ± 0.24	3.00 ± 0.67	0.87 ± 0.35
ME_7/3_CLOT-0.5%	1.10 ± 0.35	4.60 ± 0.48	1.50 ± 0.51

Q_{24hr} : cumulative permeated amount over 24 hours; Data report as mean ± SD; n=6 for each formulation; define CLOT, ME and SCE.

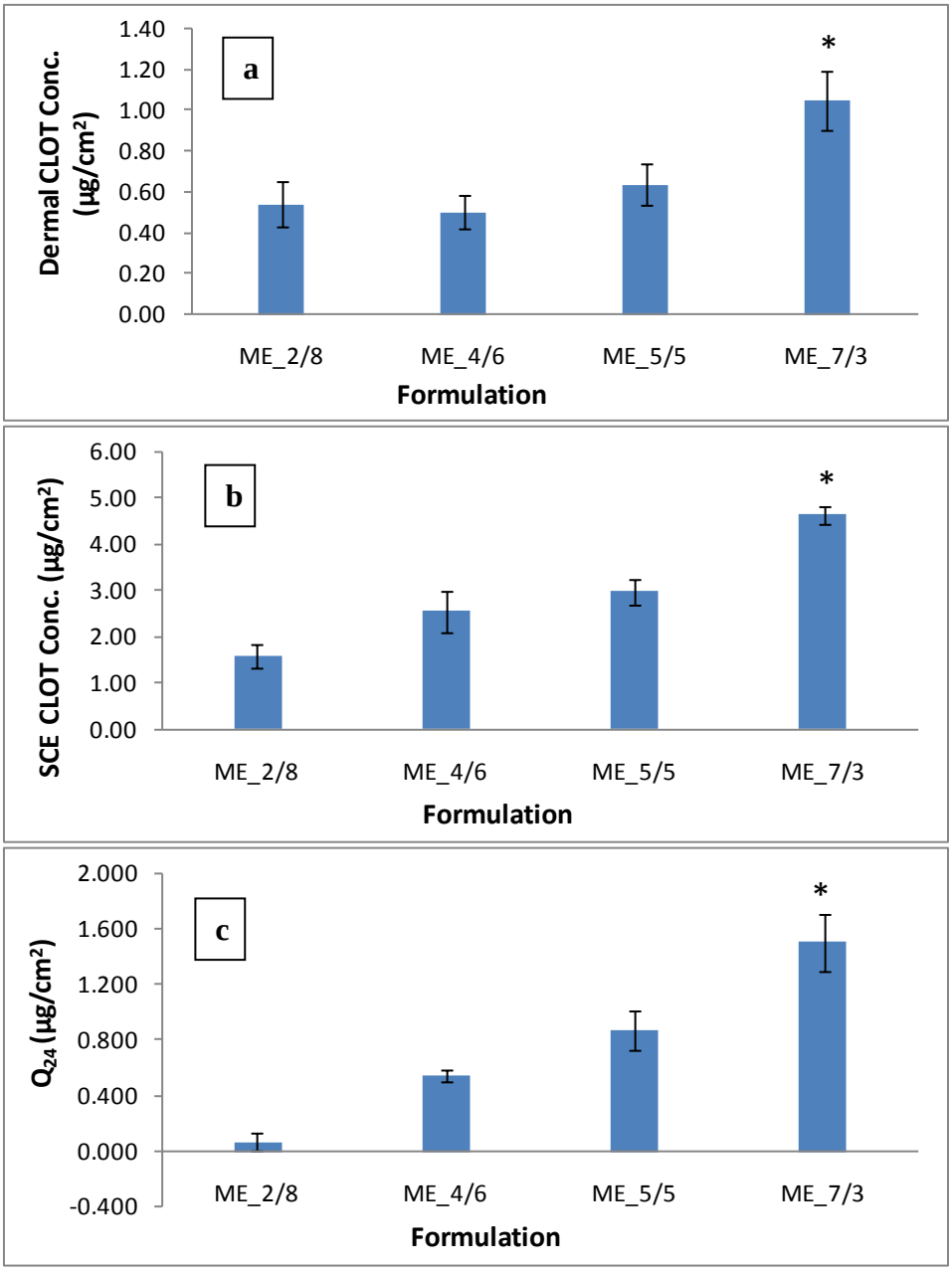

Figure 5-2. Human skin permeation testing results of MEs containing 0.5% (w/w) of CLOT: (a) Dermal CLOT concentration (µg/cm^2), (b) SCE CLOT concentration (µg/cm^2), and (c) Q_{24hr}(µg/cm^2); Data reporedt as mean ± Standard Error (SE). SCE stands for stratum corneum epidermis. n=6 for each formulation. *P < 0.05 compared to ME_2/8, ME_4/6, and ME_5/5.

5.3.3. Skin Permeation Tests for ME and ME Gel Formulations Containing 1.0% (w/w) of CLOT

Human cadaver skin permeation test results for ME, ME gel formulations, the control formulation, and Lotrimin® cream that all contained 1.0% (w/w) of CLOT, are presented in Table 5-4 and Figure 5-3.

CLOT 1.0% (w/w) solution in Propylene Glycol (PG) was first chosen as the control formulation in the study, the results (not reported here) showed that PG had noticeable dermal delivery enhancement effect for CLOT and was not suitable for being a control. Then, CLOT 1.0% (w/w) solution in Propylene Carbonate (PC) was chosen as the control formulation, because PC provided high CLOT solubility, and had been previously used as the control vehicle in atransdermal study (Sintov, 2015).

Figure 5-3 shows dermaland SCE CLOT concentrations from ME formulations. They are significantly higher than the control formulation ($P<0.05$).ME_65/35 with an O/W microstructure showed the highest dermal and SCE CLOT concentrations and adermal delivery Enhancement Ratio (ER_D) of 5.1. While dermal CLOT concentrations and ER_D from W/O ME_2/8 and bi-continuous ME_5/5 are not significantly different from each other (ER_D being 3.0 and 2.8, respectively).When CLOT load in MEs increased from 0.5% to 1.0% (w/w), the differences in thermodynamic activity of CLOT among MEs of increased water content would increase, however, the overall results of 1.0% (w/w) MEs show closely comparable extent of changeto those from 0.5% (w/w) MEs in term of dermal and SCE drug concentrations when water content increased, suggesting thatCLOT thermodynamic activity is not the main cause for observed change in dermal and SCE drug concentrations when water content increased from 20% to 65%, and rather microstructure change is the cause. In other words, ME microstructure has a

significant impact on CLOT dermal delivery, and O/W ME enables higher CLOT skin retention than W/O and bi-continuous MEs. The observed phenomena may potentially be explained based on two facts: (a) O/W ME's higher water content results in a higher degree of skin hydration which in turn increases CLOT skin penetration (Hoppel et al., 2014); and (b) CLOT, which is located at interface with surfactant/co-surfactant, will have higher mobility in O/W ME vehicle (Fanun, 2009).

For transdermal delivery as assessed by CLOT cumulative permeated amount, Q_{24hr}, the values for MEs were significantly higher than control, and increased significantly with water content.Data of CLOT dermal concentrations and transdermal Q_{24hr} from this study are in good agreement with previous literature reports on CLOT human skin permeation (Schmook et al., 2001).

If ME microstructure effects on CLOT dermal and transdermal delivery are compared, dermal delivery is moderate however, the transdermal one is significantly affected as indicated by ER_D of 3.0, 2.8, and 5.1 vs. ER_{TD} of 7.1, 11.7, and 20.4 for W/O ME_2/8, bi-continuous ME_5/5, and O/W ME_65/35, respectively. The data suggest that for dermal delivery using ME formulations, it is necessary to select the most suitable ME microstructure to get a balance between dermal and transdermal delivery in order to achieve optimal therapeutic effects for the formulation.

Additionally, Micelle_5/5 formulation that contained only surfactant/co-surfactant and water, but no oil, was also tested for CLOT human skin permeation and its dermal CLOT concentration is significantly lower than ME_5/5 ($P<0.05$). The result suggeststhat oil is a critical component in ME for drug penetration enhancement, and demonstrates the superiority of ME over a micellar vehicle for dermal delivery. The results are in

concordance with literature reports on such comparisons (Sintov, 2015; Sintov and Greenberg, 2014). One possible explanation is that oil lowers surface tension between the ME and SC, and allows better contact and penetration into SC by surfactants and the associated drug.

Furthermore, dermal CLOT concentrations of O/W ME_65/35_gel and bi-continuous ME_5/5_gel show to be equivalent to corresponding MEs, but are significantly higher compared with CLOT commercial cream, Lotrimin®. Their ER_D increased to 1.5 and 2.4 fold that of Lotrimin®, respectively. The results indicate that ME-gel formulations, which possess additional advantage of easier application vs. MEs, have the potential of providing improved dermal delivery over a conventional cream formulation. The results on ME-gels from this study are in concordance with reports of numerous previous studies that investigated ME-gel formulations for dermal delivery of various drugs (Wan et al., 2015; Fouad et al., 2013; Zhu et al., 2009).

Table 5-4. Skin Penetration Study Results of ME and Control Formulations with CLOT Load of 1.0% (w/w).

Formulation	Dermal Conc. (μg/mg)	SCE Conc. (mg/cm^2)	Q_{24hr} ($\mu g/cm^2$)	Dermal ER_D	Transdermal ER_{TD}
PC	0.022 ± 0.035	1.22±0.69	0.07 ± 0.16	1.0	1.0
ME_2/8	0.065 ± 0.018	1.71 ± 0.56	0.50 ± 0.34	3.0	7.1
ME_5/5	0.062 ± 0.007	2.61 ± 0.77	0.82 ± 0.61	2.8	11.7
ME_65/35	0.112 ± 0.022	4.53 ± 1.90	1.43 ± 0.30	5.1	20.4
Micelle_5/5	0.037 ± 0.010	1.71 ± 0.68	0.77 ± 0.30	1.7	11.0
Lotrimin®	0.046 ± 0.024	1.57 ± 1.07	0.70 ± 0.58	2.1	10.0
ME_5/5_gel	0.070 ± 0.007	1.96 ± 0.77	1.04 ±0.82	3.2	14.9
ME_65/35_gel	0.112 ± 0.055	2.47 ±0.90	1.36 ± 0.80	5.1	19.4

Data reported as means ± SD; n=3 to 5;
ER_D stands for "dermal delivery Enhancement Ratio", and is equal to ((Dermal Conc. of the formulation) / (Dermis conc. of the control));
ER_{TD} stands for "transdermal delivery Enhancement Ratio", and is equal to((Q_{24hr} of the formulation) / (Q_{24hr} of the control));

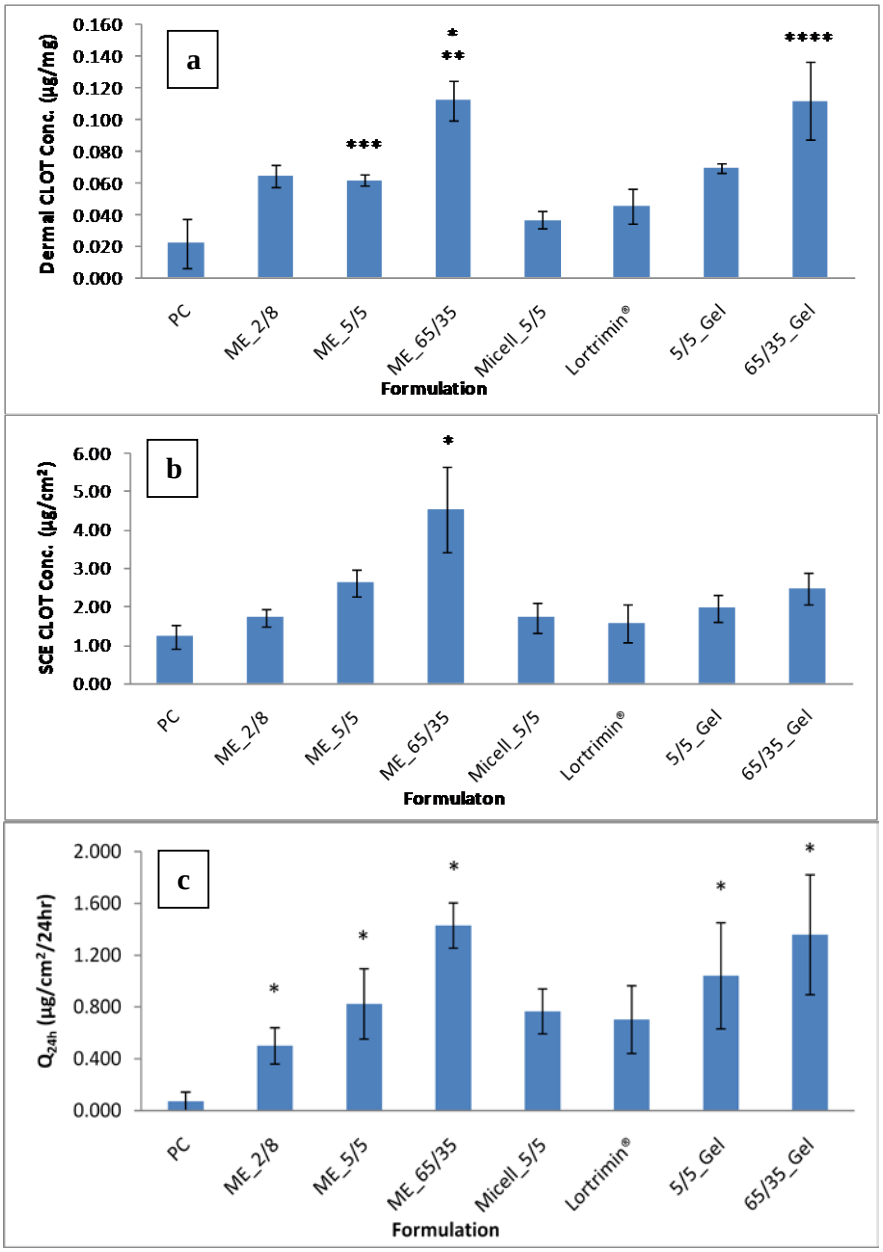

Figure 5-3. Skin permeation testing results of formulations containing 1.0% (w/w) of CLOT: (a) Dermal CLOT concentration (µg/mg), (b) SCE CLOT concentration (µg/cm^2), and (c) Q_{24hr} (µg/cm^2); Data plotted as means ± standard error. * P< 0.05 compared to PC. ** P < 0.05 compared to ME_2/8 and ME_5/5. *** P < 0.05 compared to Micelle_5/5. **** P < 0.05 compared to Lotrimin®.

5.3.4. FITC Dermal Deposition from ME Formulations in Porcine Skin Permeation Study

FITC is a hydrophobic fluorescent dye which has been used as a probing compound in skin penetration studies (Lopes et al., 2010). ME formulations possessing different microstructures containing 0.1% (w/w) FITC were used to treat porcine skin samples. The treated samples were then examined under a fluorescent microscope for FITC skin deposition profiles in different skin layers, namely the stratum corneum (SC), viable epidermis (vE), and dermis (D). FITC dermal deposition concentrations are estimated based fluorescent intensity in skin layers quantitatively analyzed by Image-J software. The results are summarized in Table 5-5 and plotted in Figure 4.Representative fluorescent microscopic images of skin samples treated by different formulations are showed in Figure 5-5.

Figure 5-4 illustrated O/W ME formulation, ME_7/3_FITC-0.1%, provided significantly higher FITC concentrations (fluorescence intensity, $P<0.05$) in all skin layers, SC, vE, and D than bi-continuous ME_4/6 and W/O ME_2/8. The results are consistent with those observed on CLOT dermal delivery in previous sections, which indicated ME microstructure plays an important role in ME dermal delivery of hydrophobic drugs, and O/W MEs enable higher dermal delivery efficiency over bi-continuous and W/O MEs under conditions set in the present study.

Fluorescent image of the skin sample that was treated by blank PBS in Figure 5e shows only skin auto-fluorescence. The image of the same skin sample by regular microscope (under bright field and the identical magnification) in Figure 5f illustrates normal skin structures. Image of the skin sample treated using PG solution containing 0.1% FITC in Figure 5a shows FITC mainly penetrated into and stayed at SC layer. Images of the skin samples treated by W/O ME_2/8_FITC-0.1% and bi-continuous

ME_4/6_FITC-0.1% in Figure 5b and 5c, respectively, show some level of deeper penetration into SC and deposition at SC layer with slightly increased depth. Finally, image of the skin sample treated by O/W ME_7/3_FITC-0.1% in Figure 5d demonstrates much deeper FITC penetration through SC and also into the dermal layer, as evidenced by relatively strong fluorescent light in wide area of full skin thickness.

Table 5-5. FITC skin deposition quantified by fluorescent intensity using Image-J software

Formulation	FITC Fluorescent Intensity (ABU [a])		
	SC	vE	D
ME_2/8_FITC-0.1%	26.2 ± 14.5	3.6 ± 2.8	1.6 ± 0.7
ME_4/6_FITC-0.1%	28.9 ± 17.3	4.1 ± 2.6	1.5 ± 0.3
ME_7/3_FITC-0.1%	55.8 ± 18.3	10.6 ± 4.3	5.6 ± 3.7

[a] Intensity was measured by the integration of pixel brightness (arbitrary units, ABU) using Image J software. n=30 for each formulations. Data expressed as means ± standard deviation.

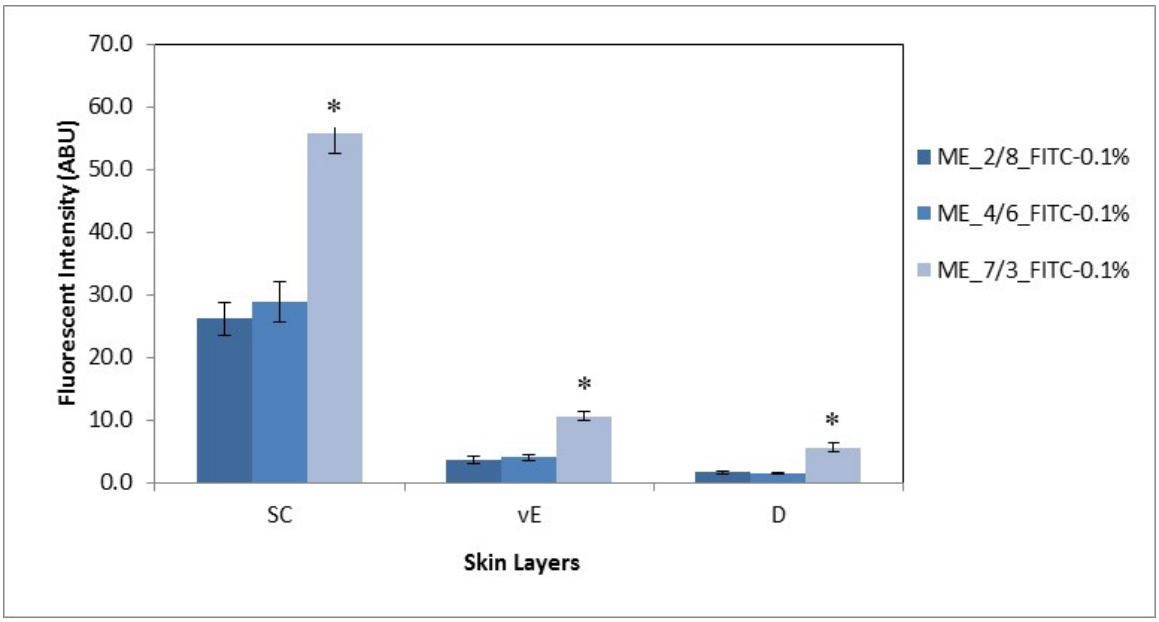

Figure 5-4. FITC porcine skin dermal deposition byME formulations containing 0.1% (w/w) of FITC, quantified based on fluorescence intensity. * P< 0.05 compared to ME_2/8_FITC-0.1% and ME_4/6_FITC-0.1%.

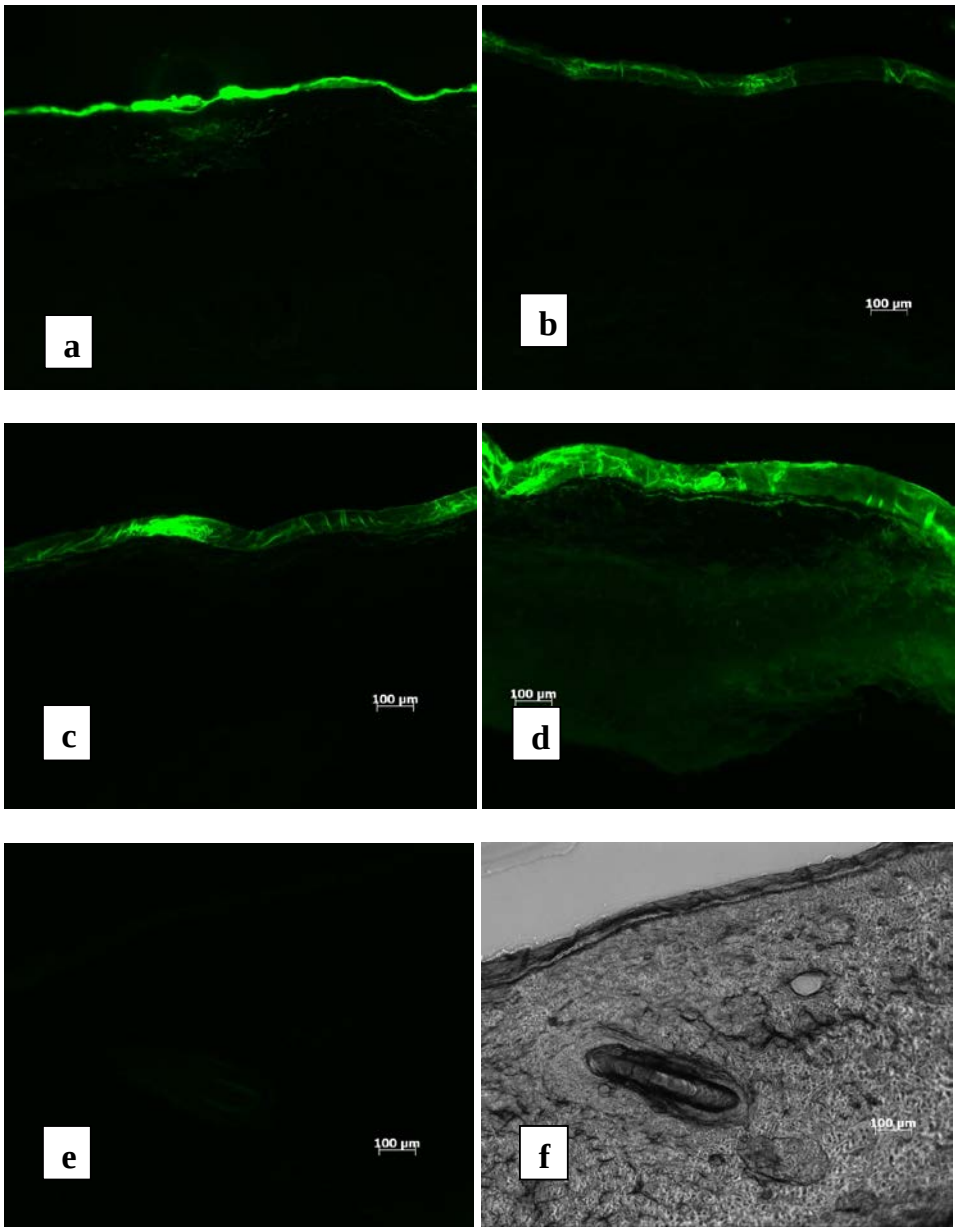

Figure 5-5. Fluorescent microscopic images of skin samples (cross-sections) topically treatedusing various formulations for 12 h: (a) PG formulation, 0.1% (w/w) of FITC, (b) ME_2/8_FITC-0.1%, (c) ME_4/6_FITC-0.1%, (d) ME_7/3_FITC-0.1%,(e)PBS, and (f) the phase-contrast image of the skin sample treated by PBS.

5.4. Conclusions

The dermal delivery of the hydrophobic drug CLOT using an alcohol-free ME formulation system and the influence of the ME microstructure were studied. Results show significant CLOT skin retention enhancement by MEs when compared with the control formulation. The dermal delivery is affected by microstructure of MEs, suggested by significantly higher CLOT depositionin dermis by O/W ME vs. W/O and bi-continuous MEs. Relatively high water content in a formulation is critical in order to form O/W microstructure and to achieve the higher dermal delivery. However, enhancement of dermal delivery as water content increase is moderate when compared with that of transdermal delivery. For example, ER_D and ER_{TD} for CLOT delivered by O/W ME_65/35 are 5.1 and 20.4, respectively. Therefore, the results suggest that to achieve an optimal drug dermal delivery by ME formulations, it is necessary to consider microstructure influence on drug percutaneous retention and also drug percutaneous retention vs. transdermal permeation to find a balance, in order to achieve the best therapeutic outcome.

Additionally, micellar formulations at the same water content showed lower dermal drug concentrations than the corresponding ME formulation, suggesting the superiority of ME vs. micellar vehicle for drug dermal delivery. Furthermore, ME-gel formulations based on O/W and bi-continuous MEs, which improved the formulation applicability, enabled significantly higher dermal drug concentration than the commercial CLOT cream product, Lotrimin®. Results of the study suggest ME formulations are potentially useful for dermal drug delivery product development.

Finally, FITC skin penetration study by MEs showed consistent results as CLOT study. O/W ME provided significantly higher FITC deposition in porcine skin layers of SC, viable epidermis, and dermis than Bi-continuous and W/O MEs. Overall, the present study highlight that ME microstructure is a critical variable in ME dermal delivery of hydrophobic drugs for skin retention enhancement. The results provide further insight toward understanding of ME permeation enhancement mechanism and also offer meaningful guiding information for ME formulation development for dermal drug delivery.

Acknowledgements

The authors would like to acknowledge the Center for Dermal Research CDR, Rutgers University for financially supporting this research work.

5.5. References

Biruss, B., Valenta, C., 2008. The advantage of polymer addition to a non-ionic oil in water microemulsion for the dermal delivery of progesterone. International Journal of Pharmaceutics 349, 269-273.

Fouad, S.A., Basalious, E.B., El-Nabarawi, M.A.,Tayel, S.A., 2013. Microemulsion and poloxamermicroemulsion-based gel for sustained delivery of diclofanacepolamine using in-skin drug depot: In vitro/in vivo evaluation. International Journal of Pharmaceutics 453, 569-578.

Ge, S., Lin, Y., Lu, H., Li, Q., He, J., Chen, B.,Wu, C., Xu, Y., 2014. Percutaneous delivery of econazole using microemulsion as vehicle: Formulation, evaluation and vehicle-skin interaction. International Journal of Pharmaceutics465, 120-131.

Hashem, F.M., Shaker, D.S., Ghorab, M.K., 2011. Formulation, characterization, and clinical evaluation of microemulsion containing clotrimazole for topical delivery. AAPS PharmSciTech. 12, 879-886.

Heuschkel, S., Goebel, A., Neubert, R.H.H., 2008. Microemulsions—moderncolloidal carrier for dermal and transdermal drug delivery. J. Pharm. Sci. 97(2), 603-631.

Hoppel, H., Ettl, H., Holper E., Valenta, C., 2014. Influence of the composition of monoacyl phosphatidylcholine based microemulsions on the dermal delivery of flufenamic acid. Int. J. Pharm. 475, 156-162.

Hoppel, M., Juric, S., Ettl, H., Valenta, C., 2015. Effect of monoacyl phosphatidylcholine content on the formation of microemulsions and the dermal delivery of flufenamic acid. Int. J. Pharm. 479, 70-76.

Kreilgaard, M., 2001. Dermal pharmacokinetics of microemulsion formulations determined by in vivo microdialysis. Pharm. Res. 18, 367-373.

Lee, P.J., Langer, R., Shastri, V.P., 2003. Novel microemulsion formulation enhancer formulation for simultaneous transdermal delivery of hydrophilic and hydrophobic drugs. Pharmaceutical Res.20, 264-296.

Lopes, L.B., VanDeWall, H., Li, H.T., Venugopal, V., Li, H.K., Naydin, S., Hosmer, J., Levendusky, M., Zheng, H., Bentley, M.V., Levin, R., Hass, M.A., 2010. Topical delivery of lycopene using microemulsions: enhanced skin penetration and tissue antioxidant activity. J. Pharm. Sci. 99(3), 1346-1357.

Mahrhauser, D., Kahlig, H., Partyka-Jankowska, E., Peterlik, H., Binder, L., Kwizda, K., Valenta, C., 2015. Investigation of microemulsion microstructure and its impact on skin delivery of flufenamic acid. Int. J. Pharm. 490, 292-297.

Montenegro, L., Carbone, C., Puglisi, G., 2011. Vehicle effects on in vitro release and skin permeation of octylmethoxylcinnamate from microemulsions. Int. J. Pharm. 405, 162-168.

Mura, P., Bragagni, M., Mennini, N., Cirri, M., Maestrelli, F., 2014. Development of liposomal and microemulsions for transdermal delivery of clonazepan: Effect of randomly methylated β-cyclodextrin. Int. J. Pharm. 475, 306-314.

Ning, M., Gu, Z., Pan, H., Yu, H., Xiao, K., 2005. Preparation and in vitro evaluation of liposomal/niosomal delivery systems for antifungal drug clotrimazole. Indian Journal of Experimental Biology 43, 150-157.

Pepe, D., Phelps, J., Lewis, K., Dujack, J., Scarlett, K., Jahan, H., Bonnier, E., Milic-Pasetto, T., Hass, M.A., Lopes, L.B., 2012. Decylglucoside-based microemulsions for cutaneous localization of lycopene and ascorbic acid. Int. J. Pharm. 434, 420-428.

Puglia, C., Bonina, F., Trapani, G., Franco, M., Ricci, M., 2001. Evaluation of in vitro percutaneous absorption of lorazepam and clonazepam from hydro-alcoholic gel formulations. Int. J. Pharm. 228, 79-87.

Ren, Q., Deng C., Meng, L., Chen, Y., Chen, L., Sha, X., Fang, X., 2014. In vitro, ex vivo, and in vivo evaluation of the effect of saturated fat acid chain length on the

transdermal behavior of ibuprofen-loaded microemulsions. J. Pharm. Sci. 103, 1680-1691.

Schmalfub, U., Neubert, R., Wohlrab, W., 1997. Modification of drug penetration into human skin using microemulsions. J. Controlled Release. 46,279-285.

Schmook, F.P., Meingassner, J.G., Billich, A., 2001. Comparison of human skin or epidermis models with human and animal skin in in-vitro percutaneous absorption. Int. J. Pharm. 215, 51-56.

Sintov, A.C., Greenberg, I., 2014. Comparative percutaneous permeation study using caffeine-loaded microemulsion showing low reliability of the frozen/thawed skin models. Int. J. Pharm. 471, 516-524.

Sintov, A.C., 2015. Transdermal delivery of curcumin via microemulsion. Int. J. Pharm. 481, 97-103.

Thomas, S., Vieira, C.S., Hass, M.A., Lopes, L.B., 2014. Stability, cutaneous delivery, and antioxidant potential of lipoic acid and α-tocopheral codrug incorporated in microemulsions. J. Pharm. Sci. 103, 2530-2538.

Todosijevic, M., Savic, M.M., Bartinic, B.B., Markovic, B.B., gasperlin, M., Randelovic, D.V., Lukic, M.Z., Savic, S.D., 2015. Biocompatible microemulsions of a model NSAID for skin delivery: A decisive role of surfactants in skin penetration/irritation profiles and pharmacokinetic performance. Int. J. Pharm. 496, 931-941.

Tsai, M.J., Huang, Y.B., Fang, J.W., Fu, Y.S., Wu, P.C., 2015. Preparation and evaluation of submicron-carriers for naringenin topical application. Int. J. Pharmaceut (2015), http://dx.doi.org/10.1016/j.ijpharm.2015.01.034.

Valenta, C., Schultz, K., 2004. Influence of carrageenan on the rheology and skin permeation of microemulsion formulations. J. Controlled Rel. 95, 257-265.

Wan, T., Xu, T., Pan, J., Qin, M., Pan, W., Zhang, G., Wu, Z., Wu, C., Xu, Y., 2015. Microemulsion based gel for topical dermal delivery of pseudolaric acid B: in vitro and in vivo evaluation. Int. J. Pharm. 493, 111-120.

Zhang, J., Michniak-Kohn, B, 2011. Investigation of microemulsion microstructures and their relationship to transdermal permeation of model drugs: ketoprofen, lidocaine, and caffeine. Int. J. Pharm. 421, 34-44.

Zhao,L., Wang, Y., Zhai, Y., Wang, Z., Liu, J., Zhai, J., 2014. Ropivacaine loaded microemulsion and microemulsion-based gel for transdermal delivery: preparation, optimization, and evaluation. Int. J. Pharm. 477, 47-56.

Zhu, W., Guo, C.,Yu, A., Gao, Y., Cao F., Zhao, G., 2009. Microemulsion-based hydrogel formulation of penciclovir for topical delivery. Int. J. Pharm. 378, 152-158.

APPENDIX A. INTRODUCTION

Chemical enhancers decrease the skin barrier function and increase drug skin permeation. Many compounds have been found to be active in increasing skin permeation and are considered as chemical enhancers. To name some, they are alkanols and alkenols (alcohols, polyethylene glycol, propylene glycol), fatty acids (lauric acid, myristic acid, stearic acid, oleic acid), fatty acid esters (isopropyl myristate, glyceryl monolaurate, glyceryl monooleaate, glyceryl monocaprylate, ethyloleate, ethyldecanoate), amides (Azone®, dimethyl formamide, dimethyl acetamide), sulfoxides (DMSO, N-decylmethyl sulfoxide), cyclic carbohydrates (β-cyclodextrin, HPβCD), terpenes (p-menthane, d-limonene, dipentene, menthol), and pyrrolidones (N-methyl-pyrrolidone, 1-ethylpyrrolidone) [1].

In general, the chemical enhancer permeation enhancement involves either disruption of lipid ordered organization structure or interaction with keratin in corneocytes, causing opening up the dense protein structure. Alteration of the chemical environment could also lead to better partitioning of the drug in the SC. Figure 5 illustrates some plausible interactions of enhancers in SC lipid layers (Barry, 2004 [2]).

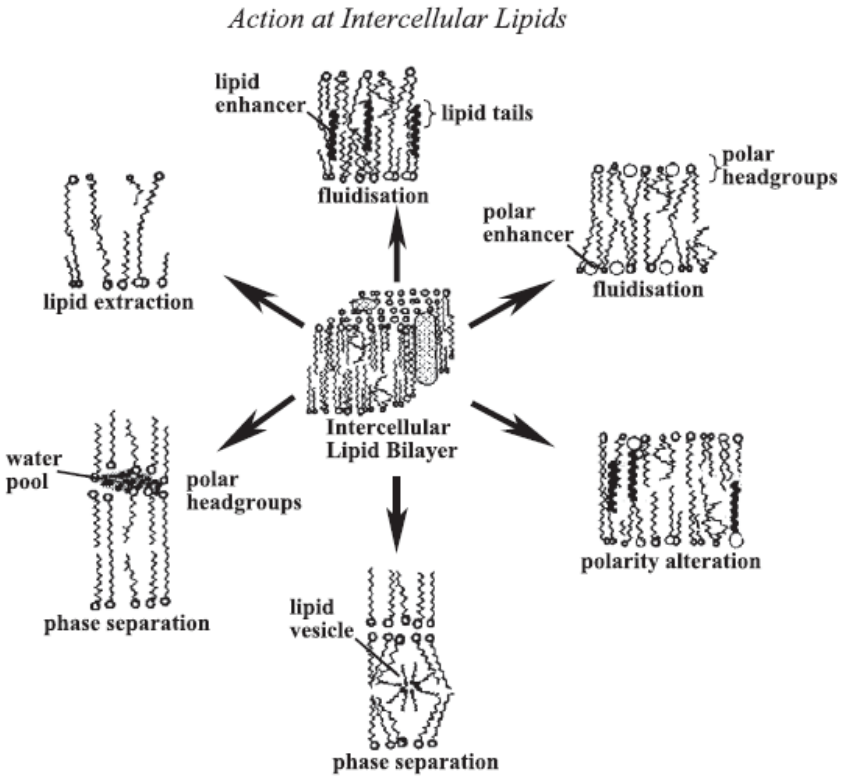

Figure 5. Plausible action mechanism of permeation enhancers within the SC intercellular domain (William and Barry, 2004 [2])

S,S-dimethyl iminosulfuranes are one new class of compounds that was discovered and investigated by Dr. Michniak's group over past years [3,4], had been showed to have the transdermal permeation enhancement or retardence activity. Among the 20 or so compounds being studied, one of the highest permeation enhancement activity is S,S-dimethyl-N-(4-bromo-benzoyl)-iminosulfurane (denoted as DMBIS) [5]. At a relatively low concentration of 0.4 M, it increased permeation of the model drug hydrocortisone 11.9 and 17.0 times over 24 hours in hairless mouse skin and human cadaver skin, respectively. The compound also showed to be relatively safe when the concentration used for skin treatment was below 0.2 M. However, the mechanism of

permeation enhancement of iminosulfurane compounds was not clearly understood, especially for DMBIS, which standed out to show sigificantly high enhancement activity. One initial graduate study effort was to try to investigate DMBIS transdermal permeation further and to gain insight of its peameation enhancement mechanism. The results from the study are presented in Appendix Chapter 2 and 3. This work in Appendix Chapter 3 was an collaboration effort with other researchers and the results was published in Journal of Controlled Release (2009) [28].

APPENDIX B. SYNTHESIS OF TRANSDERMAL PERMEATION ENHANCER S,S-DIMETHYL-N-(4-BROMOBENZOYL)-IMINOSULFURANE

B.1. Introduction

The searches and studies on new effective and safe enhancers never stop and continue to be an interested subject to pharmaceutical scientists in the area. The mechanism of enhancing dermal penetration is also a subject for persistent studies because the progresses in the area will lead to design and develop more potent and safer enhancing agents. A novel permeation enhancer bromo-aromatic iminosulfuranes had been reported to be active in enhancing skin permeation of model drugs and be relatively safe [3,4]. The mechanism of the enhancer is not well understood, and is one of the subjects of investigation in this graduate research.

In order to conduct the permeation enhancement mechanism study, DMBIS was firstly synthesized based on the literature reports [3,4]. The sythesis reaction is required to be conducted at low temperature -60 °C and anhydrous environment initially, and then to go through a series steps of base neutralization, organic extraction, and crystallization. Each step reaction conditions need to be controlled acurately to obtained good yield and purity of the the final product.

B.2. Material and Method

DMSO, trifluoroacetic anhydride, dichloromethane, sodium hydroxide, magnesium sulfate (anydrous), and 4-bromo-benzamide were purchased from Sigma (St. Louis, MO).

Iminosulfurane are conventionallyy synthesized by activation of DMSO through the reaction with an electrophilic reagent followed by treatment of the resultant intermediate active complex with an amino derivative. In this case, trifluoroacetic anhydride was used as the activating electrophilic agent.

All reactions were conducted in glassware that was dried in an over at 140 °C, assembled hot, and cooled in a streem of high purity nitrogen. A postive pressure of nitrogen was maintained during the reactions as showed in the reaction setup, Figure 1. DMSO was dried by the treatment of molecular sieves 3A.

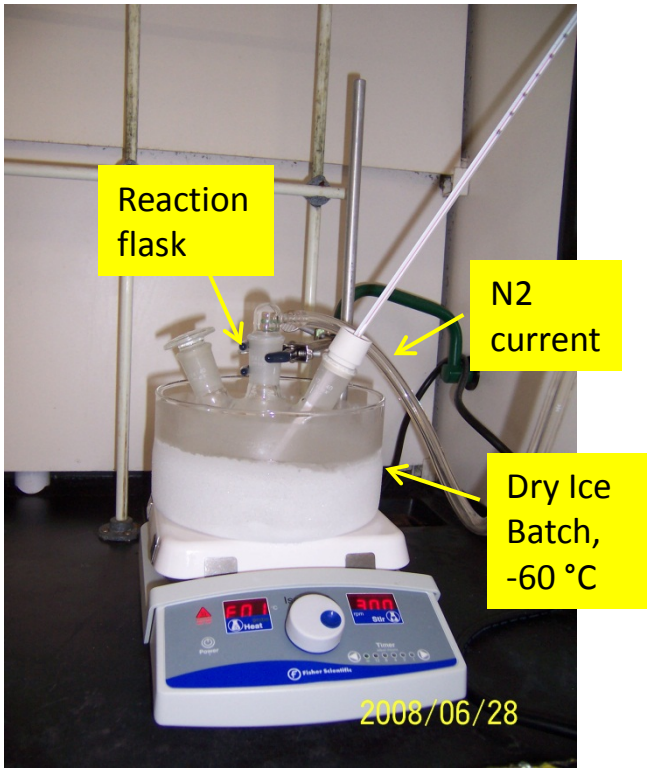

Figure 1. DMBIS synthesis reaction apparatus setup

B.3. Synthesis and Purification

The synthesis procedure used was a modification from the method by N. Kim et al. [3], and is summarized as follows. A solution of DMSO (1.3 mL, 18 mmol) in dichloromethane (5 mL) was stirred at -60 °C and treated drop wise with trifluoroacetic anhydride (1.4 mL, 10 mmol) at such a rate that the temperature did not rise above -50 °C (the reaction was exothermic). The resultant mixture containing a white precipitate was treated dropwise with a solution of 4-bromo-benzamide (10 mmol) in dichloromethan/DMSO (1:1, 4 mL) maintaining the temperature below -50 °C. Upon completion of the addition, the white precipitate disappeared and a clear solution was then stirred at -50 °C for an additional 3 h. Quenching with aqueous sodium hydroxide (10%, 12 mL) was followed by extraction with dichloromethane (2x20 mL). The extract was washed with water, dried (MgSO4), concentrated, and the residue was crystallized from ethanol. Figure 2 shows the reaction scheme.

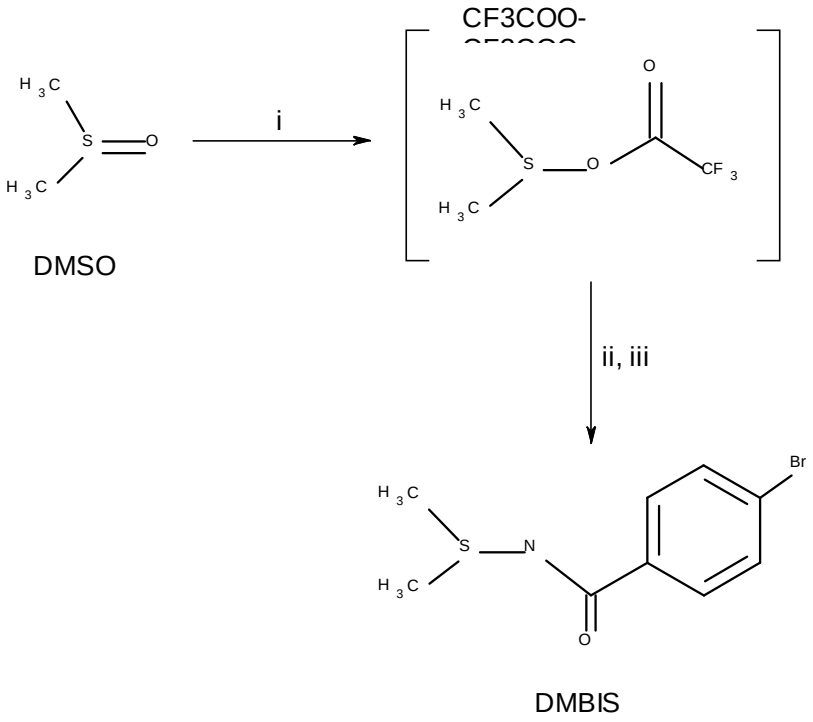

Figure 2. DMBIS synthesis reaction scheme, (i) -60 °C, a slow addition of $(CF_3CO)_2O$ (1 eq.) in CH_2Cl_2 to DMSO (2 eq.) in CH_2Cl_2; (ii) -50 °C, a slow addition of 4-bromo-benzamide (1 eq.) in CH_2Cl_2/DMSO, then 3 h at -50 °C; (iii) quenching with 10% aqueous NaOH (3 eq.) at -50 °C, extraction with CH_2Cl_2, crystallization from ethanol. Melting Point 107-109 °C;

B.4. The Final Product Testing

The final product, DMBIS was tested by ^{1}H-NMR and DSC to confirm its identy and purity. Both ^{1}H-NMR and DSC results of the synthesis product are consistent with the literature report [3]. The testing results are presented in Figure 3 and 4.

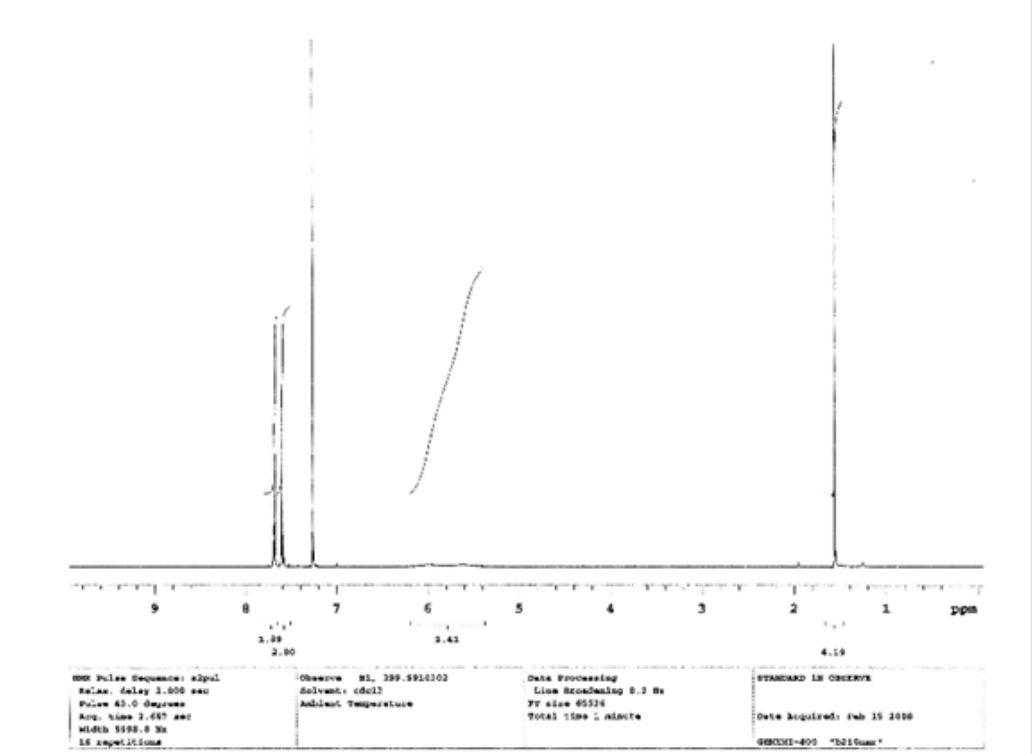

Figure 3. ^{1}H-NMR spectrum of the sample of synthesized final product of DMBIS in $CDCl_3$.

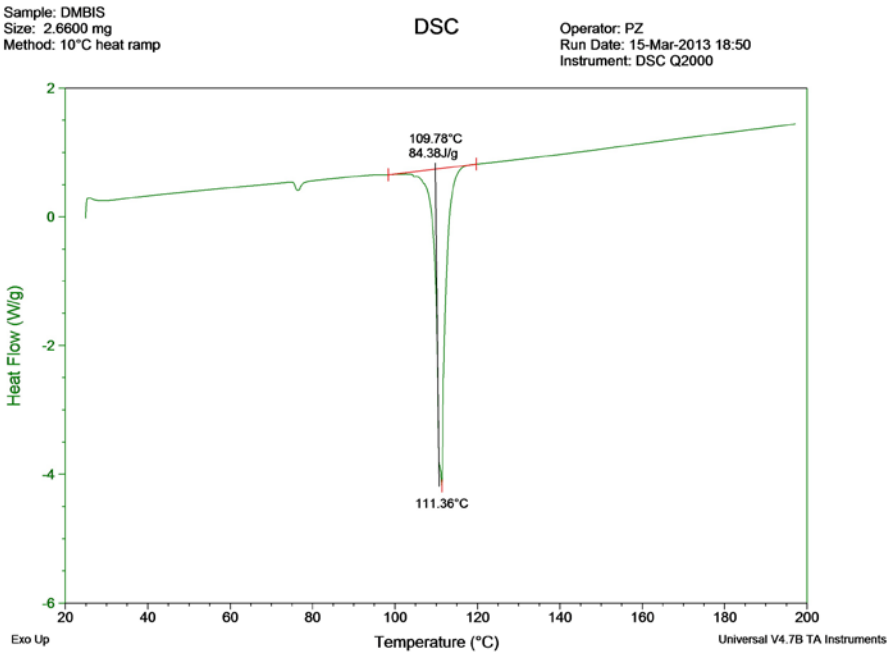

Figure 4. DSC testing result of the sample of synthesized final product of DMBIS

APPENDIX C. CUTANEOUS BIOTRANSFORMAION N-(4-BROMOBEZOYL)-S,S-DIMETHYLIMINOSULFURANE AND ITS PRODUCT, 4-BROMOBENZAMIDE, LEADING TO PERCUTANEOUS PENETRATION ENHANCEMENT OF DRUGS: INITIAL EVIDENCE USING HYDROCORTISONE

C.1. Introduction

The skin is an excellent barrier to penetration of many substances, primarily due to the lipophilic properties of the outmost layer of stratum corneum. Significant efforts have been made and numerous strategies have been proposed to overcome the impermeability of human skin in an attempt to develop and improve the transdermal drug delivery route and produce an effective alternative to oral delivery [6-17]. One of the strategy, which has ben extensively studies, is the chemical permeation enhancement (CPE) by modification of the stratum corneum. It has been suggested [18,19] that the mechanism by which these enhancers affect skin permeability are (a) disruption of the ordered lipid bilayers' structure such as fatty acids, Azone, or DMSO, and eventual fluidization of the lipid environment of the stratum corneum, (b) interaction with intracellular proteins of the stratum corneum, and (c) improvement of partitioning and solubility of the drug in the stratum corneum.

In previous reports [3,4], aromatic S,S-dimethyliminosulfurane derivatives have been introduced and studied for their CPE activities. These molecules are based on a DMSO molecule in which a nitrogen atom substituted to the arylsulfonyl, aroyl, or aryl group replaced the DMSO oxygen atom. S,S-dimethyl-N-(4-bromobenzoyl)-

iminosulfurane (DMBIS) was the most effective permeation enhancer, based on the previous studies using hairless mouse and human cadaver skin [5]. These studies have also shown that the excellent enhancement effect of DMBIS could not be achieved with other various analogs including other halobenzoyl derivatives (i.e. F, Cl, I). Thus, 4-bromo-substitution on the benzoyl imino-dimethylsulfurane molecule enables a dramatic enhancement effect while other halogeno- and various derivatives have a relatively poor or no effect. Therefore, it is hypothesize that the enhancement effect, which is specifically attributed only to the bromo-substituted iminosulfurane (DMBIS) might be related to an enzyme site selectivity, and the high concentration required to generate the effect may imply an in situ formation of a bio-product from DMBIS as a substrate of the enzymatic catalysis, while this bio-product is used as the active permeation enhancer. This hypothesis has also emerged due to the accumulating evidence of the skin's role as a highly metabolizing organ that acts as a frontal guard to protect the body from toxicants, reactive oxygen species (ROS), and various environmental pollutants [20,21,22]. As one related example, skin metabolism of dinitro-chlorobenzene to glutathione conjugate, which absorbed through mouse, rat, pig ear, and human skin, was related to skin glutathione-S-transferase activity and high levels of glutathione (GSH) [23]. As another example, the skin metabolism of nitroglyerin to 1,2- and 1,3-glyceryl dinitrate was significantly enhanced by GSH, a co-factor of glutathione-S-transferase [24].

In the present study, we attempt to understand the mechanism by which DMBIS and its immediate degradation product, 4-bromobenzamide (BBA), enhance skin permeation of drugs from the view of its metabolism in the skin. Our specific objectives were (a) to elucidate whether DMBIS and BBA are metabolized by skin tissue taken from

various species and (b) to evaluate whether the skin metabolism is correlated with the observed enhancement activity of a model drug.

C.2. Material and methods

C.2.1. Chemicals

N-(4-bromobenzoyl)-S,S-dimethyliminosulfurane (DMBIS) was synthesized as based on the method as described previously [3,4]. 4-bromobenzamide, iodine, iodoacetic acid (IAA), dl-dithiothreitol (DTT), N-ethylmaleimide (NEM), propylene glycol, and phosphate buffer saline (PBS) were purchased from Sigma-Aldrich (St. Louis, MO). Acetonitrile, methanol, and water were HPLC grade and purchased from Sigma-Aldrich (St. Louis, MO).

C.2.2. Animal and skin

Skin excised from hairless mice (NCRNU/Mcr Nude homozygous, Taconic Farms, Inc., Germantown, NY) was provided by Dr. Minko from Ernest Mario School of Pharmacy, Rutgers University (Piscataway, NJ), and used on the same day. Sprague dealey rats (male, 200-300 g) were supplied by Charles River Laboratory (Wilmington, MA). Full-thickness skin was taken from the rat carcasses, and kept at – 20 °C. Porcine skin was obtained from young Yorkshire pigs (26.5 – 28 kg, NMDNJ, Newark, NJ). The pig skin was excised and dermatomed using Padgett® Model B Electric Dermatome (Integra LifeSciences, Plainsboro, NJ). The thickness of the dermatomed skin ranged 500-600 μm. Human epidermis was separated from human cadaver skin (National Disease Research Interchange – NDRI, PA, # OD25080). The human cadaver skin was thawed at room temperature before immersion in PBS (pH 7.4) at 60 °C for 45 s to

separate the dermis from epidermis. The epidermis was peeled off gently with a pair of forceps (average thickness of 100 – 150 μm) and was then cut into appropriate size and stored at – 80 °C.

C.2.3. Skin metabolism

Excised skin (from mouse, rat or pig) was cut to small pieces and incubated at 37 C within PBS (pH 7.4); the skin-PBS ratio was 1:5 (w/v) in all experiments. Just prior to incubation, 1 mg/mL solution of DMBIS or BBA were introduced to produce an initial solution concentration of 10 μg/mL. Aliquots (0.1 mL) of the solution were withdrawn at 10, 20, 30, 40, 50, 60, 90, and 120 min. To stop further reaction, the samples were diluted with 0.2 mL of a cold methanol-water (1:1) mixture. Samples were kept at – 20 C until analyzed for remaining DMBIS or BBA, aand formed BBA by HPLC. As BBA was found to be the major and immediate product of DMBIS, inhibition of BBA biotransformation was examined by adding various modifiers into the skin-PBS system prior to BBA introduction, as described below.

C.2.3.1. Iodine

Appropriate aliquots of a concentrated iodine solution (2 mM I2 in ethanol/propylene glycol/water 1:20:79% vol) were added into the skin-PBS system to produce initial concentrations of 4-25 μM before the introduction of BBA. It was noted that in the presence of skin, the brownish solution formed after iodine addition was very rapidly decolored, and the obtained results were concentration independent within the working range of 4-25 μM. In seven control experiments (without iodine), the corresponding aliquots of the vehicle used to dissolve iodine were added.

C.2.3.2. Alkylating agents

Into skin containing PBS solutions, appropriate aliquots of 0.4 M NEM solution (in PBS, pH 8) and 1 M IAA (in 1 M NaOH) were incoporated to produce 10 mM and 20 mM final concentrations of NEM and IAA, respectively. The skin in the NEM solution was incubated for 1 h at 37 °C prior to BBA introduction. The skin in the IAA solution was left at ambient temperature for 1 h, then DTT solution was added to quench IAA (40 mM) and BBA was introduced.

C.2.4. Permeation enhancement of hydrocortisone by DMBIS and BBA in Franz cells

The permeation of hydrocortisone (HC) through various skins from different aniaml spieces was measured in vitro with numerous vertical Franz diffusion cells (Permegear, Inc., Bethlehem, PA) filled with PBS at pH 7.4. The diffusion area was 0.64 cm2, and the receptor compartment volume was 5.1 mL. The receptor fluid was maintained at 37 °C and stirred continuously at 600 rpm using a magnetic stirrer. On the day of the experiment, skin pieces were thawed and mounted on the Franz diffusion cells. After 1 h of skin equilibration, 4 μl 0.4 M DMBIS or BBA solutions (in propylene glycol) or plain propylene glycol was pipetted onto the skin. Six cells were assigned for each group (DMBIS, BBA and vehicle control). The enhancerswere allowed to permeate into the skin (and be metabolized) for 1 h. After 1 h, a 40 μl saturated solution of hydrocortisone in propylene glycol was added. Receptor samples of 300 μl were removed through the cell sampling port and immediately replaced with an equivalent volume of PBS (pH 7.4) at 0, 4, 7, 10, 18, 20, 22, and 24 h after drug application. The cellswere checked for air bubbles at each sampling point. The samples were kept at −20 °C until

analyzed by HPLC. After analysis, datawere expressed as the cumulative permeation (Qt) of BBA (only small levels of penetrating DMBIS were detected) and hydrocortisone per unit of skin surface area, Qt/S (S=0.64 cm2). The slope of the linear portion of the permeation curve provided the flux value in $\mu g \cdot cm^{-2}$ h^{-1} correct at steady state. The lag time was determined by extrapolating the linear portion of the curve to the x-axis. Enhancement ratio (ER) for flux was calculated by dividing the flux for skin treated with enhancer by the flux obtained without enhancer treatment (control).

C.2.5. Penetration enhancement of hydrocortisone after epidermal treatment with iodoacetate

The permeation of hydrocortisone through human epidermis was measured in vitro with six vertical Franz diffusion cells (Permegear, Inc., Bethlehem, PA) filledwith PBS at pH7.4. The diffusion areawas 0.64 cm^2, and the receptor compartment volume was 5.1 ml. The receptor fluid wasmaintained at 37±0.5 °C and stirred continuously at 600 rpm using a magnetic stirrer. On the day of the experiment, epidermis pieces were thawed and mounted on the Franz diffusion cells. Twenty µl of 1 M IAA solution (in 1MNaOH) was applied with 50 µl PBS (pH 8.5 in the donor compartment). After 45 min, 40 µl of DTT was added to the donor chamber and was allowed to react for 15 min. In control cells, 50 µL PBS (pH8.5) and 20 µlwater followed by another portion of 40 µlwaterwere used instead of IAA/DTT. After treatment, the fluid in the donor compartment was removed and 4 µl 0.4 M BBA solution (in propylene glycol) was pipetted onto the epidermis in all cells. The solution was allowed to permeate into the skin (and be metabolized) for 1 h. After 1 h, a 40 µl saturated solution of hydrocortisone in propylene glycol was added. Receptor samples of 300 µL were removed through the

cell sampling port and immediately replaced with an equivalent volume of PBS (pH 7.4) at 0,1, 2, 7, 20, 22, and 24 h after drug application. The cells were checked for air bubbles at each sampling point. The samples were kept at −20 °C until analyzed by HPLC.

C.2.6. Simultaneous HPLC analysis of DMBIS, BBA and hydrocortisone

Samples were analyzed using Agilent 1100 automated HPLC with diode array detector (Agilent Technologies, Inc., Santa Clara, CA). Aliquots of 20 μl from each sample were injected into the HPLC system, which was equipped with a prepacked C18 column (Brava ODS, 5 μm, 250×4.6 mm, Alltech Associates, Inc., Deerfield, IL). The simultaneous detection of DMBIS, BBA and hydrocortisonewas carried out at 242 nm. The samples were chromatographed using a mobile phase consisting of water–acetonitrile or 0.05% acetic acid solution–acetonitrile at a flow rate of 1.4 mL/min. The gradient systemwas programmed to linearly alter the solvents' mixture from water–acetonitrile ratio of 80:20 to 60:40 in 7 min. Calibration curves (peak area versus drug or enhancer concentration) were linear over the range 1–20 μg/mL (in PBS). The limit of quantitation was 0.1 μg/mL.

C.3. Results and discussion

C.3.1. Elimination of DMBIS in buffer solutions and in the presence of skin tissue

Fig. 1 demonstrates how fast DMBIS decomposes to BBA in aqueous solutions at four different pH values, i.e., up to 80% of the substance was eliminated in 8 h. The half-life of the reaction kinetics is approximately 3 h as shown form the point of intersection of DMBIS elimination-BBA formation lines. No difference in DMBIS elimination as well as in BBA formation was noted among the four buffer pHs.

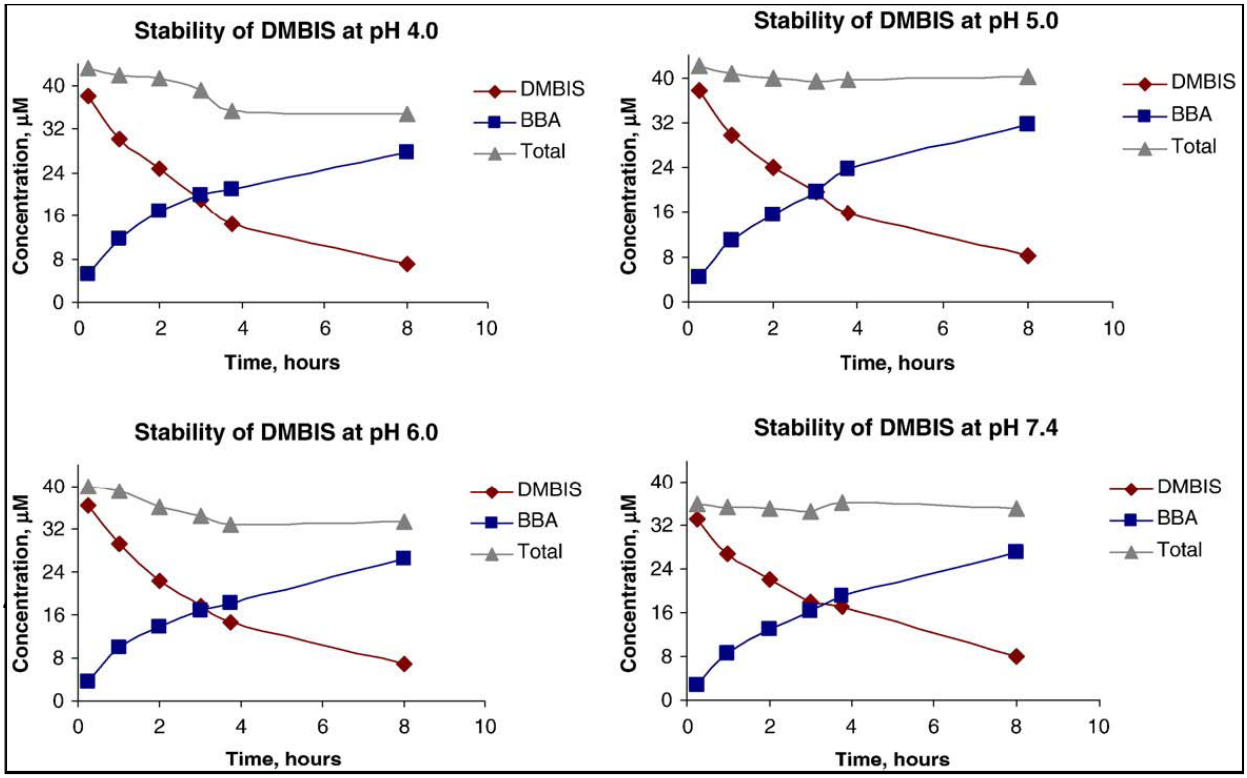

Figure 1. DMBIS hydrolysis at pH values ranged from 4 to 7.4. A simultaneous formation of BBA and the toal molar concentration of the remaining DMBIS and the formaed BBA at each time point are also shown.

A relatively more interesting phenomenon relating to DMBIS decomposition was presented in Fig. 2. The half-life of elimination in buffer solution (pH 7.4) decreased from about 3 h to 1 h when the substance had brought in contact with skin tissue at 37 °C. After 2 h, only 38.3% (±4.1%) of the initial quantity of DMBIS remained in the buffer system when it had been incubated with skin, compared to 74.8% (±4.3%) that remained with no presence of skin (Fig. 3b). It is also interesting to note that compared to the 100% mass balance (DMBIS plus BBA moles) obtained without the skin tissue, only 84% of total DMBIS and formed BBA molar quantities remained after 2 h of incubation with skin. This difference is obviously due to the skin metabolism of BBA as presented and explained further in following sections.

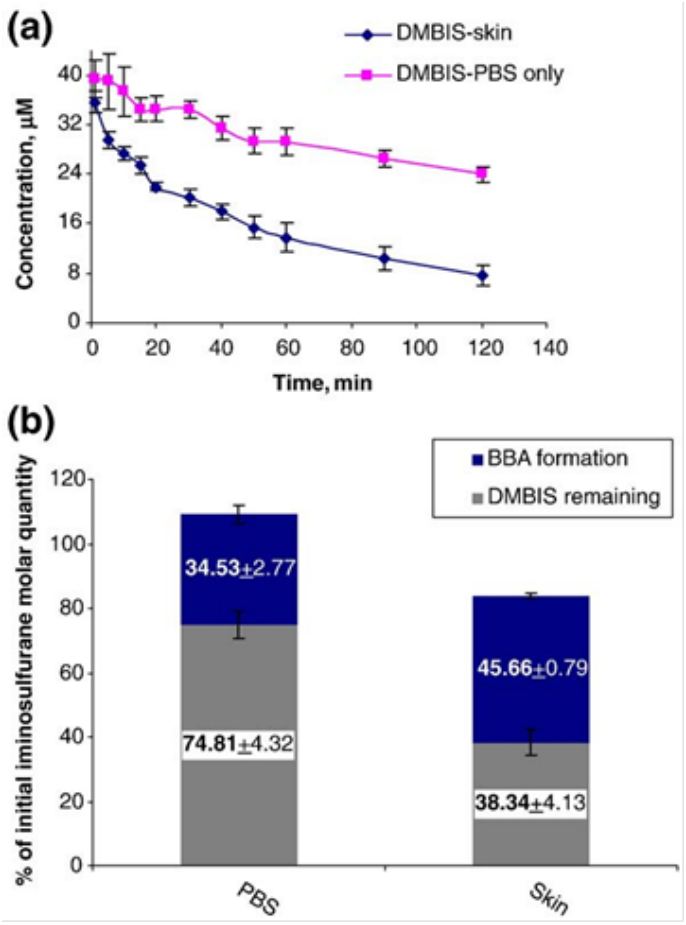

Figure 2. Elimination of DMBIS in the presence of pig skin tissue compared to the elimination without skin. (a) The kinetic profile of DMBIS dlimination, and (b) the mass balance as calculated after 120 min incubation including the molar percentage of the formed BBA.

C.3.2. Inhibition of the metabolic elimination/transformation of BBA in skin tissues — the influence of iodine

Iodine is a mild oxidant that can alter the properties and activity of proteins by a variety of reactions; however, when using small quantities of iodine at physiological conditions, its oxidation is limited primarily to cysteinyl residues (i.e., free thiol groups). The free thiol groups in the protein can be oxidized either to sulfenic acid (–SOH), sulfinic acid (–SO2H) or sulfonic acid (–SO3H) groups, and even to a disulfide bridge (–

SS–) in cases where two sulfhydryl groups exist in proximity within the protein molecule. Iodine oxidation may cause inactivation of proteins such as urease and creatine kinase [25].

As shown in Fig. 3, iodine slows down the metabolism of BBA in the presence of dermatomed porcine skin (Fig. 5a) or rat skin (Fig. 5b). It is interesting to note that we have never in any of our experiments observed a complete inhibition of the metabolic process by iodine. This may imply that iodine is involved in the inhibition of certain steps (probably the last step) in the enzymatic process, but it cannot modify all participating enzymes. As most, if not all, of the common metabolic reactions are reversible and become fixed when the next reaction step removes the product, it is reasonable to conceive that iodine intervenes in the last metabolic reaction. A greater success was achieved when iodine (in I_2/KI aqueous solution) was applied in the donor compartment of vertical Franz diffusion cells mountedwith rat skin for the entire experiment. BBA that had been exposed to the dermis side of the skin in the receptor compartmentwas rapidly eliminated without iodine in the donor, but its disappearance was completely halted after a few hours when iodine was present in the donor. Figure 3 illustrates the significant difference between the elimination of BBA exposed to iodine-treated and untreated skin, while Figure 3b presents the mass balance after 22 h, showing that I_2 inhibited approximately 30% of the metabolism of BBA by rat skin.

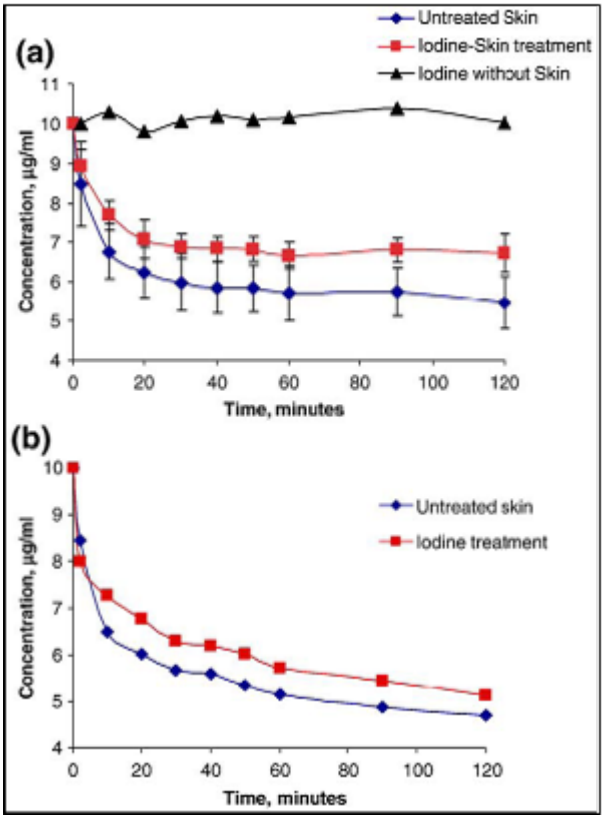

Figure 3. Elimination profiles of BBA in the presence of (a) pig skin and (b) rat skin at physiological conditions in vitro with and without iodine pretreatment of the skin (n=7).

C.3.3. Inhibition of the metabolic elimination/transformation of BBA in rat skin — the influence of alkylating agents

Since the evident inhibition of the metabolic elimination of BBA by iodine is seemingly related to oxidation reactionswith cysteinyl residues of the enzymes, we predict that covalent blocking of the free sulfhydryls by alkylating agents might be a better strategy to inhibit the enzymes involved in the process. Chemical modification of proteins by iodoacetic acid (IAA) and N-ethylmaleimide (NEM) has been known to involve reactions that occur specifically at the thiol groups of cysteinyl residues. The introduction of these S-alkylating agents to the reaction mixture of BBAandrat skin resultedin a significant inhibition of the metabolism by both agents. In particular, iodoacetate/dithiothreitol (IAA/DTT) demonstrated a greater inhibition of the enzymatic

reactions than NEM. This may be a consequence of using DTT, which reduced existing disulfide bonds to free thiols, thus increasing the availability of more thiol groups to S-carboxymethylation by IAA.

C.3.4. Percutaneous penetration of hydrocortisone co-applied with DMBIS and BBA on pig skin in vitro

Once I twas obvious that DMBIS had rapidly been transformed to BBA by skin tissue and that BBA might serve as a pivotal factor in drug enhancement, the transdermal effects of bot hmaterials were evaluated and compared. Table 1 summarizes the parameters obtained for the percutaneous hydrocortisone delivery through dermatomed pig skin. As shown in the table, the co-application of DMBIS and BBA increased drug penetration by 2 fold (the enhancement ratios were 2.4 and 2.2 for DMBIS and BBA, respectively), relative to the control group without enhancer. Simultaneous analysis of the enhancers and the cumulative drug penetration has revealed that BBA was the major substance penetrating through the skin after DMBIS application, although it was in lesser extent than after its direct application (data not shown). Only small amounts of DMBIS were detected in the receptor solutions. These results indicate that either BBA itself implements the enhancement activity, or it may be used as a precursor for another in situ formed enhancer that makes the effect.

Table 1. Parameters of in vitro percutaneous penetration of hydrocortisone through dermatomed pig skin -- enhancement by DMBIS and BBA

Test Group	Flux, J ($\mu g/cm^2/h$)	Q_{24} ($\mu g/cm^2$)	ER[a]
Control (no enhancer)	0.065 (±0.017)	0.778 (±0.355)	1

DMBIS (4 µL 0.4 M sol)	0.154* (±0.063)	2.043* (±0.973)	2.4
DMBIS (4 µL 0.4 M sol)	0.143* (±0.055)	1.653* (±0.846)	2.2
* Statistically different than the control group (ANOVA, $p<0.05$) [a] Enhancement Ratio=J of enhancer treated /J of the control			

C.3.5. The influence of iodoacetate/dithiothreitol treatment on the penetration of BBA and on the enhancement of hydrocortisone penetration by BBA through human cadaver epidermis

Once we have shown that BBA is extensively metabolized by skin, a 'proof-of-concept' is required to determine whether or not the skin metabolism is correlated with the observed enhancement activity of a model drug. Although bearing some limitations, skin penetration studies of hydrocortisone are commonly performed in vitro and their relevance to in vivo investigations is well established [24,25]. Therefore, in an in vitro permeation study using human epidermis, we compared between the permeabilities of untreated skin and IAA/DTT-treated skin to hydrocortisone in the presence of BBA. It is worth noting that a vehicle control was not used in these experiments since BBA has already been proved in a previous report to have a significant enhancing effect for hydrocortisone over propylene glycol as a vehicle control [15]. Figure 4 presents the results of these experiments. It was obvious from the previous experiments that, due to inhibition of the metabolism of BBA in the skin, more molecules would be retained and transported into the receptor than with untreated skin. Figure 4a shows a higher penetration of BBA through the IAA/DTT-treated epidermis than the untreated epidermis. Conversely, the extent of the penetration of hydrocortisone through the untreated epidermis was higher (and had much shorter lag time) than its penetration through IAA/DTT-treated epidermis

(Fig. 4b). Although the permeation fluxeswere similar in both groups, hydrocortisone started to penetrate 2 h after its application onto the untreated epidermis in contrast to the 12 h delay demonstrated after the enzymes were inhibited, as calculated by a linear regression method. It is evident, therefore, that at least one enzymatic reaction is involved in the enhancement activity of BBA; by inhibition of the enzymatic reaction, the enhancement activity is also inhibited.

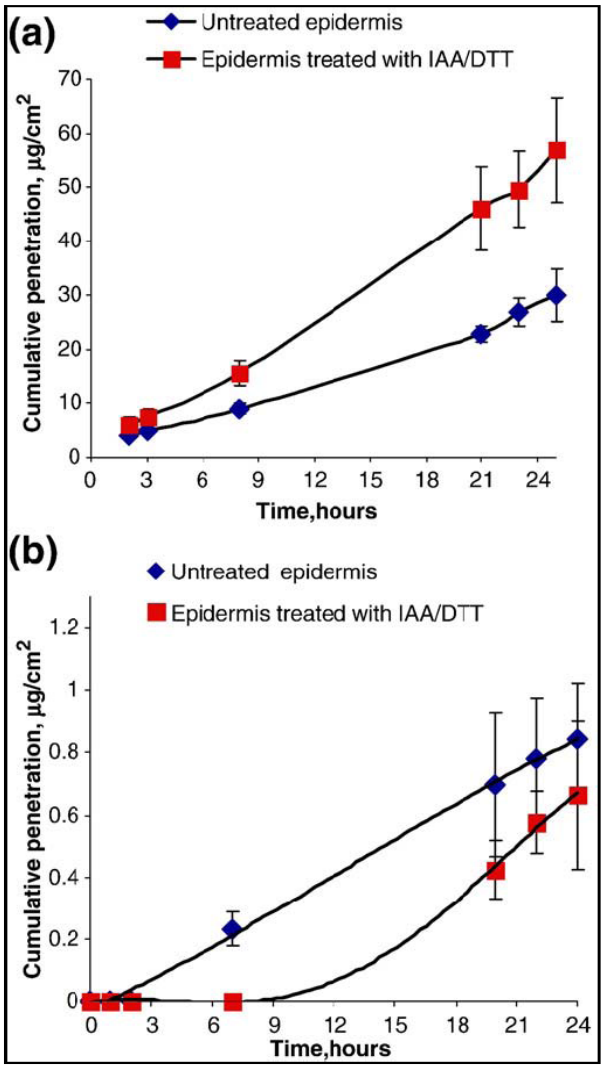

Figure 4. In vitro percutaneous penetration of BBA (a) and hydrocortisone (b) co-applied on human epidermis. Comparison between untreated epidermis and pretreatment with iodoacetate/dithiothreitol (n=6).

C.4. Conclusions

The search for an ideal skin penetration enhancer has been the focus of a considerable research effort over the last decades. Unfortunately, no chemical enhancer has yet been found to possess ideal properties; furthermore, many enhancers are toxic, acting as skin irritants or allergens at some level (depending on their concentration and

the frequency of their treatment). Generally, the toxicity of a potent enhancer is associated with its enhancement effect, indicating that its mechanism of action is related to chemical interaction with skin components or structures. In this paper, we described for the first time a new mechanism of action by which a non-irritant and powerless “enhancer” (i.e., a pro-enhancer) is activated by its own metabolism in the skin tissue. To understand the mechanism of enhancement by S,S-dimethyl-N-(4-bromobenzoyl)iminosulfurane, or more practically, by its immediate product, we evaluated its metabolic elimination of 4-bromobenzamide in the presence of skin from various species, inhibited its biotransformation by iodine and alkylating agents, and eventually proved that this biotransformation is essential for its enhancement activity. Relative to the commonly-known enhancers, greater advantages could be gained by this type of an in situ formed enhancer, such as (a) a continuous and slow release, (b) the presence of only small quantities of the active enhancer/metabolite at a given time, and (c) an enhancer's capability to being rapidly eliminated. Although it is now evident that an effective enhancement activity can be generated by a metabolite, an understanding of BBA metabolism, and in particular, the nature of the new active molecule/s is needed. Hence, it is of great interest to study and analyze the chemical structure of the active bioform of BBA; such research may trigger development of a new generation of potent enhancers and permitting a better understanding of their structure–activity relationships.

Acknowledgements

We acknowledge the use of tissues procured by the National Disease Research Interchange (NDRI) with support from NIH grant no. 5 U42RR006042-17. Funding was provided by the Center for Dermal Research.

C.5. References

1. R.K. Subedi, H-K. Choi, et al. 2010. Recent Advances in transdermal drug delivery. Arch. Pharm. Res. 33(3):339-351.

2. A.C. William and B.W. Barry. 2004. Permeation enhancers. Adv. Drug Delivery Rev. 56:603-618.

3 N. Kim, M. El-Khalili, M.M. Henary, L. Strekowski, and B.B. Michniak. 1999. Percutaneous penetration enhancement activity of aromatic S,S-dimethyliminosulfuranes. Int. J. Pharm. 187:219-229.

4. L. Strekowski, M.M. Henary, N. Kim, and B.B. Michniak. 1999. N-(4-bromobenzoyl)-S,S-dimethyliminosulfurane, a potent dermal penetration enhancer. Bioorgan. Med. Chem. Letter. 9:1033-1034.

5. Y. Song, C. Xiao, R. Mendelsohn, T. Zheng, L. Strekowski, and B.B. Michniak. 2005. Investigation of iminosulfuranes as novel transdermal penetration enhancers: enhancement activity and cytotoxicity. Pharm. Res. 22(11):1918-1925.

6. A.F. Davis, R.J. Gyurik, J. Hadgraft, M.A. Pellett, K.A.Walters, Formulation Strategies for modulating skin penetration, in: K.A. Walters (Ed.), Dermatological And Transdermal Formulations, Marcel Dekker Inc., New York, 2002, pp. 271–317.

7. D.V. McAllister, M.G. Allen, M.R. Prausnitz, Microfabricated microneedles for Gene and drug delivery, Ann. Rev. Biomed. Eng 2 (2000) 298–313.

8. P. Singh, P. Liu, S.M. Dinh, Facilitated transdermal delivery by iontophoresis, in: R.L. Bronaugh, H.I. Maibach (Eds.), Percutaneous Absorption, Drugs–Cosmetics–Mechanisms–Methodology, 3rd ed, Marcel Dekker, Inc., New York, 1999, pp. 633–657.

9. D. Marro, R.H. Guy, M.B. Delgado-Charro, Characterization of the iontophoretic permselectivity properties of human and pig skin, J. Control. Release 70 (2001) 213–217.

10. R.H. Guy, M.B. Delgado-Charro, Y.N. Kalia, Iontophoretic transport across the skin, Skin Pharmacol. Appl. Skin Physiol 14 (2001) 35–40.

11. M.R. Prausnitz, V.G. Bose, R. Langer, J.Weaver, Electroporation of mammalian skin: a mechanism to enhance transdermal drug delivery, Proc. Natl. Acad. Sci. USA 90 (1993) 10504–10508.

12. R. Vanbever, N. Lecouturier, V. Preat, Transdermal delivery of metoprolol by electroporation, Pharm. Res 11 (1994) 1657–1662.

13. J.E. Riviere, N.A. Monteiro-Riviere, R.A. Rogers, D. Bommannan, J.A. Tamada, R.O. Potts, Pulsatile transdermal delivery of LHRH using electroporation: drug delivery and skin toxicology, J. Control. Release 36 (1995) 229–233.

14. R. Vanbever, E. Le Boulenge, V. Preat, Transdermal delivery of fentanyl by electroporation I. Influence of electrical factors, Pharm. Res 13 (1996) 559–565.

15. M.R. Prausnitz, A practical assessment of transdermal drug delivery by skin electroporation, Adv. Drug Del. Rev 35 (1999) 61–76.

16. Q. Hu, W. Liang, J. Bao, Q. Ping, Enhanced transdermal delivery of tetracaine by electroporation, Int. J. Pharmaceut 202 (2000) 121–124.

17. J. Kost, S. Mitragotri, R. Langer, Phonophoresis, in: R.L. Bronaugh, H.I. Maibach (Eds.), Percutaneous Absorption, Drugs–Cosmetics–Mechanisms–Methodology, 3rd ed, Marcel Dekker, Inc., New York, 1999, pp. 615–631.

18. A.C. Williams, B.W. Barry, Terpenes and the Lipid–Protein-Partitioning theory of skin penetration enhancement, Pharm. Res 8 (1991) 17–24.

19. B.W. Barry, Lipid–Protein-Partitioning theory of skin penetration enhancement, J. Control. Rel 15 (1991) 237–248.

20. D.W. Nebert, D.W. Russell, Clinical importance of the cytochromes P450, Lancet 360 (2002) 1155–1162.

21. H.F. Merk, J. Abel, J.M. Baron, J. Krutmann, Molecular pathways in dermatoxicology, Toxicol. Appl. Pharmacol 195 (2004) 267–277.

22. N. Ahmad, H. Mukhtar, Cytochrome P450: a target for drug development for skin diseases, J. Invest. Dermatol 123 (2004) 417–425.

23. C. Jewell, J. Heylings, H.M. Clowes, F.M. Williams, Percutaneous absorption and metabolism of dinitrochlorobenzene in vitro, Toxokinet. Met 74 (2000) 356–365.

24. N. Higo, R.S. Hinz, D.T.W. Lau, L.Z. Benet, R.H. Guy, Cutaneous metabolism of nitroglycerin in vitro. I.Homogenized versus intact skin, Pharm. Res 9 (1992) 187–190.

25. L. Hellerman, M.E. Perkins, W. Mansfield Clark, Urease activity as influenced by oxidation and reduction, Proc. Nat. Acad. Sci. USA 19 (1933) 855–860.

26. C. Parkes, J. Gagnon, M.A. Kerr, The reaction of iodine and thiol-blocking reagentswith human complement components C2 and Factor B, Biochem. J 213 (1983) 201–209.

27. H. Scaefer, G. Stuttgen, A. Zesch,W. Schalla, J. Gazith, Quantitative determination of percutaneous absorption of radiolabeled drugs in vitro and in vivo by human skin, Curr. Probl Dermatol 7 (1978) 80–94.